



Norwegian University of
Science and Technology

CFD simulation of active displacement ventilation

Tollef Hjermann

Mechanical Engineering

Submission date: June 2017

Supervisor: Per Olaf Tjelflaat, EPT

Co-supervisor: Laurent Georges, EPT

Norwegian University of Science and Technology
Department of Energy and Process Engineering

EPT-M-2017-35

MASTER THESIS

for

Student Tollef Hjermann

Spring 2017

CFD simulation of active displacement ventilation

*CFD simulering av aktiv fortrenningsventilasjon***Background and objective**

There is basically a choice between mixing ventilation and displacement ventilation for rooms.

Displacement ventilation is normally designed with air supply at low speed and low temperature in the lower part of the room. Ventilation extract is placed at ceiling level.

Active displacement ventilation is a variant where the ventilation air, also at low speed and at low temperature, is supplied close to the ceiling level. Extract is still at ceiling level.

Well designed, active displacement ventilation can give benefits as sufficient air quality and thermal comfort, e.g. in class rooms, with less ventilation flow rate compared to ordinary displacement ventilation and mixing ventilation. Thus, active displacement has a potential to reduce the emission of GHG from buildings.

Active ventilation has been investigated in a project thesis in the fall of 2016. Literature has been reviewed, and design of active displacement ventilation, using empirical relations for jets and plumes, has been investigated.

Uncertainties related to application of the simple empirical relations make need for further investigations by use of CFD simulation.

The following tasks are to be considered:

- 1 Training in a relevant CFD tool.
- 2 Literature review with respect to use of CFD for room ventilation problems.
- 3 Application of the CFD tool on relevant cases from the project thesis.
- 4 Evaluation of the application of simple empirical relations used for design of active displacement ventilation.

Within 14 days of receiving the written text on the master thesis, the candidate shall submit a research plan for his project to the department.

When the thesis is evaluated, emphasis is put on processing of the results, and that they are presented in tabular and/or graphic form in a clear manner, and that they are analyzed carefully.

The thesis should be formulated as a research report with summary both in English and Norwegian, conclusion, literature references, table of contents etc. During the preparation of the text, the candidate should make an effort to produce a well-structured and easily readable report. In order to ease the evaluation of the thesis, it is important that the cross-references are correct. In the making of the report, strong emphasis should be placed on both a thorough discussion of the results and an orderly presentation.

The candidate is requested to initiate and keep close contact with his/her academic supervisor(s) throughout the working period. The candidate must follow the rules and regulations of NTNU as well as passive directions given by the Department of Energy and Process Engineering.

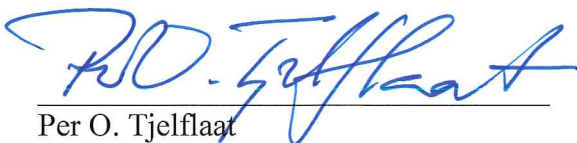
Risk assessment of the candidate's work shall be carried out according to the department's procedures. The risk assessment must be documented and included as part of the final report. Events related to the candidate's work adversely affecting the health, safety or security, must be documented and included as part of the final report. If the documentation on risk assessment represents a large number of pages, the full version is to be submitted electronically to the supervisor and an excerpt is included in the report.

Pursuant to “Regulations concerning the supplementary provisions to the technology study program/Master of Science” at NTNU §20, the Department reserves the permission to utilize all the results and data for teaching and research purposes as well as in future publications.

The final report is to be submitted digitally in DAIM. An executive summary of the thesis including title, student's name, supervisor's name, year, department name, and NTNU's logo and name, shall be submitted to the department as a separate pdf file. Based on an agreement with the supervisor, the final report and other material and documents may be given to the supervisor in digital format.

- Work to be done in lab (Water power lab, Fluids engineering lab, Thermal engineering lab)
- Field work

Department of Energy and Process Engineering, 15. January 2017



Per O. Tjelflaat
Academic Supervisor

Research Advisor: Laurent Georges

Preface

This master thesis is written at the Department of Energy and Process Engineering at Norwegian University of Science and Technology. The master thesis was carried out during the spring semester 2017. The thesis is written as a specialization in Energy Supply and Climatizing of Buildings as a part of the Master of Science degree in Mechanical Engineering.

The idea of the project was brought up by my supervisor, Per Olaf Tjelflaat. The topic of the master's thesis is a ventilation method called active displacement ventilation. It is assumed that this method will provide a sufficient indoor air quality and thermal comfort with lower temperatures and airflow rates than other methods.

The assumed background for the reader is knowledge similar to an engineering student on a master's/ bachelor's level studying energy supply and climatizing of buildings, or similar studies.

Trondheim, 2017-06-11

A handwritten signature in black ink, reading "Tollef Hjermann". The signature is written in a cursive style with a large, sweeping initial 'T'.

Tollef Hjermann

Acknowledgment

I would like to thank my supervisor, Professor Per Olaf Tjelflaat, for excellent guidance and encouragement throughout the semester. He has contributed with his great knowledge within the specialization field and has been helpful finding relevant literature. I would also like to thank my research advisor Laurent Georges for his guidance on the use of ANSYS Fluent.

T.H.

Summary

Active displacement ventilation is an air supply method that reuses the warm and polluted air in the upper zone of the room for preheating, while sufficient indoor air quality and thermal comfort are still achieved in the zone of occupancy. Air with low temperature is supplied high on the wall with low velocity, and the air "falls" down to the lower zone due to buoyant effects. Well-designed active displacement ventilation has the potential of achieving thermal comfort and sufficient air quality with lower airflow rate and air temperature compared to displacement ventilation and mixing ventilation.

CFD has been used to investigate vertical low velocity buoyant and isothermal jets, both free and along walls, since these are of relevance in the design of active displacement ventilation. Furthermore, cases of active displacement in a simple room situation were simulated for different airflow rates and temperatures. Displacement ventilation and mixing ventilation were also investigated to create a basis for comparison.

In the investigation of jets, it was concluded that empirical relations and well-known jet theory for free jets, both buoyant and isothermal, correspond with the CFD simulations. Two turbulence models, RNG $k-\epsilon$ and Realizable $k-\epsilon$, were used. When the vertical jets were moved next to a wall, it was observed that the maximum velocity was higher than for the free jets. As this result is contrary to what was expected it is assumed that the error lies in the CFD simulation. It is not clear to the author why the error occurred, but one hypothesis is that the $k-\epsilon$ models perform badly near walls.

For the room simulations, it is concluded that empirical relations together with heat- and mass balance are useful tools for the prediction of the airflow pattern, CO_2 concentration, and temperature in a room with active displacement ventilation. One must be aware of the restrictions on the diffuser size and number of diffusers per wall width to use the relations in the area where they are valid. The most energy efficient solution was when a flow rate of 7 l/(s·person) with temperature 10°C was supplied.

Displacement ventilation was in this thesis restricted to an inlet air temperature of 17°C due to the risk of cold draught. Since the only heat loss from the room was through the ventilation duct, the flow rate for displacement ventilation had to be increased to 8 l/(s·person) to meet the requirement for thermal comfort. If the atmospheric environment was the only restriction, the flow rate could be reduced to 6 l/(s·person). Mixing ventilation was modelled as complete mixing ventilation, i.e. with homogenous CO_2 concentration and air temperature. The most energy efficient solution was when the flow rate was 9 l/(s·person) and the air temperature was 11°C. The methods were compared in a $q_0 - T_i$ -chart to illustrate which combinations of flow rate and inlet air temperature that are suggested to use.

Sammendrag

Aktiv fortrenningsventilasjon er en måte å tilføre luft på som utnytter varm og forurenset luft i øvre sone av rommet til forvarming av luft mens luftkvaliteten og det termiske miljøet fremdeles er tilfredsstillende i oppholdssonen. Luft med lav temperatur blir tilført oppe på veggen med lav hastighet, og "faller" ned mot den nedre sonen grunnet termiske krefter. Godt utformet aktiv fortrenningsventilasjon har potensial for å oppnå termisk komfort og tilstrekkelig luftkvalitet med lavere luftmengde og lufttemperatur sammenlignet med fortrenningsventilasjon og omrøringsventilasjon.

CFD har blitt brukt til å undersøke vertikale lavhastighets termiske og isotermske luftstråler, både frie og langs vegger, da disse er av relevans for utformingen av aktiv fortrenningsventilasjon. Videre ble tilfeller av aktiv fortrenningsventilasjon i en enkel romsituasjon simulert for forskjellige luftmengder og temperaturer. Fortrenningsventilasjon og omrøringsventilasjon ble også undersøkt for å skape et grunnlag for sammenligning med aktiv fortrenningsventilasjon.

I undersøkelsen av luftstråler ble det konkludert med at empiriske uttrykk og velkjent luftstråleteori for frie luftstråler, både termiske og isotermske, samsvarer med CFD-simuleringene. To turbulensmodeller, RNG $k-\epsilon$ og Realizable $k-\epsilon$, ble brukt. Når den vertikale luftstrålen ble flyttet til en vertikal vegg, ble det observert at maksimalhastigheten var høyere enn for den frie strålen. Da dette resultatet er i strid med det som var forventet, antas det at feilen ligger i CFD-simuleringen. Det er ikke klart for forfatteren hvorfor feilen oppstod, men en hypotese er at $k-\epsilon$ -modellene yter dårlig langs vegger.

For romsimuleringen konkluderes det med at empiriske uttrykk sammen med varme- og massebalanse er gode verktøy for å forutsi luftmønsteret, CO_2 -konsentrasjonen, og lufttemperatur i et rom med aktiv fortrenningsventilasjon. Man må være oppmerksom på restriksjonene i størrelse og antall tilluftsventiler per veggbredde for å sørge for at uttrykkene er brukt i et område hvor de er gyldige. Det termiske og atmosfæriske miljøet var tilstrekkelig når luftmengden var $7 \text{ l}/(\text{s}\cdot\text{person})$ med temperaturen 10°C .

Fortrenningsventilasjon var i denne oppgaven begrenset til en tilluftstemperatur på 17°C på grunn av risiko for kaldt trekk. Siden det eneste varmetapet fra rommet var gjennom ventilasjonskanalen, måtte luftmengden for fortrenningsventilasjon økes til $8 \text{ l}/(\text{s}\cdot\text{person})$ for å tilfredsstille kravet til termisk komfort. Hvis det atmosfæriske miljøet var den eneste begrensningen, kunne luftmengden reduseres til $6 \text{ l}/(\text{s}\cdot\text{person})$. Omrøringsventilasjon ble modellert som komplett omrøringsventilasjon, dvs. med homogen CO_2 -konsentrasjon og lufttemperatur. Den mest energieffektive løsningen var når luftmengden var $9 \text{ l}/(\text{s}\cdot\text{person})$ og lufttemperaturen var 11°C . Metodene ble sammenlignet i et $q_0 - T_i$ -diagram for å illustrere hvilken kombinasjon av luftmengde og tilluftstemperatur som er anbefalt.

Contents

Preface	i
Acknowledgment	ii
Summary	iv
Sammendrag	vi
List of figures	xiv
List of tables	xv
List of symbols	xvi
Abbreviations	xx
1 Introduction	1
1.1 Background	1
1.2 Scope	1
2 Theory	3
2.1 Indoor climate	3
2.1.1 Thermal environment	3
2.1.2 Atmospheric environment	4
2.2 Ventilation and its categorization	4
2.2.1 Displacement ventilation	5
2.2.2 Mixing ventilation	10
2.3 Building integrated ventilation	11
2.3.1 The Swedish model	12
2.4 Active displacement ventilation	15
2.4.1 Active displacement ventilation in the industry	16
2.4.2 Active displacement ventilation in school buildings	18
2.5 Flows in rooms and empirical relations	18
2.5.1 Archimedes number	19
2.5.2 Comparing supply methods using $\mathbf{q}_0 - \Delta\mathbf{T}_0$ - charts	20
2.5.3 Flow elements in rooms	21
2.5.4 Vertical jet supplied by wall	26
2.5.5 Indoor air quality indices and energy efficiency	27
2.6 Basis for CFD	28
2.6.1 Governing equations	28
2.6.2 Turbulence modeling	30
2.6.3 Near wall turbulence	32
2.6.4 Mesh	33
2.6.5 Solution of transport equations	34
2.7 CFD for room air distribution	38
2.7.1 Turbulence models for HVAC simulations	38
2.7.2 Influence of radiation	40
2.7.3 CFD-studies relevant for simulation of free jets and wall jets	41

2.7.4	Previous CFD research relevant for active displacement ventilation . . .	41
3	Method	45
3.1	Geometrical model and boundary conditions	45
3.1.1	Thermal and isothermal jets	45
3.1.2	Active displacement ventilation	48
3.1.3	Model for ordinary displacement ventilation	50
3.2	Mesh	51
3.3	Setup	53
3.4	Method for analyzing jets	54
3.5	Method for design of active displacement ventilation using empirical relations	55
3.6	Method for design of displacement ventilation using empirical relations	56
3.7	Method for design of complete mixing ventilation	57
4	Results and discussion	59
4.1	Simulation of buoyant jet	59
4.1.1	Initial discussion of the simulations	59
4.1.2	Similarity profile, jet angle and pole distance	66
4.1.3	Centerline distribution	67
4.1.4	Local Archimedes number	68
4.2	Simulation of buoyant wall jet	69
4.2.1	Validation of mesh	69
4.2.2	Comparison of buoyant wall jet and free buoyant jet	70
4.2.3	Discussion of errors	74
4.3	Simulation of isothermal jets	74
4.4	Simulation of active displacement ventilation	77
4.4.1	Inlet airflow rate 6 l/s for active displacement ventilation	77
4.4.2	Inlet airflow 7 l/s for active displacement ventilation	82
4.5	Discussion of active displacement ventilation	88
4.5.1	Humidity	88
4.5.2	Comparison with ordinary displacement ventilation	90
4.5.3	Comparison with mixing ventilation	92
4.5.4	Energy use and reduction of greenhouse gases	93
4.5.5	Application of the results	94
4.5.6	Design of a classroom situation	99
5	Conclusion	105
5.0.1	Application of CFD on buoyant and isothermal jets	105
5.0.2	Evaluation of the application of simple empirical relations used for design of active displacement ventilation	106
5.0.3	Comparison of supply methods	107
6	Further Work	109
A	Appendix	111
A.1	Relevant guidelines and regulations	111
A.2	Clothing, activity and human metabolism	112
A.3	Integration constants	112
A.4	Matlab script for calculations of active displacement ventilation	113

List of Figures

2.1	Simple principle sketch of displacement ventilation	6
2.2	Schematic of two-zone model	7
2.3	Concentration of CO_2 in the breathing zone	8
2.4	Distribution of CO_2 in a room with one source	9
2.5	Temperature distribution in a room with one heat source	10
2.6	Principle sketch of mixing ventilation	11
2.7	Schematic of the principles of the Swedish model	13
2.8	Driving forces for different outdoor temperatures	14
2.9	Sketch of active displacement ventilation	16
2.10	Sketch of active displacement ventilation in the industry	17
2.11	$q_0 - \Delta T_0$ - chart	19
2.12	$q_0 - \Delta T_0$ - chart indicating restrictions on the flow rate and temperature difference ΔT_0	20
2.13	The zones of a jet	21
2.14	Schematic view of a vertical buoyant jet structure along a wall	23
2.15	Heat source generating thermal convective flow	24
2.16	Method of calculating flow along wall	26
2.17	Illustration of displacement thickness	27
2.18	The effect of refining grid	36
2.19	First order upwind scheme and false diffusion	37
2.20	CFD simulation of displacement ventilation rooms	42
2.21	CFD simulation of displacement ventilation in artium	43
3.1	Geometrical model for modeling of buoyant jet	46
3.2	Geometrical model for simulation of wall jets	47
3.3	Geometrical model for simulation of active displacement ventilation	49
3.4	Geometrical model for simulation of displacement ventilation	51
3.5	Mesh for simulation of jet and active displacement ventilation	52
3.6	Mesh independence test for the simulation of the jet	53
3.7	Illustration of method of analyzing jets	55
4.1	Contour of velocity in y-direction for free buoyant jet	60
4.2	Contour of velocity in y-direction for free buoyant jet	61
4.3	Contour of air temperature distribution for free buoyant jet	62
4.4	Plot of streamlines for buoyant jet	63
4.5	Temperature stratification	64
4.6	Analysis of spreading of buoyant horizontal jet	64
4.7	Analysis of spreading of buoyant horizontal jet	65
4.8	Velocity in horizontal direction along centerline for free buoyant jet	67
4.9	Temperature distribution along centerline for free buoyant jet	68

4.10	Local Archimedes number for buoyant jets	69
4.11	Contour of y-plus for wall jet	70
4.12	CFD simulation of free buoyant jet and buoyant jet along wall compared to empirical relation by Skåret [1]	71
4.13	CFD simulation of free buoyant jet and buoyant jet along wall compared to empirical relation by Skåret [1]	72
4.14	Relative velocity in y-direction 2.5m over the floor	72
4.15	Shifting of centerline for isothermal wall jets	73
4.16	Velocity profile for free buoyant jet and buoyant wall jet	73
4.17	CFD simulation of free isothermal jet and isothermal jet along wall	75
4.18	CFD simulation and analysis of the velocity profile development of an isothermal free jet with k- ϵ RNG model	75
4.19	Shifting of line of maximum velocity for isothermal wall jets	76
4.20	CFD simulation of free isothermal jet and isothermal jet along wall	76
4.21	Red line indicating where vertical CO_2 - concentration and temperature distribution are studied	77
4.22	Flow pattern calculated from empirical relations	78
4.23	CO_2 concentration from floor to ceiling	80
4.24	Contour of concentration of CO_2 for active displacement ventilation	81
4.25	Contour of air temperature for active displacement ventilation	81
4.26	CO_2 concentration from floor to ceiling	83
4.27	Concentration of CO_2 for active displacement ventilation	84
4.28	Contour of air temperature for active displacement ventilation	85
4.29	Contour of air temperature for active displacement ventilation	85
4.30	Contour of air speed (velocity magnitude) for active displacement ventilation for $T_i = 8^\circ C$	87
4.31	Draught at ankle height for active displacement ventilation	88
4.32	Sketch of suggested occupancy zone	88
4.33	Mollier diagram for active displacement ventilation	89
4.34	Contour of CO_2 -concentration for ordinary displacement ventilation with and airflow rate of 6l/s	90
4.35	Contour of temperature for ordinary displacement ventilation	91
4.36	Explanation of design chart	97
4.37	Graphical illustration of the use of supply methods	98
4.38	Illustration of the restrictions for each of the supply methods	99
4.39	Illustration of the restrictions for each of the supply methods	100
4.40	Suggestions on other inlet air devices	101

List of Tables

3.1	Boundary conditions for simulation of thermal and isothermal jets	46
3.2	Boundary conditions for simulation of thermal and isothermal jets	48
3.3	Geometry for simulation of active displacement ventilation	49
3.4	Boundary conditions for simulation of active displacement ventilation	50
3.5	Geometry for simulation of ordinary displacement ventilation	50
3.6	Boundary conditions for simulation of ordinary displacement ventilation	51
3.7	Boundary conditions for simulation of mixing ventilation	52
3.8	Distance of the first node for simulation of jet	52
3.9	Setup for simulations	54
3.10	Ratio between concentration in the breathing zone and in the ambient	57
4.1	Values inserted in empirical relations	66
4.2	Summary of comparison of results from empirical relations and CFD simulations for active displacement ventilation with $Q_i = 6\text{ l/s}$	80
4.3	Key values from the calculation of active displacement ventilation based on empirical relations for $Q_s=7\text{ l/s}$	82
4.4	Efficiency indices for active displacement ventilation	84
4.5	Summary of comparison of results from empirical relations and CFD simulations for active displacement ventilation with $Q_i=7\text{ l/s}$	86
4.6	Calculations for complete mixing ventilation	93
4.7	Overview of results for winter condition where the energy use is minimized while an acceptable thermal and atmospheric environment is still achieved	96
4.8	Distance before jet is developed	100
4.9	Design of classroom with active displacement. Inlet diameter 0.2 m	103
4.10	Design of classroom with active displacement. Inlet diameter 0.25 m	104
A.1	Relevant guidelines and regulations	111
A.2	Relevant guidelines and regulations	112
A.3	Table for clothing, activity and human metabolism	112
A.4	Integration constants	112
A.5	Integration constants	113

List of symbols

Roman letters

A_i	Total inner area of room [m^2]
$A_{imaginary}$	$2A_{real}$. Area of imaginary inlet opening for wall jet. [m^2]
A_k	Area of surface k
A_{per}	Surface area of person [m^2]
Ar	Archimedes number
A_{real}	Area of inlet opening for wall jet. [m^2]
A_w	Window area [m^2]
Ar_0	Archimedes number at inlet
a	Factor for convective plume calculations
a_0	The total area of the supply openings [m^2]
b	Jet width [m]
C_{1e}	Constant in RNG k- ϵ
C_2	Constant in RNG k- ϵ
C_b	$\tan(\alpha)$
C_e	CO_2 -concentration in exhaust [ppm]
C_f	Skin friction
C_{zone}	CO_2 -concentration in zone [ppm]
c_{e1}	Experimental konstant in SKE
c_{e2}	Experimental konstant in SKE
c_μ	Experimental konstant in SKE
D_H	Hydraulic diameter [m]
d_{per}	Diameter of a cylinder approximated as a person [m^2]
E	Energy
F_{jk}	View factor
G_b	Generation of turbulence kinetic energy due to buoyancy
G_k	Generation of turbulence kinetic energy due to mean velocity
Gr	Grashof number
g	Gravity acceleration [m/s^2]
h	Heat transfer coefficient [$W/(m^2K)$]
h_{avg}	Average height [m]
h_c	Convective heat transfer coefficient [$W/(m^2K)$]
h_{per}	Height of person [m^2]
h_r	Radiative heat transfer coefficient [$W/(m^2K)$]
i	1) Momentum factor 2) Integration constant
J_j	Diffusion flux
k	1) Conductivity 2) Kinetic turbulent energy
K_a	Constant for air terminal device
k_{eff}	Effective conductivity
k_t	Turbulent conductivity
l_0	Characteristic length [m]
M	Molecular weight of gas
m	mixing number

P	Power / heat [kW]
P_c	Convective heat [kW]
P_{cl}	Convective heat per length [kW/m]
P_f	Heat from floor [kW]
P_{per}	Heat from person [kW]
p	Pressure [Pa]
p_{op}	Operating pressure [Pa]
Q_0/q_0	Inlet airflow rate [l/s] or [m^3/h]
Q_B	Airflow due to material emission [l/s] or [m^3/h]
$Q_{b,l}$	Airflow from boundary layer approximations [l/s] or [m^3/h]
Q_d	Airflow at cold/ warm surface [l/s] or [m^3/h]
Q_i	Inlet airflow [l/s] or [m^3/h]
Q_p	Airflow per person [l/s] or [m^3/h]
Q_{plume}	Airflow from convective plume [l/s] or [m^3/h]
Q_v	Airflow at a distance y from a jet/plume [l/s] or [m^3/h]
$Q_{v,l}$	Airflow per length at a distance y from a jet/plume [$l/(s \cdot m)$] or [$m^3/(h \cdot m)$]
Q	Energy flux [W]
$q_{out,k}$	The radiative energy leaving a surface k
$q_{in,k}$	The radiative energy entering a surface k
R	Universal gas constant
R_i	Rate of production of species by chemical reactions
S_h	Production term for volumetric heat sources
S_i	Source term
T_m	1) Mean temperature for stack effect. 2) Maximum temperature for jets [$^{\circ}C$]
ΔT	Temperature difference. Are specified in text for which temperatures [$^{\circ}C$]
ΔT_0	Temperature difference between inlet air and ambient/exhaust [$^{\circ}C$]
ΔT_m	Maximum temperature difference between jet and ambient [$^{\circ}C$]
$\Delta T_{U_{maxd}}$	Maximum temperature difference for draft along cold/ warm surface [$^{\circ}C$]
T_1	Temperature in lower zone [$^{\circ}C$]
T_2	Temperature in upper zone [$^{\circ}C$]
T_e	Temperature of exhaust air [$^{\circ}C$]
T_f	Temperature of floor [$^{\circ}C$]
T_i	Temperature at inlet [$^{\circ}C$]
T_s	Temperature of supply air [$^{\circ}C$]
$T_{s'}$	Temperature of supply air entering the double wall [$^{\circ}C$]
T_{s2}	Temperature of supply air entering the room [$^{\circ}C$]
U	Velocity [m/s]
U_m	Maximum velocity [m/s]
U_{maxd}	Maximum velocity of air along cold/ warm surface [m/s]
U_{disc}	Value of U by discretizing [<i>dependsonwhatUis</i>]
U_{model}	Real value of U in the model [<i>dependsonwhatUis</i>]
u	Velocity
\bar{u}	Mean value
u'	Fluctuating value
$-\rho \overline{u_i u_j}$	Reynold stress tensor
v	Wind velocity [m/s]
x_p	Pole distance in x- direction
Y_M	Dilatation in compressible turbulence for high Mach numbers
y	Distance from jet inlet [m]
y_l	Distance for $Gr = 10^9$ [m]
y_p	Pole distance in y- direction
y_{pt}	Distance at which turbulent boundary layer begins [m]
y^+	Y plus. Dimensionless distance from wall to first node
z	Height over a reference level [m]

Greek letters

α	1) Jet angle [°] 2) absorptivity 3) Experimental constant in SKE
β	1) Thermodynamic beta 2) Experimental constant in SKE
Δ	Difference
δ	Boundary layer thickness [°C]
δ^*	Displacement thickness [°C]
ϵ	1) Contraction coefficient 2) emissivity 3) Dissipation rate
ϵ^c	Contaminant removal effectiveness
ϵ^T	Temperature effectiveness
ϵ_{disc}	Discretization error
η^T	Kolmogorov length scale
η_0	Experimental constant in SKE
μ	Kinematic viscosity m^2/s
ν	Dynamic viscosity m^2/s
ν_T	Eddy viscosity m^2/s
ρ	Density [kg/m^3]
ρ_o	Density of inlet air [kg/m^3]
ρ_r	Density of room air [kg/m^3]
$\bar{\rho}$	Average density [kg/m^3]
σ	Stefan-Boltzman constant
σ_k	Turbulent Prandtl number for k
σ_ϵ	Turbulent Prandtl number for ϵ
τ_w	Wall shear stress

Abbreviations

ADV	Active displacement ventilation
AHU	Air handling unit
BC	Boundary condition
CAV	Constant air volume
CFD	Computational fluid dynamics
DCV	Demand controlled ventilation
DNS	Direct numerical simulations
DV	Displacement ventilation
EWT	Enhanced wall treatment
GHG	Green house gasses
HVAC	Heat, ventilation and air conditioning
IAQ	Indoor air quality
MV	Mixing ventilation
NS	Navier-Stokes equation
PPM	Parts per million
RANS	Reynolds averaged Navier-Stokes equation
RKE	Realizable $k-\epsilon$ model
RNG	Renormalized group $k-\epsilon$ model
SFP	Specific fan power
SIMPLE	Semi-Implicit Method for Pressure Linked Equations
SIMPLEC	SIMPLE-Consistent
SFP	Specific fan power
SKE	Standard $k-\epsilon$ equations
S2S	Surface to surface
TDC	Top down chimney
TI	Turbulence intensity
VAV	Variable air volume
QUICK	Quadratic Upstream Interpolation for Convective Kinematics

Introduction

Computational fluid dynamics (CFD) is a tool for predicting and analyzing fluid flows numerically by the use of computers. In the ventilation industry, the tool can be used to analyze important factors affecting the thermal and atmospheric environment such as the airflow pattern, contamination, humidity and heat distribution in rooms. The tool is therefore perfect for design and research of ventilation. Active displacement ventilation (ADV) is a method of supplying air to a room, and it has the potential of competing with other more established supply methods. This thesis will, by the use of CFD, hopefully, give some answers on how active displacement ventilation should be designed to take full advantage of its potential.

1.1 Background

The goal for a ventilation designer is to provide a healthy and comfortable indoor environment with as little effort as possible to save energy and reduce the emission of greenhouse gasses (GHG) from buildings. Natural driving forces and smart ways of preheating air will contribute to the reduction of the energy demand. This is partly achieved by reducing pressure losses in the system, recover heat from waste air and processes, utilizing natural driving forces, and creating buildings designed to interact with the outdoor environment when it is beneficial.

Active displacement ventilation is a method of supply that has the potential of being more energy efficient than methods such as mixing ventilation and displacement ventilation. If the method is designed correctly, it is assumed that one can supply air with lower temperatures and lower flow rate than for other methods. The concept is simple; reuse of warm and polluted room air while acceptable indoor air quality and thermal comfort are still achieved in the zone of occupancy.

1.2 Scope

Active displacement ventilation has been investigated in the project thesis in the fall 2016 where empirical relations were used in the design. Due to uncertainties related to the use of

1.2. SCOPE

such equations in the design, CFD simulations are used for further investigation.

A limitation of the scope is done to help clarify the problem and open for a greater depth of the study. Four main tasks are to be considered:

1. Training in a relevant CFD tool
2. Literature review with respect to use of CFD for room ventilation problems
3. Application of the CFD tool on relevant cases from the project thesis
4. Evaluation of the application of simple empirical relations used for the design of active displacement ventilation

The first task will mainly be answered in the literature review in section 2.6 where important aspects and governing theory related to CFD are explained. In addition, the presentation of the methodology and results will give an insight into the CFD skills of the author.

The second task is answered in the theory section. Especially section 2.6 and 2.7 reflects this task where one of the focus areas is the investigation of earlier publications on the topic. The choice of turbulence models, treatment of wall turbulence, density for non-isothermal flow, radiation, solution methods and sources of errors are topics that have been in focus.

In addition to answering task one and two in the theory section, some additional theory and relevant theory from the project thesis from the fall 2016 are included to give the reader a deeper insight into indoor climate, ventilation and its categorization, building integrated ventilation and of course active displacement ventilation. This literature will be useful in the discussion of the CFD simulations.

Task three is answered when the results and discussion are presented. The task has been limited to analysis of vertical jets in rooms where simple empirical relations has been used for comparison. Also, jet theory related to the development and spreading of the jet is investigated. Both vertical positive buoyant and isothermal jets are examined, and the jets are also investigated when supplied along a wall. The following four points describe the main aspects of the analysis of jets:

- Free buoyant jets
- Buoyant wall jets
- Free isothermal jets
- Isothermal wall jets

The last task to be considered is answered by simulating and discussing simple cases of active displacement ventilation where a heated cylinder, representing a person, is placed in a room with one air supply and one air extract. The cylinder pollutes and heats the room similarly to an adult person at rest. This means that the case typically is valid for offices and classrooms. The main focus will lie on what is happening inside the room, while the building design and energy solution will be discussed to a lesser degree.

The results are compared to cases where empirical relations are used to calculate the flow pattern, degree of contamination and temperature distribution for the same room. Cases of displacement and complete mixing ventilation will also be examined and compared to active displacement ventilation.

Theory

In this chapter theory and relevant perspectives will be presented in order to shed light on the topic in a scientific matter. The theory presented will be put to use when the methodology, results, discussion, and conclusion are presented.

The first part of this chapter will give insight to the concept of active displacement ventilation and important concepts related to this method of supply. Indoor climate, categorization of ventilation and building integrated ventilation will be in focus. Then, an introduction to the empirical relations used for comparison with CFD simulations will be presented. The last part of the section is the literature study of CFD for room ventilation problems.

2.1 Indoor climate

Indoor climate are influenced by several physical parameters. Normally, the indoor climate is divided into the following categories:

- Thermal environment (temperature, air velocity, humidity)
- Atmospheric environment (air pollution, perceived air quality)
- Acoustic environment (sound pressure, frequency, reverberation)
- Actinic environment (light, radiation, field phenomena)
- Mechanical environment (geometry, furniture / fixtures etc.)

The thermal and atmospheric environment are most relevant for this thesis, and will, therefore, be the main focus. The acoustic environment is normally also a very important factor for ventilation design, but will not be in focus in this thesis. Typical ventilation related factors affecting the acoustic environment are noise from the air handling unit (AHU), noise due to high air velocity, and over-hearing in the ducts.

2.1.1 Thermal environment

A popular measure of the thermal environment is whether the occupants are in thermal comfort or not. The definition of thermal comfort according to NS-EN ISO 7730 [2] is "a state of mind where we express full satisfaction with the thermal environment". A person's

thermal perception depends on the following factors:

- Air temperature [$^{\circ}\text{C}$]
- Air velocity (Draught) [m/s]
- Mean radiant temperature [$^{\circ}\text{C}$]
- Relative humidity
- Clothing [clo]
- Activity level [met]

Being in thermal comfort is not the same as being thermal neutral. Thermal neutrality is the state where the body as a whole is in heat balance with the environment. When a person is exposed to high levels of draught and temperature gradients, thermal comfort might not be achieved, while thermal neutrality might be achieved. Radiative asymmetry and cold floor temperature are other examples. From a ventilation designers perspective, draught, air temperature, and humidity are important factors for the thermal environment. Draught is a complicated issue as it depends on air velocity, air temperature, clothing, and which body part that is exposed. Typically, neck, head, and ankle regions are vulnerable to draught.

The relative humidity does not have a large impact on the thermal environment, but is important for the health. For low relative humidity (15-20 %) dry and irritated eyes and respiratory tract can occur. For high relative humidity, the occurrence of microbes will increase. Ideally, the relative humidity is between 20 % and 40 % [3].

2.1.2 Atmospheric environment

The atmospheric environment is associated with the indoor air quality (IAQ). It exists many definitions of IAQ. One of them is: "an indicator of the types and amounts of pollutants in the air that might cause discomfort or risk of adverse effects on human or animal health, or damage to vegetation". The smell in rooms can be used as a criterion for ventilation. Traditionally, the CO_2 level is used as an indicator on the air quality in rooms when people are the dominating source of the smell, and the suggested ventilation rate is normally around $8 \text{ l}/(\text{s}\cdot\text{person})$ where l is liter [4]. To overcome the smell/ pollution from materials a ventilation rate of $0.7 \text{ l}/(\text{s}\cdot\text{m}^2)$ for category two for low polluting buildings is suggested. The unit " l/s " will in this thesis be used instead of m^3/h which is a unit that is also frequently used for ventilation airflow rates. For classrooms, the maximum CO_2 -concentration according to the guidelines is 1000 ppm. This is equivalent to approximately 600 ppm over outdoor concentration. Appendix A.1 give an overview of relevant standards and guidelines for this thesis. For cases where the values depend on the type of building, values for classrooms are chosen.

2.2 Ventilation and its categorization

Ventilation is used to control the indoor environment, and the goal is to keep people healthy and comfortable, and facilitating for a productive working environment. When discussing

ventilation, it is convenient to categorize different ventilation types. Typically one categorize ventilation after the type of heat-, ventilation- and air conditioning (HVAC) system, the method of supply, and by which forces the air is driven. For this thesis, the method of supply and driving force is of highest relevance since we are mainly looking on what happens inside a room.

Air can be delivered to a room in many ways depending on the desired air movement, the room design and the thermal and atmospheric requirements for the room. One typically differ between buoyancy-driven and momentum-driven flow. Different methods of supply utilize these two flow types. The two most common methods for supply are displacement ventilation and mixing ventilation. Ordinary displacement ventilation is in this thesis used as a synonym for displacement ventilation, and will sometimes be used to separate it from active displacement ventilation. In short, we can say that ordinary displacement ventilation utilizes thermal forces displacing air from the supply near the floor to the extract in the ceiling. Mixing ventilation, on the other hand, utilizes momentum forces causing a mixing of the air in the room where the temperature and contaminant concentration in the entire room, ideally, are uniform. Active displacement ventilation is also utilizing buoyant forces, but the air is supplied high on the wall and with a lower temperature than ordinary displacement ventilation. Active displacement ventilation will be discussed in chapter 2.4. Another method of supply is piston ventilation. It is a supply method where the air moves through the room like a piston with a minimum of turbulence. The method is typical for clean rooms, and will not be used for comparison with active displacement ventilation in this thesis.

2.2.1 Displacement ventilation

To obtain a better basis for comparison between the three methods of supply, which are displacement ventilation, mixing ventilation and active displacement ventilation, a more detailed description will be given in the coming sections.

Displacement ventilation is, as already mentioned, a type of ventilation where the air is mainly driven by buoyant forces. The momentum forces have no practical importance in displacement ventilation. Air is supplied near the floor, displaced to higher levels, and extracted at ceiling height. Originally displacement flow is supplied through the floor, but for practical reasons, the air is supplied either by floor supply air devices or by side wall air devices near the floor [5]. The goal for displacement ventilation is to achieve nearly as good air quality in the breathing zone as in the air supply. Achieving the same air quality in the breathing zone as for mixing ventilation with lower flow rates will also be a goal. The thermal environment is characterized by a vertical temperature gradient. A sketch of displacement ventilation is shown in figure 2.1 where we see how fresh air from the lower zone is transported to the occupants breathing zone, and to the exhaust. In this case, the person is both a convective heat source and a pollution source.

The fresh supply air enters the room at a relatively low speed with a lower temperature than the room temperature and flows into the zone of occupancy. The zone near the supply air outlet is often referred to as the near zone and is a zone where people are normally

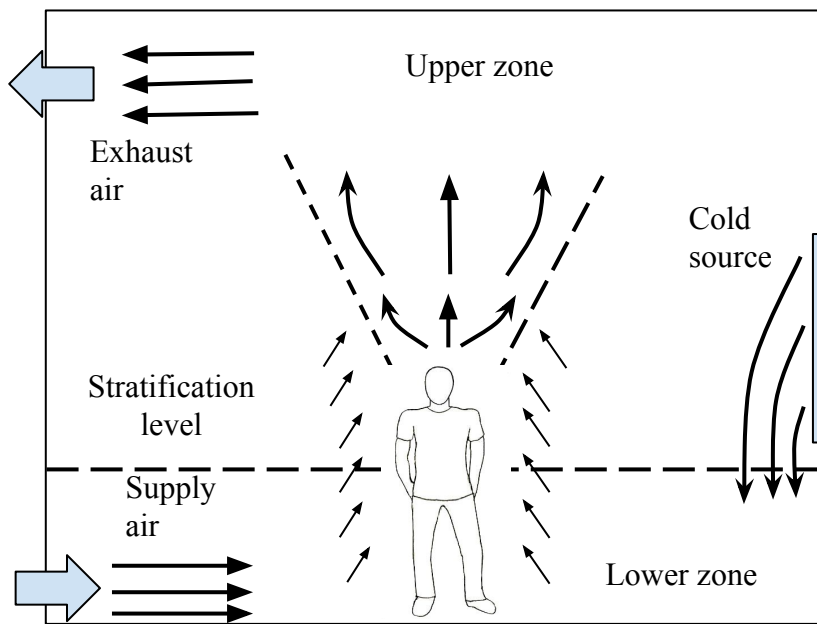


Figure 2.1: Simple principle sketch of displacement ventilation

not present due to a higher chance of cold draught. When cold and fresh air approaches the heat source a convective plume is generated by free convection from the heat source. A vertical flow is generated. As the air passes the person, CO_2 -emission from exhalation pollutes the air and brings the contaminants to the upper zone. How the stratification level between the two zones is defined will be further discussed in section 2.2.1.1. The design of displacement ventilation requires knowledge of the plumes from people, and flow due to other flow elements in the room generated from warm or cold sources. Knowing how the air flows makes it possible to estimate the air quality and air temperature in the zones for a given inlet airflow rate. A common way of designing a room with displacement ventilation is to apply the *two-zone model* which will be introduced in section 2.2.1.1. *Ventilation Systems* edited by Hazim Awbi is used for the description of this topic [6, Chap. 5].

Supply airflow rates for displacement ventilation vary, but for school buildings flow rates in the range of 6-8 l/(s·person) is achievable. Two Norwegian schools called Mediå school and Jaer school were investigated in an article by Wachenfeldt et al. [7], where "the resulting airflow rates are almost identical for the two schools", and equal 7 l/(s·person). This will give a good indication when simple cases of displacement ventilation are designed later in the thesis.

2.2.1.1 The two-zone model

The two zone model is an idealistic room model where the room is divided into two zones. The properties of each zone are homogenous and are decided by a mass balance of air. The temperature in the lower zone equals the supply temperature T_s , and the temperature in the

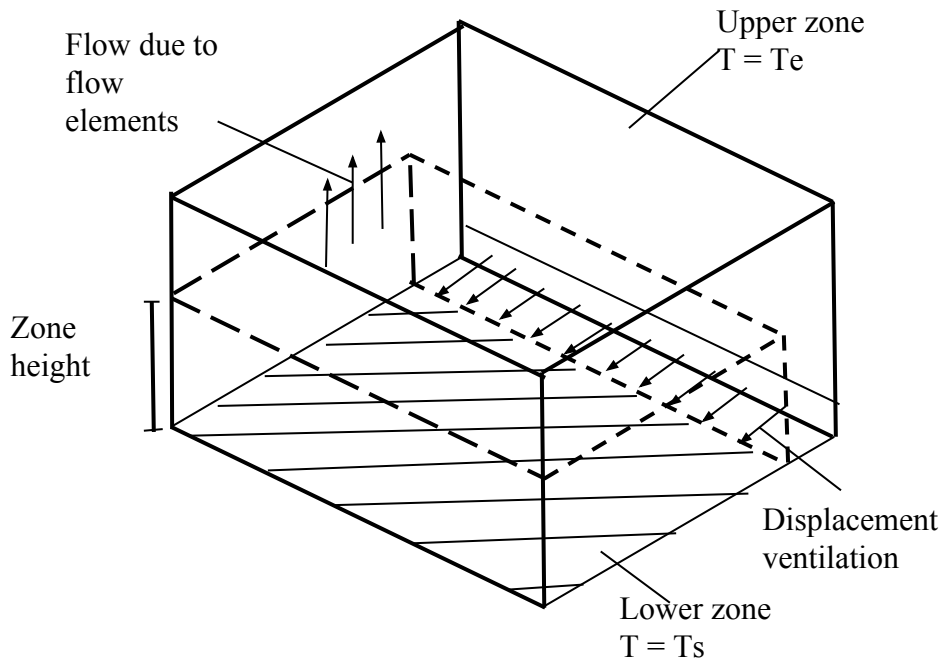


Figure 2.2: Schematic sketch of the two zone model

upper zone equals the exhaust temperature T_e . In the model, there is a lower zone with an acceptable concentration of contaminants and comfortable air temperature. The height of this zone must be designed so that it ensure sufficient air quality and thermal comfort for the occupants. There is also an upper zone where the concentration of CO_2 and the temperature are not specified. The only mass flow between the zones is flow caused by flow elements. The model is practical for calculations and design of displacement ventilation. Figure 2.2 illustrates how a room is divided into two zones.

The stratification level, or the neutral level, is defined by a mass balance. If the lower zone is a control volume, the height, H , of the stratification level is where the total flow into the control volume equals the total flow out of the control volume. The occupied zone is typically 1.8 m over the floor when standing, and 1.3 m when sitting [6, p.266], but that does not mean that the stratification level should be at these heights which we will see in section 2.2.1.2. For a room where all heat sources are defined the only way of changing the height of the stratification level is increasing or decreasing the ventilation rate. Flow elements in a room will be presented in section 2.5.

It is convenient to have a large upper zone. The volume will, in the same way as an exhaust hood, work as a buffer for the polluted and warm air if an overload of people or heat were to occur. The two-zone model assumes a steady state problem, but for real cases, where the pollution and heat load may vary, the stratification line will be in constant movement. A large upper zone is therefore convenient.

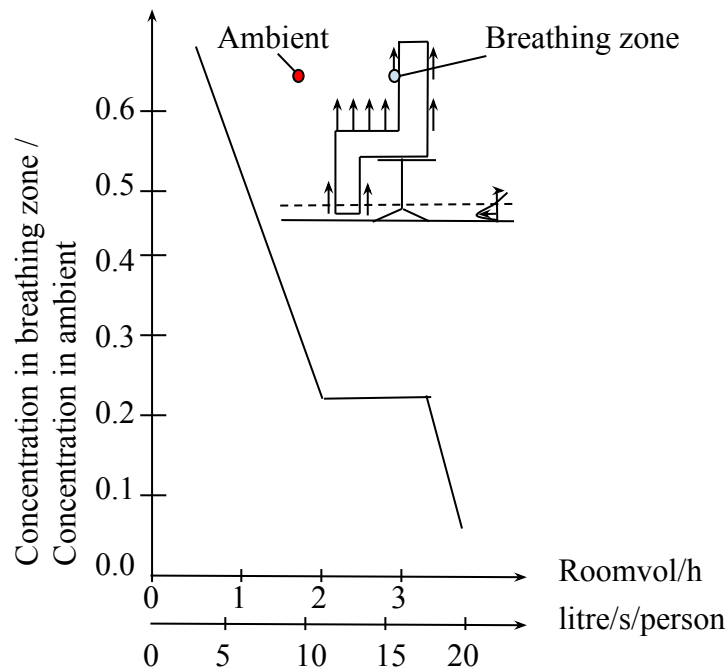


Figure 2.3: Concentration in the breathing zone compared to the concentration in the ambient. Figure adapted from Sandberg [8, Chap.8]

2.2.1.2 CO_2 -concentration in rooms with displacement ventilation

Since people create plumes due to their convective heat air in the breathing zone will be of higher quality than the ambient air at the same height. This can be seen in figure 2.3 adapted from Sandberg [8].

The y-axis shows the relationship between the CO_2 -concentration of air in the breathing zone and the CO_2 -concentration of the air in the ambient. The x-axis shows how this ratio varies for different airflow rates. The study is valid for displacement ventilation. As an example, we see that if we ventilate with supply flow rate $Q_i = 10 \text{ l/(s-person)}$ the concentration of the air in the breathing zone will be approximately 5 times lower than in the ambient. A similar study is done by Mattsson and Sandberg [9] using a movable dummy. The results show that even though the dummy is moving, the concentration in the breathing zone is much lower than in the ambient. This is of importance in the design of displacement ventilation since one can accept the stratification line to be somewhat lower than the zone of occupancy. The experiments might also be related to active displacement ventilation, but for active displacement ventilation, the CO_2 -concentration in the lower zone will normally be higher.

Other studies show similar results. Xing et al. [10] concluded that "the perceived air quality (represented by the mean age of air) for a seated mannequin in a room ventilated using displacement systems was between 35 % and 50 % better than the average air quality in the occupied zone. This difference depends on the type of air terminal device (DV unit) which is used for supplying the air". These values correspond with figure 2.3 for supply flow rate

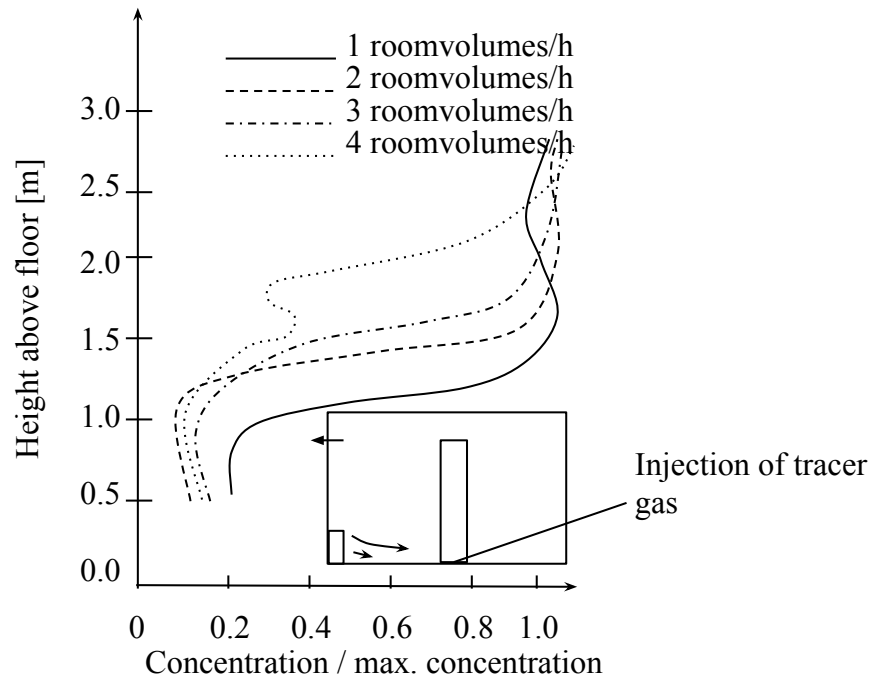


Figure 2.4: Concentration of CO_2 in a room with a single source. Figure is adapted from Sandberg [8, p.452]

between approximately 6 and 8 l/(s·person).

The two zone model is a good approximation when calculating the CO_2 -concentration in a room. The concentrations can be calculated using a mass balance of CO_2 -sources and CO_2 -sinks, and the airflows generated from the flow elements. The reason that applying the two-zone model for calculations of the CO_2 -concentration is possible is that there will be a defined stratification line for the two zones. Studies are done with tracer gas show this. One of the studies is done by Heiselberg and Sandberg [11], and the results can be seen in figure 2.4.

This experiment is done using a heated cylinder with tracer gas to simulate the movement and concentration of CO_2 . The results show how the CO_2 concentration suddenly changes at a certain height above the floor, and that the two zone model is a good approximation. As an example, one see that for an air exchange rate of 1 room-volumes/h the relative concentration will shift from approximately 0.2 concentration/max.concentration to 1 concentration/max.concentration between 0.5 m and 1.5 m height above the floor. The stratification height will be within this range.

2.2.1.3 Temperature in rooms with displacement ventilation

The temperature distribution does not correspond to the two zone approximation as good as for the CO_2 -concentration. The temperature and contaminants have in common that their quantities can be transported due to diffusion and convection. If these two transport

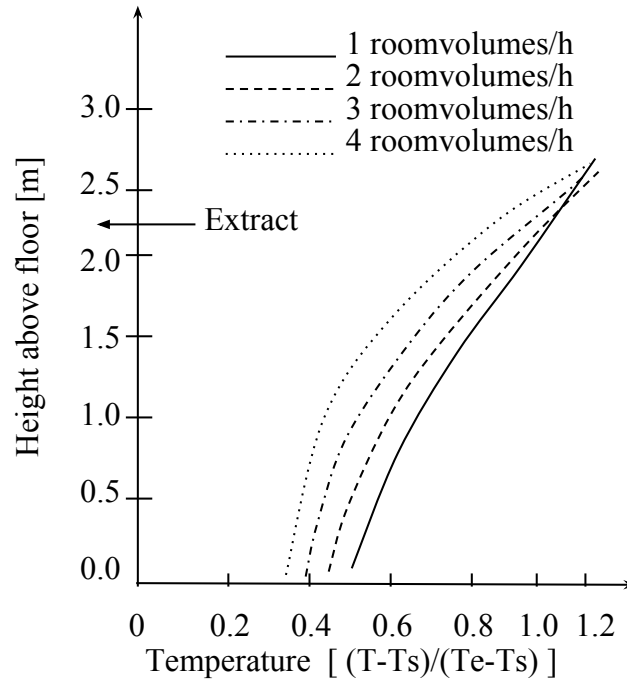


Figure 2.5: Temperature distribution in a room with one heat source. Adapted from Sandberg [8, p.453]

mechanisms where the only mechanisms for the temperature distribution, the two zone model would be suitable. However, temperature, or heat, is transported due to another mechanism in addition to these, namely radiation. Radiation is the reason for the gradual increase of temperature with the height as it is not affected by the flow pattern in the room. Figure 2.5 shows the temperature distribution in a room with one heat source for the same experiment as presented for the contaminant distribution in section 2.2.1.2.

In a paper by Mundt [12] the conclusion is that the temperature gradient in the room is dependent on ventilation rate and not so much on the position of heat sources, and that the gradient can be approximated to be linear. A typical approximation is known as the "50 %-rule", and is described by, among others, Nilsson [5]. The technique says that half of the temperature rise from supply air to exhaust air occurs at the floor, i.e. $T_f = 0.5 \cdot (T_e - T_s)$, and that the temperature in the vertical direction increases linearly to the exhaust temperature at $h = H$. Here T_f , T_e and T_s are the floor temperature, exhaust temperature and supply temperature respectively, and H is the height of the room. Figure 2.5 correspond well as the floor temperature, $T_f = \frac{T_f - T_s}{T_e - T_s} \approx 0.5$.

2.2.2 Mixing ventilation

Mixing ventilation is a somewhat simpler concept than displacement ventilation. As mentioned in section 2.2 the principle of mixing ventilation is simply to mix the air so that both the temperature and contaminant concentration is homogeneous. Air is supplied with high velocity in order to mix with a large amount of air [5, chp. 4]. Figure 2.6 shows

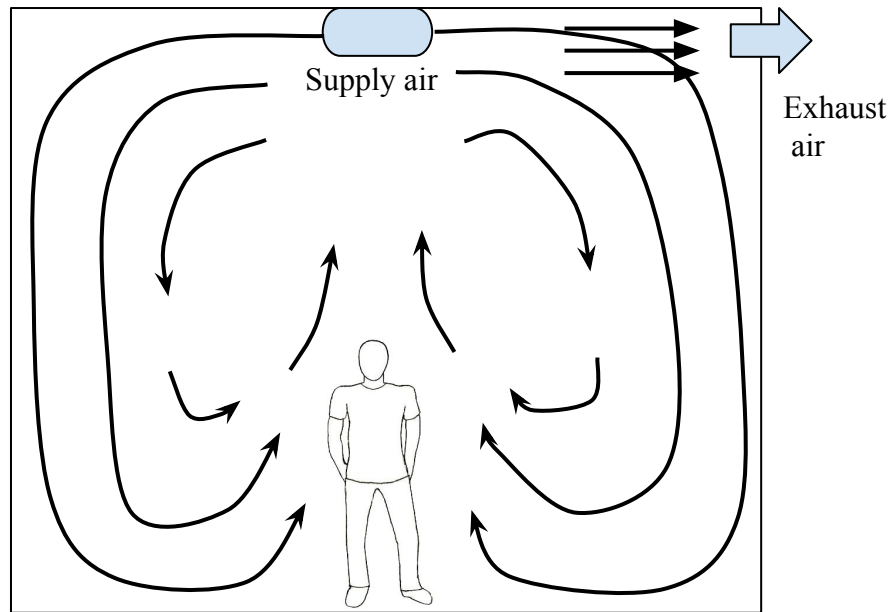


Figure 2.6: Principle sketch of mixing ventilation

a simplified sketch of how mixing ventilation is applied. To avoid draught for mixing ventilation, the throw length $L_{U_{max}}$ (depending on the draught requirement) must be less or equal to the distance from the diffuser to the occupied zone. The throw length is simply defined as the length of where the velocity has decreased to a certain level indicated by the subscript. Mixing ventilation is typically compared to other methods of supply by the use of ventilation indices. Ventilation indices will be presented in section 2.5.5.

2.3 Building integrated ventilation

Before going more deeply into active displacement ventilation the concept of building integrated ventilation will be presented. Building integrated ventilation is when a building is constructed and designed in way that facilitates for air movement due to the nature's natural forces. In other words, the goal is to make the indoor environment interact with the outdoor environment when it is beneficial. In most cases of building integrated ventilation hybrid ventilation is applied [13, 14].

The term hybrid ventilation is important in the understanding of building integrated ventilation. Hybrid ventilation can simply be defined as a method combining both elements from natural and mechanical ventilation. Natural ventilation uses only natural forces such as wind and temperature differences to drive the air, while mechanical ventilation uses mechanical forces such as pumps and fans driven by electrical power. The goal for hybrid ventilation is to take the best sides of each of these two methods. Fans are used as in mechanical ventilation, but since natural forces and smart architecture is used as a

supplement, low fan power is often required.

The need for fan power is reduced due to two main factors. These are low-pressure losses in the system and the contribution of natural driving forces. How much these two factors contribute to the reduced fan power is very unevenly distributed. Approximately 99 % of the saved fan energy in a building integrated system is due to reduced pressure losses in the system, while approximately 1 % is due to the contribution of natural driving forces. This means that it is essential to have low pressure losses to make a hybrid system work if low fan power is desirable [13, p.8]. For systems with higher pressure losses, the natural driving forces will be negligible.

Since there are many ways of applying building integrated ventilation, a categorization is done by investigating how dependent the building is of natural driving forces. They are classified from most to least equal the principle of natural ventilation, and they are named the Swedish, Danish, German, Norwegian and Finnish model respectively. This is illustrated below. The Swedish model will be discussed more in detail since buildings built after this principle is most relevant for active displacement ventilation.



2.3.1 The Swedish model

The Swedish model is a fan assisted version of natural ventilation where active displacement ventilation is used. It came to Norway after it became popular in Sweden, and today several Norwegian schools are built after this principle. Examples are Gjerde Barneskule, Frei barneskole, Jaer barneskole and Kjeldsås skole.

The Swedish model is a temperature controlled concept where the airflow rate depends on the outdoor temperature and not the indoor CO_2 -concentration. The airflow rate is typically controlled with a demand controlled ventilation system (DCV) by throttling the air. It is no heat exchange of exhaust air or heating coils installed. This means that the inlet air temperature is strongly dependent on the outside temperature.

For the winter season higher indoor CO_2 concentrations are expected. Low outdoor temperatures mean one must decrease the airflow rate to ensure acceptable indoor temperatures and thermal comfort. Floor heating, or other heating equipment, is, of course, an alternative, but the heating demand and energy cost would increase drastically if high quantities of cold air were supplied. In addition to the economical aspect, cold draught can occur if air with low temperature is supplied.

The concept of the Swedish model is illustrated in Figure 2.7. There are three main ways of supplying air to the building for this model. These are:

- Air supplied through a culvert (A)

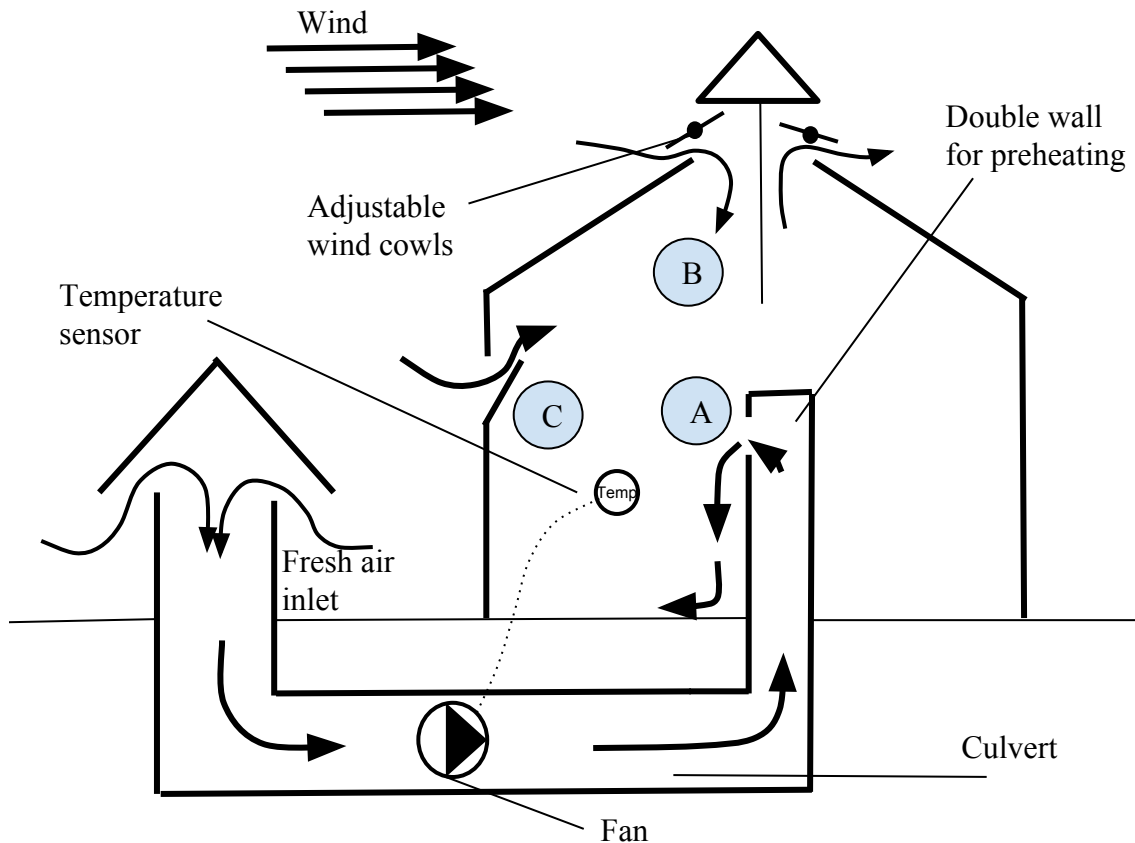


Figure 2.7: Schematic of the principles of the Swedish model. Figure adapted from Andersson and Gillbro [15]

- Air supplied through a chimney / air cowl (B)
- Air supplied through windows (C)

Air is passed through a culvert and a double wall where it is preheated or precooled depending on the outdoor temperature and season of the year. The heating/ cooling of the air in the culvert is due to the concept of thermal inertia. For winter season there will be a preheating, while it in the summer season will be a precooling. The double wall illustrated in the figure at inlet A exchanges heat between the room and the fresh air.

Several driving forces work together. Convective heat sources in the building ensure a buoyant flow, and creates, together with the wind, the fan, and the stack effect, the necessary force to drive the air through the building. The fan will only be used when the other driving forces do not fulfill the required flow rate to ensure an acceptable indoor environment.

All the three supply methods will not be present at all times of the year. Supplying air through windows and the air cowl is not done for low outside temperatures since this air is not preheated and would result in thermal discomfort and cold draught. Therefore, the only supply method for the winter season is through the culvert. Also for the culvert, throttling is necessary since the air is not sufficiently heated. This is illustrated in figure 2.8 where we see how the air change rate in the building decreases for lower outside temperatures. For higher outdoor temperatures the air change increases, and lower indoor CO_2 concentrations are

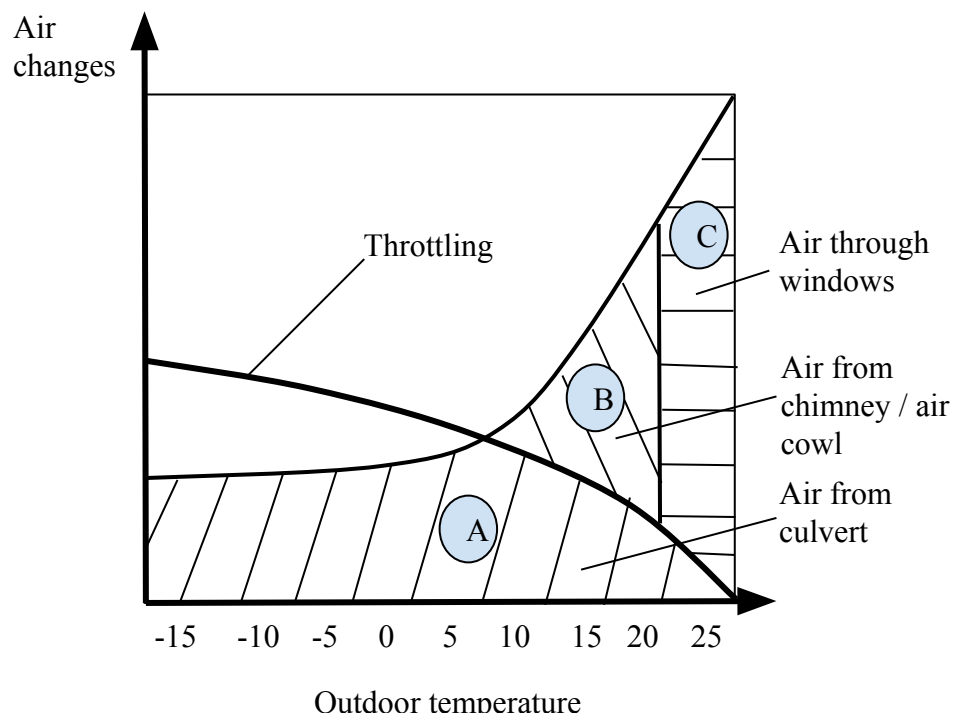


Figure 2.8: Driving forces for different outdoor temperatures. Figure adapted from [15]

expected.

Two of the first Swedish schools built after this concept was Fredkullaskolan and Riesbergsskolan. A description of these is given in the article *Fredkulla- och Riesbergsskolan - två av många moderna självdragsskolor* by Andersson and Gillbro [15] where a detailed study of the function of the schools where given.

Measurements of the atmospheric environment is done in Fredkullaskolan where the outdoor temperature increased from 1°C at 8:00am to 7°C at 1:00pm. In this case opening the window did not make sufficient influence on the thermal environment, and the temperature was held at 19°C even though the windows had to be opened 25% of the time to maintain a sufficient atmospheric environment. No studies for lower temperatures where presented in the article.

In the case of temperatures below 0°C the inlet air through the culvert should be preheated to avoid the water system in the building that is in contact with the culvert to freeze. A run-around heat exchanger and/or an electrical heating coil are both solutions that would contribute to the necessary heating demand for very cold days when the heat from the culvert is not sufficient.

2.4 Active displacement ventilation

Active displacement ventilation is an air supply method well suited for ventilating, cooling and in special cases heating. It is, among others, described in an article published by Elforsk in Danmark called *Energioptimering af procesventilation og udvikling af fleksible procesudsug til store industrielle emner* [16]. The term used is "active *thermal* displacement ventilation" and is characterized by a flow pattern in both positive and negative vertical direction as indicated in figure 2.9.

The diffusers, or terminal devices, are located high on the wall and are constructed so that air flows downwards and entrains old room air. The supplied air has a temperature lower than the room air in addition to low supply velocity. Thermal forces will make the air "fall" down towards the floor. Heat sources are treated as in ordinary displacement ventilation where the contaminants are transported to the polluted zone in the higher part of the room due to the convective flows. The supplied air has, as for ordinary displacement ventilation, the purpose of replacing old air with new air, and maintain the polluted zone outside the occupied zone. The idea of active displacement ventilation is that one can achieve an acceptable indoor climate by supplying air with a lower temperature than ordinary displacement ventilation. It will also be a goal to supply air with lower flow rate.

Supplying less air than for ordinary displacement ventilation can be obtained since the stratification line can be held at the same height for a lower amount of supply air. This can be seen from a mass balance where the entrained air contributes to the height of the stratification line. One must, on the other hand, be aware of a higher concentration of CO_2 in the lower zone.

One important concept for active displacement ventilation is the fact that jets will stick to the wall due to the Coanda effect. The Coanda effect is the tendency of a fluid to attach to a surface due to a lower pressure on the wall side. The pressure drop occurs when the air is entrained from the surroundings. For horizontal jets supplied close to the ceiling, the jet will stay attached to the wall as long as the attachment force is larger than the gravitational force.

If there is a need for heating in the room, the diffusers can guide air towards the heat sources in order to counteract the convective flows. This will cause warm air to stay in the occupied zone. This is only desirable if the convective airflow is clean and does not influence the atmospheric environment negatively.

In the design of active displacement ventilation, one must also be aware of discomfort due to cold draught since the cold air can fall at velocities over the recommended values. A typical solution is designing the room in a way that ensures the cold draught to fall down in an area where people are not normally present.

Ventilasjonsteknisk håndbok by Eimund Skåret [1] describes active displacement ventilation as a special case of "top-down" ventilation for rooms with sharply rising temperatures. It is described how the amount of fresh air supplied to maintain the stratification line at a certain level decreases for lower inlet air temperatures. This happens since the cold supply air will entrain more air than warm air will. In the design of active displacement ventilation, it is

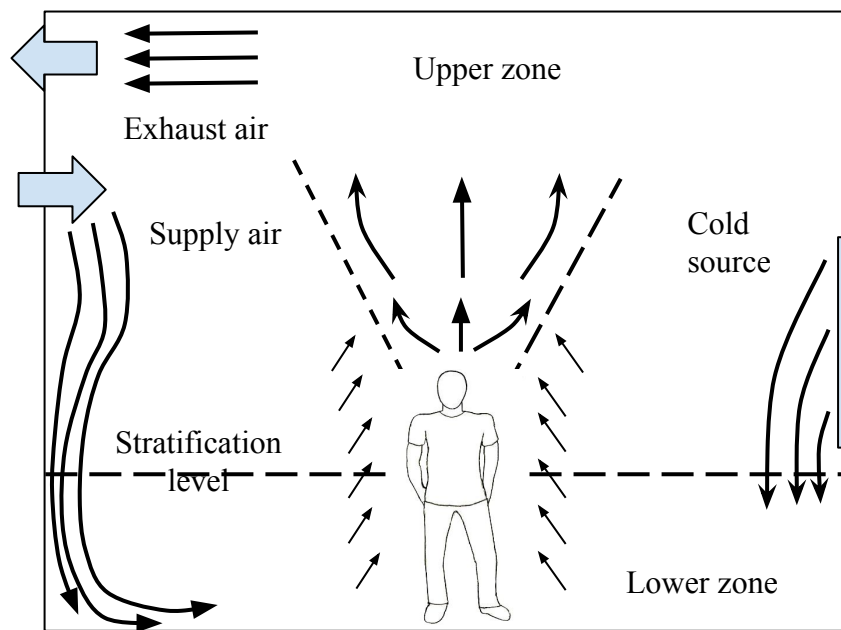


Figure 2.9: Sketch of active displacement ventilation

important to keep in mind that the supply air has the opposite direction of the convective plumes generated from heat sources and that the diffusers should not be an obstacle for the convective flows.

2.4.1 Active displacement ventilation in the industry

In this section, active displacement ventilation in industry buildings will be discussed. The way it is used in the industry might differ from other applications. Even though no design of active displacement ventilation for industrial buildings will be done in this thesis, the section is included to give a deeper insight to the application of the supply method.

2.4.1.1 Thermal and atmospheric zones

In industry buildings, the indoor climate must meet the requirements for both industrial processes as well as for persons working in the building. The requirement for the atmospheric and thermal environment will vary for different activities and processes. Smell, dust, fibers, gasses and steam are typical factors that will affect a person's perception of the indoor climate, and processes might have different requirements for the cleanness of the air. For example, machines with electrical equipment might require lower temperatures and cleaner air in order to remove heat and avoid damages.

Rooms are therefore typically divided into zones. The two zone model is already presented

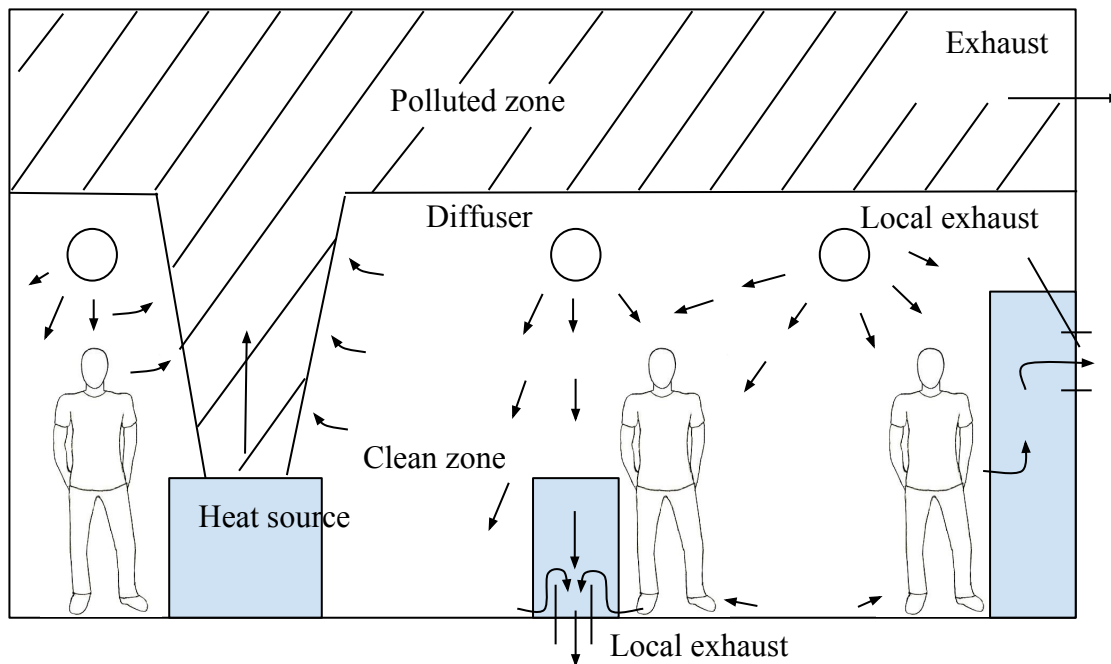


Figure 2.10: Sketch of active displacement ventilation in the industry. The figure is adapted from Sørensen [18]

in section 2.2.1, but one might also divide a room into more than two zones. One often divide the total zone, which is the whole room, into controlled and uncontrolled zones. Controlled zones are typically occupancy zones, working zones or other zones where there are requirements for thermal and atmospheric environment. The uncontrolled zones are zones where there is no requirements. Theory from the design guidebook *Industrial Ventilation* edited by Goodfellow and Tahti [17] is used for this description.

2.4.1.2 Design and function

In *Håndbog i industri ventilation* by Sørensen [18] active displacement ventilation in the industry is explained. Also here the term "active thermal displacement ventilation" is used. The principle is described as very effective in both removing heat and contaminants. A simple sketch of how active displacement can be applied in the industry is given in figure 2.10.

The figure needs some comments as many ventilation techniques are applied at the same time. Local ventilation is applied where jets are pointed directly on occupants and machines. The person to the left uses a machine generating heat. This is seen from the convective plume generated. Air is entrained to the upper zone. The second and third person use machines that do not generate heat. The machines do, on the other hand, generate some particles that are unhealthy for the occupants. The particles are therefore led directly to exhaust channels on the floor and wall respectively. The clean zone is in the lower zone at which the occupants are present.

The technique of active displacement ventilation is also applied for the automotive industry [19] and inside aircrafts [20]. The descriptions of these two applications correspond to how active displacement ventilation is described in this section.

2.4.2 Active displacement ventilation in school buildings

The principle of active displacement ventilation is also applied in school buildings and classrooms. Air is then supplied thorough plate diffusers, fabric ducts or other inlet air devices with low inlet velocity. There is no need for local ventilation as for industrial buildings. Active displacement ventilation is found in classrooms in Norway where the Swedish model, introduced in section 2.3.1, is applied. It is important to emphasize that active displacement ventilation also can be applied for other building types than buildings built after the Swedish model even though no examples are presented.

There are some factors that are important to be aware of in the design of active displacement ventilation in classrooms, and some are already mentioned. The following list summarize these factors.

- Cold draught from supply diffusers might be a problem. The diffusers should be placed so that the cold draught does not enter the zone of occupancy.
- High CO_2 -concentrations in the occupancy zone might occur. This will especially be the case if the supply air is not heated sufficiently and the airflow rate is limited by the thermal environment. Heating the room otherwise is needed if a large amount of cold air is supplied
- Sudden load change in classrooms can cause difficulties for the function. High ceilings are often suggested to create a buffer for the case of where the problem is transient.
- Air flow from flow elements go in different directions, so care must be taken in the design to avoid undesirable interaction of the different flow elements.
- The height and inlet airflow of the diffusers have a large influence on the atmospheric and thermal environment in the occupancy zone

2.5 Flows in rooms and empirical relations

It can be hard to predict the air flow pattern in a room. We can say that we have a problem where everything is dependent on everything as described in Building Ventilation by Etheridge and Sandberg [21, Chap. 8]. In most cases, the flow in a room is three dimensional. This means that the velocity vectors have components in both x-,y- and z-direction, and analytical solutions for describing the flow are hard to achieve. Examples of parameters affecting the flow in a room are inlet conditions at diffusers, the geometry of the diffusers, the geometry of room, location of diffusers, location of exhaust, furnitures, moving objects, temperature differences in supply air, heating of the room, radiation, and wall materials causing variation in surface temperatures. In this section theory used in the design of ventilation in rooms and validation of the CFD results will be presented.

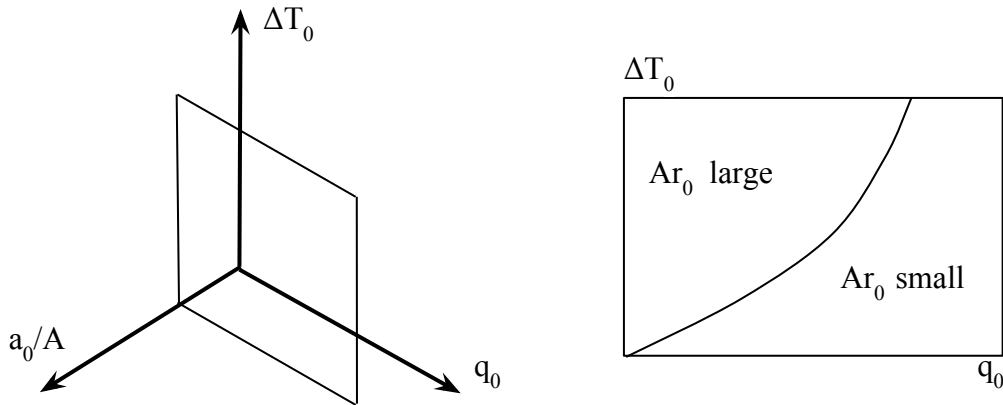


Figure 2.11: $q_0 - \Delta T_0$ - chart. Figure is adapted from Nielsen [22]

2.5.1 Archimedes number

Dimensionless numbers are formed when governing fluid mechanical equations are nondimensionalized. The numbers are used when different systems are compared, and they tell us how a system will behave. They make it easier to solve a problem and to predict the outcome of the initial and boundary conditions. The Reynolds number is a well-known dimensionless number in fluid mechanics and is defined as $Re = UL/\nu$ where U is the fluid velocity, L is the characteristic length and ν is the kinematic viscosity.

The Archimedes number is a measure of the relative magnitude of the buoyant and inertial forces acting on a fluid element [21]. When performing experiments in small scale models it is important to make sure that the Archimedes number is the same as in the real scenario. Unless the experiment will not be scalable. For a jet, one distinguishes between the local Archimedes number Ar_x and the nominal Archimedes number at the inlet opening Ar_0 . The general definition of the Archimedes number is here given as Ar .

$$Ar = \frac{gl\beta\Delta T}{U^2} \quad (2.1)$$

$$Ar_x = \frac{gb\beta\Delta T_m}{U_m^2} \quad (2.2)$$

$$Ar_0 = \frac{gl_0\beta\Delta T_0}{U_0^2} \quad (2.3)$$

In the equations, l and b are the characteristic length given as the width of the jet for Ar_x , and as the inlet diameter l_0 for Ar_0 [1]. ΔT , β , g , and U are the temperature difference between the centerline and ambient, the thermal expansion coefficient, gravitational constant and velocity respectively. The indices m and 0 stands for maximum local and initial.

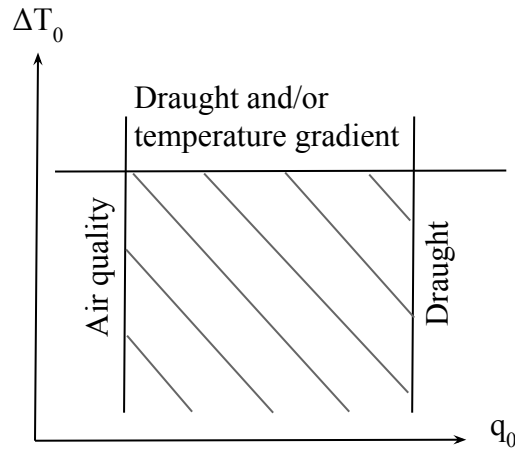


Figure 2.12: $q_0 - \Delta T_0$ - chart indicating restrictions on the flow rate and temperature difference ΔT_0 Figure is adapted from Nielsen [22]

2.5.2 Comparing supply methods using $q_0 - \Delta T_0$ - charts

Comparing supply methods can be done in many ways. In the article "The Family Tree of Air Distribution" by P.V. Nielsen [22] the flow in a room is divided into the following primary variables which is used for a categorization of different supply methods:

- Cooling mode or heating mode
- Archimedes number $\Delta T_0/q_0^2$, or flow rate of air supplied to the room, q_0 and the temperature difference between return and supply air, ΔT_0
- The ratio between the total area of the supply openings and the wall area, a_0/A
- Location, high or low, of the supply opening(s)

So-called $q_0 - \Delta T_0$ - charts are used for the comparison, where each chart has its ratio a_0/A . The ratio a_0/A is typically low for mixing ventilation since high momentum forces are required, while it is high for ordinary and active displacement ventilation. The charts define the combination of q_0 and ΔT_0 that fulfills thermal comfort and is illustrated in figure 2.11.

The upper limit for the flow rate, q_0 , is typically limited by draught in the occupancy zone, while the lower limit is limited by the air quality. For mixing ventilation Nielsen et al. [23] suggested an upper limit of 18 l/(s-person) to avoid draught for a typical office situation for a specific diffuser (Annex 20). For complete mixing ventilation one assumes constant CO_2 -concentration in the entire room, but obtaining complete mixing is not easy for low flow rates. Therefore, a lower limitation is that the penetration length should be larger than half the room, i.e. $x_s/L > 0.5$ [23]. Another lower limitation could be to follow Norwegian standards (see A.1) and use 7 l/(s-person) as the lower flow rate limit. The temperature also has its restrictions. A lower limit of $\Delta T_0 = 12.5^\circ C$ is suggested for mixing ventilation [23]. The upper lower limit of ΔT_0 for complete mixing ventilation is given by a heat balance of the room. A simple illustration of the restrictions on the flow rate and temperature difference is given in figure 2.12

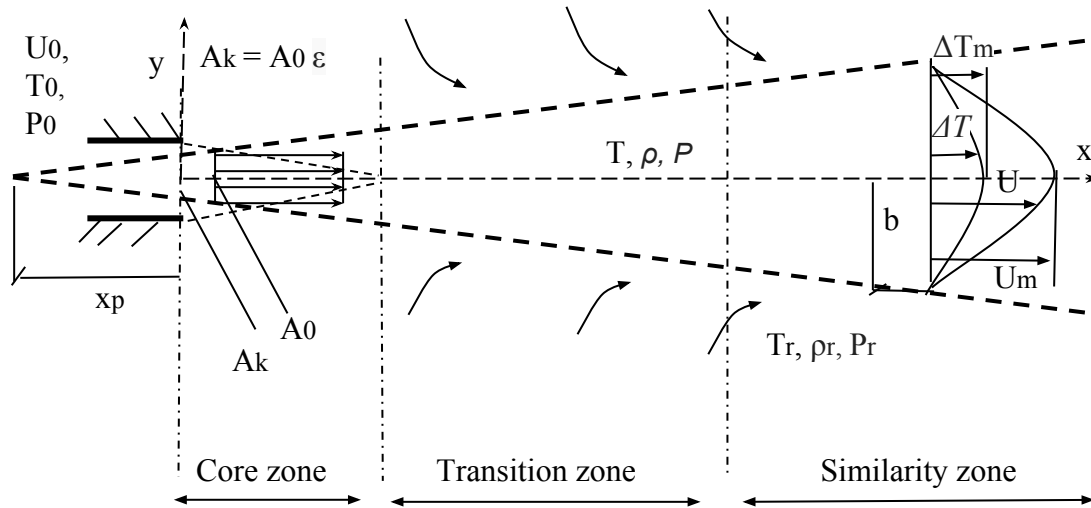


Figure 2.13: The zones of a jet and indication of important symbols in jet calculations. Figure is adapted from [1]

2.5.3 Flow elements in rooms

A room might be divided into flow elements where each element can be treated independently [24]. It is possible to divide these elements into isothermal flow, non-isothermal flow and buoyant flow. In this section empirical relations for jets and plumes will be introduced. The fundament for the empirical relation presented in this chapter is the momentum equation, the continuity equation, and the energy equation. Derivations of the relations will not be done in this thesis.

Jets and plumes are characterized by its self-preservation character giving the velocity and temperature profile a characteristic shape after it is developed. An isothermal jet can, as described by Malmström et al. [25], be divided into a core zone, a transition zone and profile similarity zone. In the core zone, the velocity is equal to the inlet velocity. In the transition zone the centerline velocity starts to decrease, and in the profile similarity zone the relative velocity profile is the same for all distances from the inlet. The same principle yields for non-isothermal jets, but here the profile will depend on whether the jet is positive or negatively buoyant. The similarity zone is the zone where the empirical relations presented in this section are valid. Typically, the region is expected to start between 6 and 10 diameters from the inlet [1]. Awbi [26] describes the similarity region, also called the axisymmetric decay region, as a region dominated by a highly turbulent flow generated from viscous shear at the edge of the shear layer. Figure 2.13 illustrates the zones.

Abramovich [27] suggested the following relations between the maximum velocity, U_m , and the velocity U , at a distance y from the centerline for a jet with width b . He also suggested a relation between the temperature difference at the centerline ΔT_m and the temperature

difference ΔT at a distance b from the centerline. Both relations are for the similarity zone.

$$\frac{U}{U_m} = \left(1 - \left(\frac{y}{b}\right)^{1.5}\right)^2 \quad (2.4)$$

$$\frac{\Delta T}{\Delta T_m} = \left(\frac{U}{U_m}\right)^{1/2} \quad (2.5)$$

2.5.3.1 Isothermal jets

Isothermal jets are jets where the inlet air temperature equals the ambient temperature. For a free isothermal jet, the momentum over the cross section is constant. For buoyant jets, this will not be valid because of the buoyant forces. A schematic illustration of an isothermal jet is presented in figure 2.13. The jet area increases with x as air is entrained into the jet. The jet width, $b(x)$, is given by the angle of the jet and the pole distance x_p which is the distance from the jet opening to the point where the boarder lines of the profile meet. P and ρ are the pressure and density respectively.

The half angle α of the jet is normally suggested to have a value between 10° and 13° [28]. 12.5° was suggested by Awbi [26]. The momentum factor i describes the momentum losses, while ϵ is the contraction coefficient describing the relation between the inlet flow area and the light opening.

Empirical relations for isothermal jets given by Skåret [1] is given in equation 2.6 and 2.7.

$$\frac{U_m}{U_0} = \left(\frac{\rho_0 i A_0}{\rho_r \epsilon A_s I_4}\right)^{1/2} \quad (2.6)$$

$$\frac{Q_v}{Q_0} = \frac{U_m A_s I_2}{U_0 A_0} \quad (2.7)$$

I_2 and I_4 are integration constants, and are solutions of the integral $\int_0^1 \left(1 - \left(\frac{y}{b}\right)^{1.5}\right)^n \frac{dA}{A_s}$ for different n . The integral constants arises from equation 2.4 and 2.5 and is different for plane symmetric and rotational symmetric flow. The integration constants are listed in appendix A.3. The densities ρ_0 and ρ_r are the density of the air in the room and the inlet respectively. A_0 and A_s describes the area of the jet opening and the area of the jet at a distance y from the inlet. A_s is calculated from the relation

$$A_s = \pi b^2 = \pi (\tan \alpha (x + x_p))^2 \quad (2.8)$$

where α is the half jet angle, x is the distance from the inlet and x_p is the pole distance. The pole distance can be hard to predict, and will be given some attention later in the thesis.

2.5.3.2 Non-isothermal jets

Non-isothermal jets, or buoyant jets, are jets where the inlet temperatures differs from the ambient temperature. This means that both momentum and thermal forces will influence the jet. Buoyant jets where the thermal forces act in the direction of the flow (positive

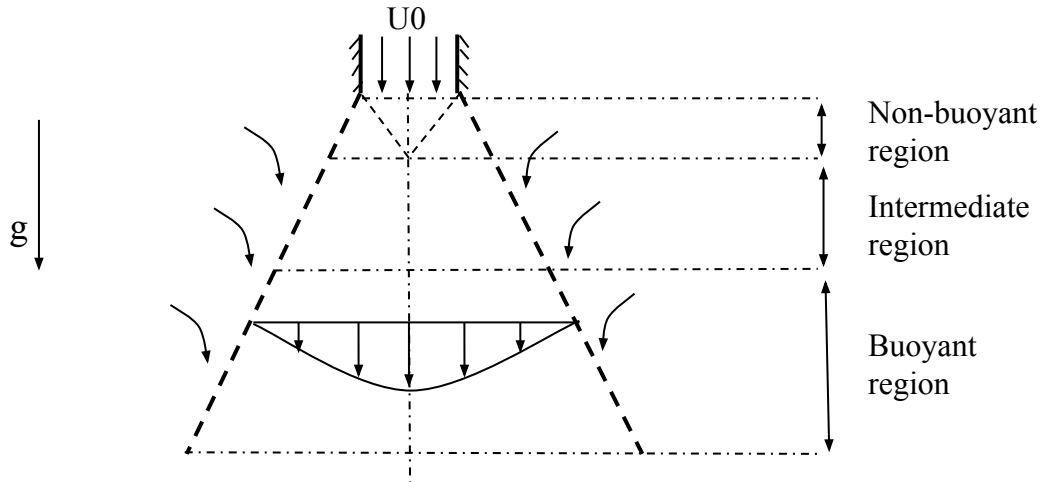


Figure 2.14: Schematic view of a vertical buoyant jet structure

archimedes number) are typically called positive buoyant. This happens if air with an under-temperature is supplied for a downward pointing jet, or if air with over-temperature is supplied for an upward pointing jet. For the contrary case the flow is called negative buoyant. The buoyant jet is typically divided into three regions as seen in figure 2.14. The first region is the non-buoyant region where the momentum forces are dominating. The next region is the intermediate region where both the momentum and buoyant forces are of importance. The last region is the buoyant region where the momentum forces are negligible compared to the buoyant forces. A publication by Guangyu [29] is used for this description of non-isothermal jets.

Empirical relations for the velocity, the air flow rate and the change in centerline temperature for a buoyant jet is given by Skåret [1] and is presented in equation 2.9, 2.10 and 2.11 respectively. These relations are for vertical jets with no influence from walls. The amount of entrained air increases with the distance from the inlet.

$$\frac{U_m}{U_0} = \left(Ar_0 \frac{\rho_0}{\rho_r} \frac{4.3}{C_b^2} \frac{\sqrt{A_0}}{y + y_p} \pm \left(\sqrt{\frac{\rho_0 i}{\rho_r \epsilon}} \frac{1.54}{C_b} \frac{\sqrt{A_0}}{y + y_p} \right)^3 \right)^{1/3} \quad (2.9)$$

$$\frac{Q_v}{Q_0} = \frac{U_m A_s I_2}{U_0 A_0} \quad (2.10)$$

$$\frac{\Delta T_m}{\Delta T_0} = \frac{\rho_0}{\rho_r} \frac{U_0 A_0}{U_m A_s I_3} \quad (2.11)$$

The " \pm "-sign depends on whether the jet is positive or negative buoyant. C_b is defined as $\tan(\alpha)$, and x_p is here replaced with y_p since we now look on a vertical jet.

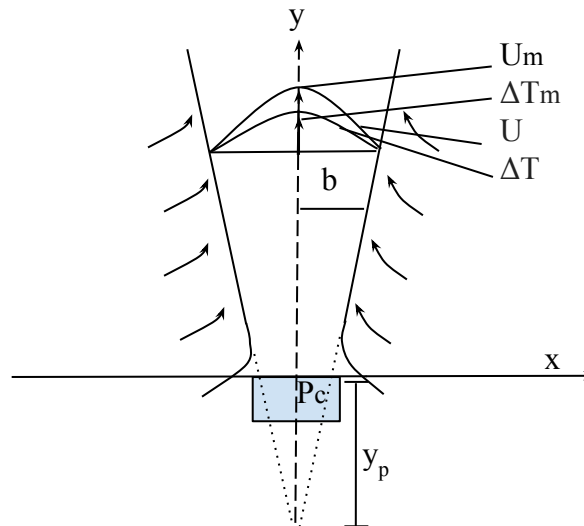


Figure 2.15: Heat source generating thermal convective flow. Figure is adapted from [1]

2.5.3.3 Buoyant flow

An important principle in the design of ventilation is to understand how heat sources generate convective plumes. Sources of thermal convective flows in classrooms and offices are typically people, office equipment, windows, walls that are not insulated properly, heating and cooling equipment, lighting and equipment/ machines in the process industry.

Empirical relations for flows over a point source it used to predict the flow over warm and cold elements in a room. Relations for line sources also exist, but will not be introduced here. The point source creates a circular flow. For a heat source generating a convective power P_c , given in kW, maximum velocity, the air flow rate and maximum temperature difference can be found from the empirical relations in equation 2.12, 2.13 and 2.14 respectively [1]. Figure 2.15 illustrates the thermal convective flow from a heat source where the velocity and temperature profile is shown.

$$U_m = \frac{1.63}{C_b^{2/3}} \left(\frac{g\beta}{\rho c_p} \right)^{1/3} \left(\frac{P_c}{y + y_p} \right)^{1/3} \quad (2.12)$$

$$Q_v = 1.31 C_b^{4/3} P_c^{1/3} (y + y_p)^{5/3} \quad (2.13)$$

$$\Delta T_m = 20.9 \cdot P_c^{2/3} \cdot (y + y_p)^{-5/3} \quad (2.14)$$

The value of y_p can be hard to predict. Skistad [30] suggested a maximum case and a minimum case. The maximum case was when the border of the plume passed through the source. This corresponds to $y_p \approx 2.25d_0$. This can be assumed for low-temperature sources. For high-temperature sources he suggested $y_p \approx 0.8d_0$. Skåret [1] suggest $0.7d_0$ for high-temperature sources. For jets, the inlet air device will have a large impact on the pole distance.

2.5.3.4 Convective plume over a person

The velocity and air flow over a person are important to calculate in order to predict the air flow pattern in a room. One important factor is the convective heat from the person. The more convective heat from the person, the higher air flow rate is generated. The activity level, clothing level, and physiological characteristics are some of them. Typically, the convective heat from a person is 50 W, but the value will vary. Table A.3 in appendix A.2 shows how the convective heat varies with the activity level, clothing, and temperature. With this variation, it is obvious that the choice of activity level, clothing, and indoor temperature will give significant differences when estimating the convective plumes.

People come in different sizes and shapes, and this will affect the convective plumes. When doing the estimation of the plumes, one typically chooses values for an average person. Many studies exist on this topic. Typical values for the average height of Norwegian males and females are 1.8 m and 1.67 m respectively [31] giving an average height $h_{avg} = 1.73$ m. A typical value for the surface area of a person are $A_{per} = 1.8$ m² [32]. It is also developed empirical equations for calculating the surface area of a person. One of them is $A_{per} \approx 0.2 m^{0.425} \cdot h^{0.725}$ where m and h are mass and height of the person respectively [33]. In the calculations of convective plumes, the geometry of the person must be simplified. Examples of simplifications are designing the body as a cylinder or estimating the person as a point and/or a line source.

Another factor that is important in the calculations of the convective plumes is the height at where people are sitting. The lower the person is sitting, the higher the generated airflow becomes at a given point over the floor since the plume has more time to develop and entrain air from the ambient. For a classroom, a reasonable assumption is that everyone is sitting still. Therefore this parameter is important. Heights between 1.1 m and 1.3 m are normal to use.

The values for the plumes are uncertain and will vary. Steensaas [28] suggested that typical values for convective plumes for normal air conditions for a sitting person are 10-12 l/s 1.2 m over the floor, and 20-30 l/s 1.8 m over the floor. Other references suggest other values. Sørensen [18] suggest that one may expect 15-20 l/s for a seated person 1.1 m over the floor, and 40-50 l/s 1.8 m over a seated person.

Dokka and Tjelflaat [34] did a study on this topic where the person was modeled as a cylinder, and the model was compared to experimental data. The cylinder that was studied was 1 m high and had a surface area 1.38 m². If the stratification line was below the height of the person it was assumed that flow due to free convection would be the best way of modeling the air flow. For the transition region between free convection and plume flow, the largest of the calculated values was chosen. The simplified model for the human-induced convective flow rate used by Dokka and Tjelflaat [34] is presented in equation 2.15 and 2.16 where $a \approx 1.9$ where suggested.

$$Q_{plume} = 6.0 \cdot (P_{per})^{1/3} (z - h_{per} + a \cdot d_{per})^{5/3} \quad (2.15)$$

$$Q_{b.l} = 8.61 \left(\frac{P_{per}}{A_{per}} \right)^{0.3} z^{1.2} d_{per} \quad (2.16)$$

Q is the airflow rate, P_{per} is the power, both convective and radiative, generated by the

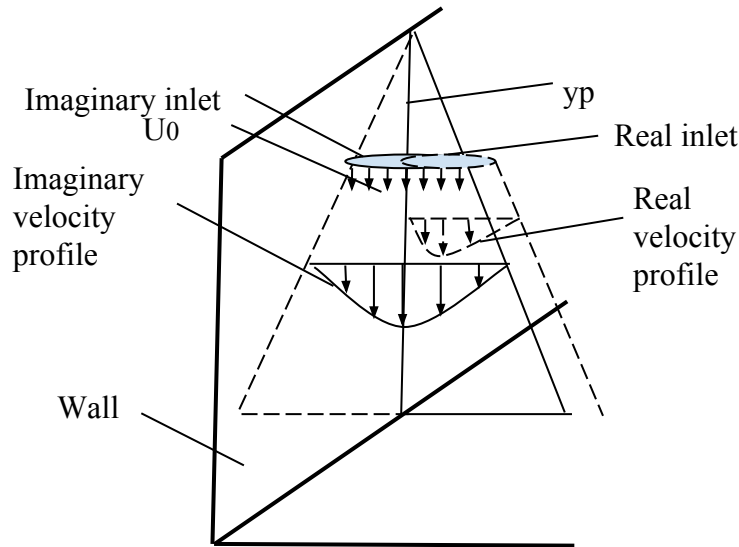


Figure 2.16: Method of calculating flow along wall with empirical relations

person, z is the distance from the floor and h_{per} is the height of the person. The model was compared to experimental data by Kofoed [35] and a gradient model by Mundt [36], and shows that choosing a value for a between 1.7 and 2.5 can give realistic results.

2.5.4 Vertical jet supplied by wall

Inlet air diffusers are often placed close to walls, and a boundary layer is created as air flows along the wall. According to Skåret [1], the maximum velocity of a wall jet is approximately equal to the maximum velocity for a free jet since the friction is almost negligible.

A typical simplification for calculating the velocity, flow and temperature difference is assuming an imaginary inlet area $A_{imaginary} = 2A_{real}$, with an imaginary airflow, $Q_{imaginary} = 2Q_{real}$, where the wall divides the flow in two equal parts. The wall is assumed not to affect the flow, and friction and the boundary layer is neglected. A schematic sketch is seen in figure 2.16.

Calculations are done as for a free jet, except for that the flow must be corrected in the end by dividing it on two. The velocity U_m and temperature difference ΔT_m is the same for the imaginary flow as for the real flow. The same argument is used for point sources, where the power source P_c must be multiplied with two. The fact that friction is not taken into consideration means that the calculated maximum velocities and the airflow might be higher than in reality.

The line of maximum velocity for a wall jet will, due to the displacement thickness, slowly move away from the wall. When a fluid at velocity U shear against a no-slip wall the velocity will show a smooth drop-off to zero at the wall. To satisfy the conservation of mass, the streamlines must be deflected away. The displacement thickness is defined as the distance the streamlines outside the boundary-layer δ , defined as the height $\delta_{99\%}$ where $u(y) = 0.99U$,

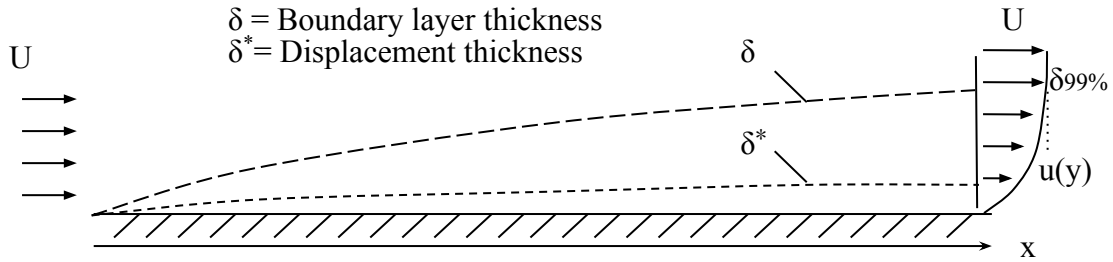


Figure 2.17: Illustration of displacement thickness

will deflect. The definition of the displacement thickness take the form

$$\delta^* = \int_0^{Y \rightarrow \infty} \left(1 - \frac{u}{U}\right) dy \quad (2.17)$$

and is derived from conservation of mass over a control volume defined by the streamline indicated on figure 2.17. U is the free stream velocity and $u(y)$ is the velocity in the boundary layer.

For a jet, there is no free stream velocity as for this example, but the case is similar, and one can imagine the maximum jet velocity to be the free stream velocity.

2.5.5 Indoor air quality indices and energy efficiency

An effective ventilation system is a system that uses as little energy, or resources, to achieve an acceptable indoor climate as possible. Resources will typically be the cost of running the ventilation system, and one is therefore dependent on having low supply airflow in order to reduce fan power and avoid unnecessary heating or cooling [37]. Two indices that will be used in this thesis is contaminant removal effectiveness and temperature effectiveness. The indices are useful for comparison of different ventilation methods.

2.5.5.1 Contaminant removal effectiveness

The contaminant removal efficiency is the ventilation's ability to remove contaminants. The concentration is compared to the complete mixing scenario where the concentration of contaminants are homogenous and can be found by a mass balance for the whole room. The concentration of complete mixing will equal the concentration in the exhaust for other methods. The equation take the form

$$\epsilon_o^c = \frac{C_e}{C_{zone}} \quad (2.18)$$

where C_e is the CO_2 concentration in the exhaust, similar to the upper zone for the two zone model, and C_{zone} is the CO_2 concentration in the zone investigated. The relations are obtained from *Assessment of Ventilation- and Energy- Efficiency in Design for Large Enclosures* by Tjelflaat and Sandberg [37].

2.5.5.2 Temperature effectiveness

Heat can be treated in the same way as the contaminants, and Etheridge and Sandberg [21] suggested the following expression for the calculation of temperature effectiveness.

$$\epsilon^T = \frac{T_i - T_2}{T_i - T_1} \quad (2.19)$$

The indices 1,2 and i stand for the lower zone, the upper zone and the inlet respectively. Similarly to the contaminant removal effectiveness, the temperature effectiveness tells us how well heat is removed from the room.

2.6 Basis for CFD

The aim for this section is to describe the technique used to obtain the solution using CFD. ANSYS Fluent is the software that will be used in the thesis. The topic is very wide, and it is not possible to give a complete explanation in this thesis. More detailed description of CFD and turbulence modeling can be found in Computational Fluid Mechanics and Heat Transfer by Tannehill et al. [38], Computational Fluid Dynamics by Bates et al. [39], Computational Fluid Dynamics: Principles and Applications by Blazek [40], Turbulent Flows by Pope [41] and A First Course in Turbulence by Tennekes and Lumley [42], which has frequently been used in the description of this section.

CFD is a technique of solving the Navier-Stokes equations (NS) and other equations governing a flow field numerically. Conservation of energy, transportation of species and radiation are examples. In this section the basis for CFD will be presented, and the focus will lie on governing equations, turbulence, treatment of walls for turbulence models, meshing and the solution of transport equations. Section 2.7 will in a higher degree focus on CFD for room ventilation and suggestions for the use of the CFD tool.

2.6.1 Governing equations

In CFD several equations are solved simultaneous, and the purpose is finding out how heat, mass, and species are transported due to mechanisms as diffusion, advection, convection, conduction, radiation and chemical reactions. The fundamental equations relevant for this theses will be presented in this section.

2.6.1.1 Continuity equation

The mass-conservation, or continuity equation, take the form

$$\frac{\partial \rho}{\partial x} + \nabla(\rho U) = 0 \quad (2.20)$$

where ρ is the density and U is the velocity. The equation state that the mass must be preserved for a fluid element.

2.6.1.2 Navier-Stokes equation

For incompressible Newtonian fluids with constant properties, the NS equation is given by

$$\frac{DU}{Dt} = -\frac{1}{\rho}\nabla p + \nu\nabla^2 U + g \quad (2.21)$$

where U , ∇ and g are vectors in the x,y and z- direction. Together with the continuity equation 2.20 the four unknowns U_x , U_y , U_z and p can be resolved.

2.6.1.3 Energy equation

The energy equation may take the form

$$\frac{\partial}{\partial t}(\rho E) + \nabla \cdot (\vec{U}(\rho E + p)) = \nabla \left(k_{eff} \nabla T - \sum_j h_j \vec{J}_j + (\tau_{eff} \cdot \vec{U}) \right) + S_h \quad (2.22)$$

where the three terms in the bracket on the right-hand side of the equation represent conduction, species diffusion, and viscous dissipation respectively. The coefficient k_{eff} is the effective conductivity $k + k_t$ where k_t is the turbulent thermal conductivity, J_j is the diffusion flux and S_h is the production term for volumetric heat sources [43]. S_h can also include a radiation source term. The simplest physical models are the one that only involves conduction and convection, while problems involving radiation and buoyant forces are more complex.

2.6.1.4 The S2S Model equations

The surface to surface (S2S) model in ANSYS Fluent is used to calculate radiation in an enclosure. The model assumes the surfaces to be gray and diffuse [44]. For gray surfaces emissivity (ϵ) and absorptivity (α) are independent of the wave length. In addition, $\epsilon = \alpha$ according to Kirchoff's law for gray surfaces [45]. The amount of energy exchange between two surfaces is decided by the view factor. The energy q_{out} leaving a surface k is given by equation 2.23 where ϵ , σ , T , ρ and q_{in} are the emissivity, Stefan-Boltzman constant, temperature, reflectivity, and energy flux from the surroundings respectively. Further, q_{in} is found by equation 2.24 where N is the number of surfaces and F_{jk} is the view factor.

$$q_{out,k} = \epsilon_k \sigma T_k^4 + \rho_k q_{in,k} \quad (2.23)$$

$$A_k q_{in,k} = \sum_{j=1}^N A_j q_{out,j} F_{jk} \quad (2.24)$$

The S2S radiation model is computationally very expensive when there are a large number of radiating surfaces. Therefore, the radiating surfaces can be divided into so-called "clusters" in ANSYS Fluent if the geometry is complex. [44]

2.6.1.5 Natural convection and buoyancy

For room simulation where cold air is supplied in a heated room, natural convection and buoyant forces must be taken into consideration in the CFD simulations. This is done by not treating the density as a constant but rather calculating it based on the local temperature and/or pressure.

The Boussinesq model is a popular model and has been applied with success in CFD simulations for room simulations [46–48]. However, the Boussinesq model has some restrictions. It should not, according to the ANSYS users guide [44], be used for transportation of species. Another limitation of the model is that it should only be used when the temperature differences are small, i.e., $\beta(T - T_0) \ll 1$.

The incompressible ideal gas law has also shown good performance in room simulations. Among others in the simulation of displacement ventilation by Gilani et al. [49]. When the incompressible ideal gas law is turned on in the solver settings, ANSYS Fluent calculate the density from

$$\rho = \frac{p_{op}}{\frac{R}{M_w} T} \quad (2.25)$$

where p_{op} is the operating pressure, R is the universal gas constant and M_w is the molecular weight of the gas [44].

2.6.1.6 Species Transport

Mixing and transport of chemical species can be modeled in ANSYS Fluent, where the local mass fraction Y_i is calculated for species i . Both convection, diffusion, and reaction are described. The conservation equation takes the form:

$$\frac{\partial}{\partial t} (\rho Y_i) + \nabla \cdot (\rho \vec{U} Y_i) = -\nabla \cdot \vec{J}_i + R_i + S_i \quad (2.26)$$

where R_i is the rate of production of species by chemical reactions, S_i is the source term and J_i is the diffusion flux of species. This diffusion arises due to gradients of temperature and concentration [43]. When no reactions are present, as for the case with a transport of CO_2 in a room, R_i becomes zero.

2.6.2 Turbulence modeling

The NS equations are solved by discretizing the equations using finite element techniques. The equations can be solved directly by performing direct numerical simulations (DNS). Solving a problem using DNS would require the grid to be finer than the smallest eddies, and large computational power are required. The length scale, η , of these eddies are called Kolmogorov length scales, and can be found from dimensional analysis of the dissipation rate, ϵ and viscosity ν . The larger length scales, L , can be related to the dissipation rate and

velocity since the kinetic energy production rate must equal the dissipated energy. The time scale U/L is also used since we want the energy dissipation rate. The equations are given as:

$$\eta = \left(\frac{\nu^3}{\epsilon} \right)^{1/4} \quad (2.27)$$

$$\epsilon \propto \frac{U^2}{L/U} \propto \frac{U^3}{L} \quad (2.28)$$

$$\eta = \left(\frac{\nu^3 L}{U^3} \right)^{1/4} \quad (2.29)$$

Equation 2.29 can be applied to estimate the size, and thus the number of cells, for the problem if DNS is used. For room simulations, this number is expected to be high since the viscosity is low compared to the velocity.

It will normally not be necessary to resolve all the details in the flow pattern including the fluctuations due to turbulence. Therefore, the fluctuating variables (velocity and pressure) are averaged so that only the information about the mean flow is resolved. The flow variables are assumed to be on the form $u = \bar{u} + u'$ where \bar{u} is the mean value and u' is the fluctuating value. Some information is lost due to this averaging, but for most engineering applications the information will be sufficient. The Reynolds averaged Navier- Stokes equation (RANS) look almost like NS, but an additional term is added. The term added is $\frac{1}{\rho} \frac{\partial}{\partial x} (-\rho \overline{u_i u_j})$ where $-\rho \overline{u_i u_j}$ is called the Reynolds stress tensor, even though it is not an actual stress tensor. The tensor has 9 unknowns as it is a 3x3 tensor, so the equation contains many unknowns. The time averaged continuity and momentum equations become:

$$\frac{\partial \overline{u_i}}{\partial x_j} = 0 \quad (2.30)$$

$$\frac{\partial \overline{u_i}}{\partial t} + \overline{u_j} \frac{\partial \overline{u_i}}{\partial x_j} = -\frac{1}{\rho} \frac{\partial \overline{p}}{\partial x_i} + \frac{\mu}{\rho} \nabla^2 \overline{u_i} + \frac{1}{\rho} \frac{\partial}{\partial x} (-\rho \overline{u_i u_j}) \quad (2.31)$$

The problem is then to formulate a model that describes the Reynold stresses. Turbulence models are often classified by the number of equations that must be solved in addition to the mean flow equations [50, p. 183-208]:

- Zero equation models
- One equation models
- Two equation models
- Stress equation models

Boussinesq suggested that the Reynold stress tensor could be expressed in terms of the eddy viscosity, ν_T , which is a flow property that changes from one flow to another and is therefore not a physical property. Both the zero-, one- and two equation models use this model. The original idea was to define the Reynold stresses by relation 2.32.

$$-\rho \overline{u_i u_j} = \rho \nu_T \frac{\partial U}{\partial y} \quad (2.32)$$

The Eddy viscosity now have to be modeled, and form the basis for many turbulence models. The two equation model, k- ϵ , which will be used in this thesis, solves this term by expressing

it in terms of the kinetic turbulent energy, k , and the dissipation rate, ϵ which again is solved in two separate transport equations. In the standard k - ϵ model (SKE), the viscous effects are neglected. This must be taken into account when calculating the flow close to walls where the viscous effect can not be neglected. The equations become

$$\rho \frac{\partial k}{\partial t} + \rho u_j \frac{\partial k}{\partial x_j} = \frac{\partial}{\partial x_i} \left(\left(\frac{\mu + \mu_t}{\sigma_k} \right) \frac{\partial k}{\partial x_i} \right) + P - \rho \epsilon \quad (2.33)$$

$$P = (\mu + \mu_t) \left(\frac{\partial u_i}{\partial x_j} + \frac{\partial u_j}{\partial x_i} \right) \frac{\partial u_i}{\partial x_j} \quad (2.34)$$

$$\rho \frac{\partial \epsilon}{\partial t} + \rho u_j \frac{\partial \epsilon}{\partial x_j} = \frac{\partial}{\partial x_i} \left(\left(\frac{\mu + \mu_t}{\sigma_\epsilon} \right) \frac{\partial \epsilon}{\partial x_i} \right) + c_{\epsilon 1} \frac{\epsilon}{k} P - c_{\epsilon 2} \frac{\epsilon}{k} \rho \epsilon \quad (2.35)$$

where the constants typically take the values $c_{\epsilon 1} = 1.44$, $c_{\epsilon 2} = 1.92$, $\sigma_k = 1.0$ and $\sigma_\epsilon = 1.3$, and μ_t , μ , σ_k and σ_ϵ are the turbulent viscosity, viscosity and turbulent Prandtl number for k and ϵ . [39].

The SKE still need some modification for various effects such as buoyancy and rapid compression [51]. Other versions of the k - ϵ are developed and will be introduced and discussed in section 2.7.

2.6.3 Near wall turbulence

It is important to consider the near wall turbulence since this an important region in terms of the production of turbulence. In addition, the region close to walls is important in ventilation design. At the wall, we have the no-slip condition $u(0) = 0$ for turbulent flows as well as for laminar flows. But, this boundary condition can not be used for the equations in the k - ϵ model because the turbulence model assumes fully turbulent flow, i.e most of the diffusion and production terms are uninfluenced by molecular properties. This is not the case near walls where the viscosity can not be neglected. For example, the production term in the k - ϵ model is a function of ν_t which is only a function of k and ϵ meaning that this is a purely turbulent quantity and therefore only valid for high Reynolds numbers. We can, therefore, say that the k - ϵ is a high Reynolds number turbulence model.

The boundary condition will therefore not be at $u(0) = 0$, but at where the so-called log-law region starts. The log-law region is also called the fully turbulent region. The log-law region start at where $y^+ \approx 30$ where y^+ is defined as

$$y^+ = \frac{y \sqrt{\frac{\tau_w}{\rho}}}{\nu} \quad (2.36)$$

In equation 2.36 y is the distance from the wall, and τ_w is the wall shear stress. For $y^+ < 30$ we move into the buffer layer and the viscous sublayer where viscous forces are not negligible.

The distance to the first node should be estimated to ensure that the y^+ is not within the viscous sub layer. Several online webpages have tools to estimate the size of the first grid point. It can also be solved by estimating the wall shear stress from the skin friction

coefficient C_f from the equation 2.37.

$$\tau_w = \frac{1}{2} C_f \rho u^2 \quad (2.37)$$

C_f can be obtained from empirical equations. For internal flows $C_f = 0.079 Re^{-0.25}$. However, the value of y^+ should be checked after the simulation is performed to ensure it is within the recommended range [39, 41, 51].

Traditionally there are two types of wall functions; the wall function approach and the near-wall model approach. For the wall function, the viscous layer is not resolved, while for the near-wall model approach this region is resolved. Except for the scalable wall function, a disadvantage of wall functions are that the numerical result deteriorates by the refinement of the mesh in normal direction. Values of y^+ should therefore be kept under a certain value. Because of this, ANSYS Fluent introduced a y^+ -independent formulation called the Enhanced Wall Treatment (EWT) [43] where the requirement for the value of y^+ is not as strict as for other wall function methods. The EWT divides the near wall region into a viscous sublayer and fully turbulent flow. In the viscous layer, only the k -equation is solved, while in the turbulent layer the k - ϵ equation is solved [52]. With the EWT the first cell should be placed in the order $y^+ = 1$, but higher than 1 is acceptable as long as it is well inside the viscous sublayer ($y^+ < 3$ to 5). Flow around complex geometries or geometries where the velocity varies makes it hard, or even impossible, to achieve a uniform y^+ . This means that there will be areas where the wall function will not be valid [53].

2.6.4 Mesh

The mesh has a large impact on the numerical result, accuracy of simulations and convergence. When creating the mesh it is important to have higher resolution at where the gradients are high. Elsewhere the mesh can be coarser. One must, therefore, analyse the problem before the simulations are performed. It is not obvious how fine the mesh should be and how many cells or nodes your domain should contain. This will be further discussed in section 2.6.5.3 where the grid refinement study is explained.

The number of cells/ nodes at the inlet and outlet is important for convergence. If for example the pressure outlet has a coarse grid, the solution can "jump" between different solutions as the quantities in the coarse cells change.

The mesh quality plays an important role for the accuracy in CFD. ANSYS Fluent let you check important quality parameters of the elements. Two important indicators are the orthogonal quality and the skewness. The range for orthogonal quality is 0 to 1 where 0 is the worst and 1 is the best. For the skewness 0 is best and 1 is worst [43]. For all quality indicators, it is the worst cell that defines the quality, and one should check where these cells are located to find out whether they affect important areas of the simulation.

2.6.5 Solution of transport equations

The transport equation for momentum, energy, concentration and the turbulence scales all have the same general form which is convenient when they are discretized and solved numerically. The discretized form of the equations are solved numerically by the finite volume method (FVM) in ANSYS Fluent [26]. In this section, the strategy of solving these equations will be described in addition to a description of accuracy and errors in CFD.

2.6.5.1 Solution of the discretization equations

The flow field is initialized before iterative methods are used to solve the nonlinear transport equations. To achieve a converged solution, the velocity components must satisfy the continuity equation and the correct pressure field. This link between pressure and velocity is referred to as Pressure-linked discretization methods.

Different options for coupling of velocity and pressure exists. The semi-implicit method for pressure coupling (SIMPLE) is the most common in the studied literature, but in some cases Coupled are used when SIMPLE is not sufficient to reach convergence. Coupled is a more robust algorithm. For complicated flows involving turbulence SIMPLE-Consistent (SIMPLEC) will improve convergence only if it is being limited by the pressure-velocity coupling [44]. Normally SIMPLE and SIMPLEC will give similar convergence rate. Menchaca-Brandan et al. [54] used SIMPLE in their calculation of natural ventilation with radiation and buoyant forces and is an example of a case where it was not necessary to use the Coupled pressure-velocity coupling. For convergence problems turning on the Coupled pressure-velocity coupling might help.

In order to reach convergence false time steps are in many cases necessary. Examples are the simulation of natural ventilation with buoyant forces and the wind by Cook et al. [55], air terminal devices by Huo et al. [56] and displacement ventilation in an enclosure by Ji et al. [47]. Cook et al. [55] used false time steps on each of the momentum equations in their simulations to achieve convergence where pressure and velocity were coupled using the SIMPLEC algorithm. In the design of active displacement ventilation and jets one can experiment with using SIMPLE and Coupled. More computational power is required when using Coupled, so this should only be considered when there are convergence problems.

2.6.5.2 Boundary conditions

Conditions on all boundaries must be specified when performing CFD simulations. In general, the boundary conditions (BC) for CFD are solid walls, far-field in external flows, inflow and outflow in internal flows, injection boundary, symmetry, coordinate cut and periodic boundary and boundary between blocks [40]. For this thesis, the wall boundary, and inflow and outflow in internal flows are of relevance in addition to symmetry BC. For the inlet boundary the mass flow, temperature and species concentration must be specified. Alternatively, the velocity can be specified instead of the mass flow since the area is fixed.

In that case, we say we have a Dirichlet BC since the values are specified at the inlet. Walls where the no-slip condition is chosen will result in a Dirichlet BC for the velocity. For the temperature both constant temperature and heat flux are alternatives. For constant flux we have a Neumann BC since the derivative is specified while constant temperature gives a Dirichlet BC. The outflow is defined differently than the inlet since both velocity and temperature depends on the other boundaries and numerical solution. Typically, a pressure outlet boundary condition is chosen where the gauge pressure must be specified in addition to backflow conditions. According to the ANSYS Fluent User's guide [44] convergence difficulties will be minimized when the backflow quantities are set to realistic values.

When defining the inlet and outlet boundary conditions the turbulence intensity must be defined as well as the hydraulic diameter. The hydraulic diameter is defined as

$$D_H = \frac{4A}{P} \quad (2.38)$$

where A is the cross sectional area and p is the wetted perimeter. For a circular pipe the hydraulic diameter is equal to the pipe diameter. The turbulence intensity (TI) is defined as

$$TI \equiv \frac{u'}{U} \quad (2.39)$$

where u' is the root-mean-square, or the turbulence velocity fluctuation, and U is the mean velocity. It is not easy to estimate u' . Russo and Basse [57] was the first to document the scaling behavior of the TI with Re , according to themselves. The scaling for the turbulence intensity over a pipe cross sectional area where found to be

$$TI = 0.140Re^{-0.0790} \quad (2.40)$$

2.6.5.3 Accuracy of CFD simulations

The accuracy of CFD simulations depends in particular on the following factors, and some of the issues related to these factors will be discussed in this section.

- The discretization scheme
- The computational grid
- The near-wall boundary conditions
- The convergence criteria

Numerical diffusion is a common phenomenon in CFD. The phenomenon arises due to the discretization scheme and computational grid. Numerical, or false, diffusion is when the diffusion has increased due to the numerical solution. Although stability is obtained in the simulations, the results may not be accurate. When cells are large, the first order upwind scheme shows a significant influence on the false diffusion when the grid cells are large [58]. Figure 2.18 is adapted from a study by Nielsen [58] and show a simulation of the velocity distribution of air coming out from an opening close to the ceiling. The measurements are done 1 m from the opening. It is obvious that the number of cells affects the false diffusion. The larger cell size, the higher degree of false diffusion.

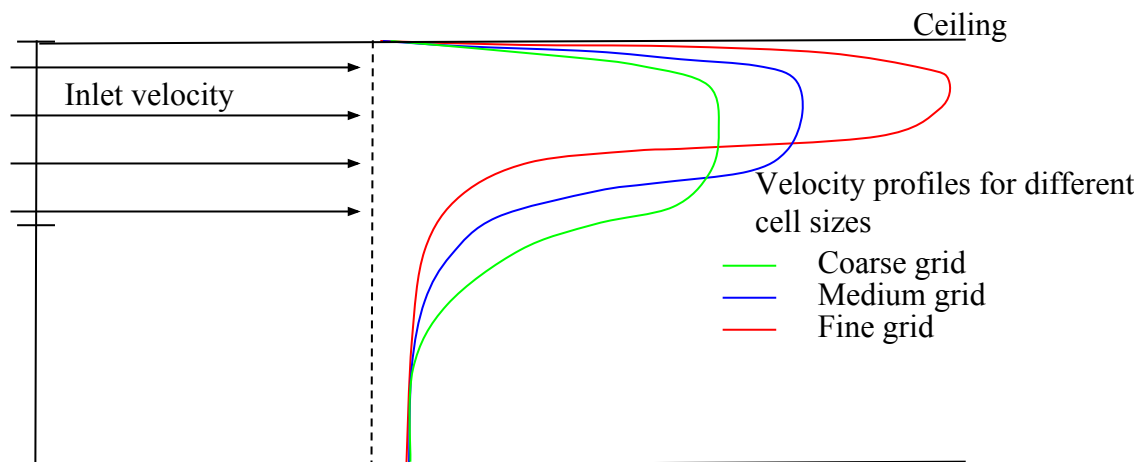


Figure 2.18: Velocity distribution downstream of the opening in a room for different grid sizings illustrate the importance of grid refinement to resolve the physics. Figure is adapted from Nielsen [58] and is only meant as an illustrative figure

The second order upwind scheme and the QUICK scheme are improvements compared to the first order schemes. They are both second-order accurate, and reduces the false diffusion. For the same problem as in figure 2.18 a new simulation with a second order upwind scheme was done, and the result can be seen in figure 2.19. Today it is possible to use a large number of grid points, and the errors due to the choice of the scheme can be reduced. However, higher order schemes are necessary to obtain high accuracy. First order accurate schemes are typically used for initialization and quick simulations where the accuracy is of less importance [43]. When the flow is aligned with the mesh the first-order upwind discretization is acceptable. If not, the first-order upwind will lead to discretization errors and to numerical diffusion. For most applications, it is therefore recommended to use the second-order scheme from the start [44].

The accuracy can be increased by performing a grid refinement study. A grid refinement study is when you perform the same computation several times, with an increasingly fine grid and monitor certain points and values. Even though the residuals has reached the convergence criteria, typically $10E-03$ or $10E-04$, one must make sure that the solution also is independent on the mesh resolution. This technique is used to reduce the error from the computational grid. Plotting key values for the different grids in one figure indicates how the grid size effects the accuracy of the computations. A key value can, for example, be the velocity, temperature or pressure at a certain point in the domain, or the sum of a defined line or surface. When the result does not change significantly, the solution is said to be mesh independent. The computational power may be a restriction for the number of elements one can afford to have.

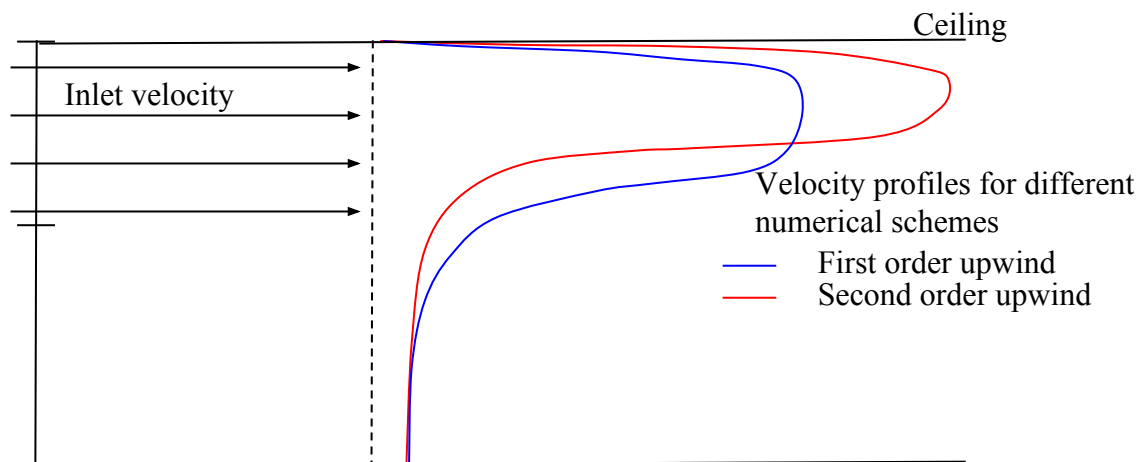


Figure 2.19: Velocity distribution downstream of the opening in a room for different numerical schemes illustrate the importance of a scheme of high order when accurate results are required. Figure is adapted from Nielsen [58]

2.6.5.4 Errors in CFD

Errors, accuracy, and convergence are factors that are closely connected together in CFD. It is important to be aware of potential errors when performing CFD simulations. Today it is relatively easy to obtain results that, at first glance, looks realistic and correct using commercial CFD software. This makes it even more important to be aware of errors that have affected the accuracy and quality of the simulation. There are many types of errors in CFD, and the main errors that may arise in a CFD simulation are

- Truncation error
- Rounding error
- Iteration error
- Discretization error
- Modeling error

The truncation error comes from approximating an infinite sum, often derivatives, to approximate a finite sum. Rounding errors arise since the computer has limited floating point numbers that can be stored. Iteration errors occur if the iterative method has not sufficiently converged. This error is connected to convergence and can be seen from the residual values in ANSYS Fluent. Convergence occurs when the pre-defined requirement for the iteration error is not reached. Discretization errors are errors due to the discretization of the equation and is defined as $\epsilon_{disc} = U_{disc} - U_{model}$ where U is the discretized quantity. The last error mentioned here is the modeling error. This is the error of the mathematical expression U_{model} with respect to the real flow physics U_{real} [59].

2.7 CFD for room air distribution

CFD in the ventilation industry was first introduced in the 1970s and has since then been increasingly used, and is today used both for research and as a design tool. About 60-70 peer-reviewed articles are, per 2015, published per year, and the interest for the topic is increasing [58].

One can not expect to calculate the indoor climate perfectly. The indoor climate is affected by a number of factors that each has its uncertainty. Examples of such factors are the weather, the behavior of occupants and thermophysical properties [60]. In addition, several simplifications are often made when CFD calculations are performed. It is therefore important to make realistic simplifications that not move the solution too far away from the real solution.

There are many focus areas in CFD for room ventilation and HVAC design. Some focus on accurate simulations of specific parts or elements in a room, while others perform simulations of entire rooms and buildings where there is not the same need for details. Examples of CFD studies relevant for room air distribution are heated manikins [61–63], temperature stratification in rooms with displacement ventilation [49], buoyant and free jets [64], convection from windows [60, 65], atria geometries [47, 66–68], the agricultural industry [69], large industrial premises [70], displacement ventilation in rooms [47, 71] and natural ventilation [54, 72]. In addition, several studies are done where turbulence models are compared and evaluated for different applications. This will be discussed in section 2.7.1, 2.7.3 and 2.7.4.

The purpose of this section is to extract out relevant information from earlier studies and adapt it to this CFD study. Turbulence models, numerical solution methods, meshing techniques and strategies, suggestions for geometry simplification and boundary conditions will be discussed continuously.

2.7.1 Turbulence models for HVAC simulations

A large number of articles are written where the focus is finding the best suited turbulence model for different applications. CFD for room ventilation and HVAC design is no exception. A study of various turbulence models in predicting airflow and turbulence in enclosed environments was performed by Zhai et al. [73] where it is pointed out that for room simulations "the most critical factors are the selection of an appropriate CFD approach and a turbulence model". An investigation and literature study of turbulence models for HVAC design is therefore important. Different HVAC scenarios require different turbulence models and the conclusion on which turbulence model that perform best is not always consistent as pointed out by Gilani et al. [49]. The most discussed turbulence models for room ventilation are the renormalized group (RNG) $k-\epsilon$ model, the realizable $k-\epsilon$ (RKE), the standard $k-\epsilon$ (SKE) and the SST $k-\omega$ model. These models are therefore given the main attention in this section.

Even though the coefficients of the SKE are determined from case studies of simple turbulent

flows, the SKE has a limitation when it comes to the complexity of the flow due to inaccuracies in the ϵ -equation [70]. The SKE has also turned out to over-predict the rate of entrained air in buoyant plumes which is not ideal when buoyant flow is analyzed in detail as in this thesis. The over-prediction results in a deeper stratified layer and is not consistent with analytical models according to Cook et al. [55]. Both the RKE and RNG $k-\epsilon$ are versions of SKE where the weaknesses of the SKE are improved. Even though the SKE has its weaknesses, the model has been used with success by, among others, Kong and Yu [74] and Wan and Chao [48].

RNG $k-\epsilon$ gives better predictions due to the lower amount of entrained air. It performs well for the simulation of flows with a large degree of strain in the fluid and for boundaries with large curvature. The idea of RNG $k-\epsilon$ is to filter out the smallest eddies. This is done by the parameter η which is the ratio between the time scale of the turbulence and the mean flow. The basic idea of the RKE is removing values of variables from the predictions by so-called numerical clipping. Numerical clipping is when one remove unphysical values of variables, such as negative normal stresses, from the predictions [52]. Both the RKE and RNG $k-\epsilon$ have shown significant improvements compared to the standard model where the flow features include strong streamline curvature, vortices, and rotation [26, 43].

In 2011 Zhang et al. [75] published an article where eight turbulence models, potentially suitable for indoor airflow, were compared in terms of accuracy and computer cost. Not all of these turbulence models are an option in ANSYS Fluent. The RANS based turbulence models RNG, low Reynolds number $k-\epsilon$ and SST $k-\omega$ were investigated. In addition, a hybrid RANS, large eddy simulation (LES), a three-equation $V^2 - f$ model and a Reynold-stress model (RSM) were studied. The conclusion was that the RNG $k-\epsilon$ and the three-equation model V^2-f model had the best overall performance compared to the other models in terms of accuracy, computing efficiency, and robustness. The accuracy was measured by comparing the simulations to experimental data where both natural, forced and mixed convection were present. The accuracy for strong buoyancy were also taken into account. The SST $k-\omega$ performed well for strong buoyant flows, but was poor for low Reynolds numbers.

It is not clear whether the RNG, RKE or SST $k-\omega$ is best to use for the application in this thesis. In general, all of these three turbulence models are frequently used in HVAC design and research. In the studied literature there is a slightly overweight of the use of RNG $k-\epsilon$ [54, 55, 67, 68, 70–72, 76–78], while the RKE [65, 79, 80] and the SST $k-\omega$ [73, 75, 81–84] in a lower degree is represented. However, due to a large amount of published articles that is not investigated, it can not be concluded that the RNG $k-\epsilon$ is more popular than other methods. The turbulence models will be discussed further in section 2.7.3 and 2.7.4 where they will be related to the specific type of airflow simulations that performed in this thesis.

2.7.1.1 RNG $k - \epsilon$ and RKE equations

The equations of RNG $k-\epsilon$ and RKE will in this section be presented since these are the models that will be used in the thesis. The equations of the RNG $k-\epsilon$ are similar to the SKE, but with some improvements. One of them is the parameter R is important for anisotropic

large scale eddies [39]. The equations are

$$\frac{\partial}{\partial t}(\rho k) + \frac{\partial}{\partial x_j}(\rho k u_j) = \frac{\partial}{\partial x_j} \left(\alpha (\mu + \mu_t) \frac{\partial k}{\partial x_j} \right) + P - \rho \epsilon \quad (2.41)$$

$$\frac{\partial}{\partial t}(\rho \epsilon) + \frac{\partial}{\partial x_j}(\rho \epsilon u_j) = \frac{\partial}{\partial x_i} \left((\mu + \mu_t) \frac{\partial \epsilon}{\partial x_i} \right) + c_{\epsilon 1} \frac{\epsilon}{k} P - c_{\epsilon 2} \frac{\epsilon}{k} \rho \epsilon - R \quad (2.42)$$

$$R = \rho \frac{c_\mu \eta^3 \left(\frac{1-\eta}{\eta_0} \right) \epsilon^2}{1 + \beta \eta^3} \frac{1}{k}, \quad \eta = \frac{k}{\epsilon} \sqrt{2S_{ij}S_{ij}}, \quad S_{ij} = \frac{1}{2} \left(\frac{\partial u_i}{\partial x_j} + \frac{\partial u_j}{\partial x_i} \right) \quad (2.43)$$

where the constants normally take the values $c_\mu = 0.0845$, $c_{\epsilon 1} = 1.42$, $c_{\epsilon 2} = 1.68$, $\alpha = 1.3$, $\beta = 0.011 - 0.015$ and $\eta_0 = 4.38$ [85, 86]. These constants are very similar to the one found in the SKE, but in the RNG the constants are found theoretically while the constants in the SKE is found experimentally.

The RKE contains an alternative formulation of the turbulent viscosity compared to SKE and a modified equation for the dissipation rate [43]. The equations are

$$\frac{\partial}{\partial t}(\rho k) + \frac{\partial}{\partial x_j}(\rho k u_j) = \alpha \frac{\partial}{\partial x_j} \left(\left(\mu + \frac{\mu_t}{\sigma_\epsilon} \right) \frac{\partial k}{\partial x_j} \right) + G_k + G_b - \rho \epsilon - Y_M + S_k \quad (2.44)$$

$$\frac{\partial}{\partial t}(\rho \epsilon) + \frac{\partial}{\partial x_j}(\rho \epsilon u_j) = \frac{\partial}{\partial x_j} \left(\left(\mu + \frac{\mu_t}{\sigma_\epsilon} \right) \frac{\partial \epsilon}{\partial x_j} \right) + \rho C_1 S_\epsilon - \rho C_2 \frac{\epsilon^2}{k + \sqrt{\nu \epsilon}} + C_{1\epsilon} \frac{\epsilon}{k} C_{3\epsilon} G_b + S_\epsilon \quad (2.45)$$

$$C_1 = \max \left(0.43, \frac{\eta}{\eta + 5} \right), \quad \eta = S \frac{k}{\epsilon}, \quad S = \sqrt{2S_{ij}S_{ij}} \quad (2.46)$$

where the constants G_k and G_b represent the generation of turbulence kinetic energy due to the mean velocity and buoyancy respectively. Y_M represent the dilatation in compressible turbulence for high Mach numbers. This factor will not be of relevance in this thesis. C_2 and $C_{1\epsilon}$ are constants.

2.7.2 Influence of radiation

Radiative heat transfer accounts for a large part of the heat transfer in a room. In 2016 Menchaca-Brandan et al. [54] investigated the influence of radiative heat transfer in rooms with natural ventilation by performing CFD simulations. They concluded that when radiation was ignored, the temperature difference of the air surrounding occupants was 2-4°C. The surface temperature of heat sources was also investigated and was up to 17°C higher when radiation was ignored. The air velocity in the room was higher in simulations including radiation.

The internal emissivity needs to be defined for all surfaces in ANSYS Fluent. The value can be set to 1 for simplicity since most materials in a classroom/ office have emissivities above approximately 0.9 according to Menchaca-Brandan et al. [54].

2.7.3 CFD-studies relevant for simulation of free jets and wall jets

One of the objectives of this thesis is performing CFD simulations and compare them to relevant empirical relations for active displacement ventilation. Today we know how a jet should behave under certain conditions. The spreading, velocity distribution and temperature distribution are examples. One can, therefore, check whether the simulations are realistic since many empirical relations, lab experiments and CFD simulations are done for jets.

An investigation of wall jets and how they interact in contact of obstacles was carried out by Awbi and Setrak [87, 88] both numerically and experimentally. For the numerical solution the momentum equations, energy equation, concentration equation and mean equation was solved. It was necessary with a fine grid close to the wall where large diffusion occurred. The grid used was an exponentially expanding grid both in the axial and normal direction.

Problems can be met when flow along walls are studied. According to a study performed by Lindner et al. [89] in 2007 where different turbulence models were studied for cases of indoor airflow "the standard $k-\epsilon$ model reproduced quite well the behavior of the experimental data, except near the floor (...)". They also claim that "It over-predicted the velocity close to the floor (...)". This was also the case for the $k-\omega$ -model. In fact, the $k-\omega$ model showed slightly worse accordance with the measurements than the standard $k-\epsilon$

CFD simulations of cold draught from cold window surfaces are almost analog to the prediction of buoyant flow along a wall. Jurelionis and Isevicius [90] did in 2010 a CFD study of air movement induced by cold window surfaces. The first grid point was 2 cm from the window surface, and the SKE model was used. The velocity in the CFD simulation gives about 15 % lower values close to the window than experimental results. The shape of the velocity profile is analogous. It was believed that the error is due inequalities of the boundary conditions and limitations of $k-\epsilon$ turbulence model.

In 2003 Schlin and Nielsen [91] performed CFD simulations on free jets and wall jets where both the $k-\epsilon$ model and Reynold stress model (RSM) was used. The results show that the $k-\epsilon$ model performs well for many situations in room air movement, but that the model has hidden problems. An example is that it does not always yield an asymmetrical flow pattern. For the wall jets the value of y^+ was between 20 and 40.

2.7.4 Previous CFD research relevant for active displacement ventilation

CFD of active displacement ventilation involves buoyant flows where, ideally, equations related to radiation and transportation of species also are resolved. In this section the focus will be to investigate literature that is of relevance for the design of active displacement ventilation. This can typically be studies where CFD is used to investigate ordinary displacement ventilation and natural ventilation.

Nielsen [92] did, in 2008, a CFD study of displacement ventilation with an end wall mounted low-velocity diffuser in a symmetric room where it was pointed out that symmetrical

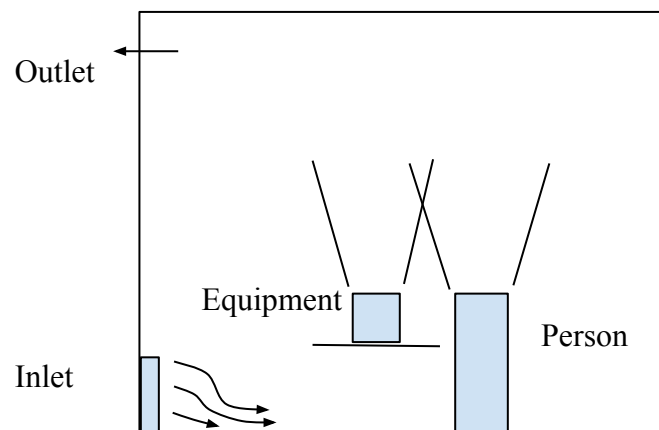


Figure 2.20: Figure of CFD simulation of displacement ventilation adapted from Nielsen [92]

boundary conditions are chosen for the problem as it saves grid points. See figure 2.20. He says that this is only recommended for ordinary displacement ventilation since stratified flow for displacement ventilation often move in a symmetrical pattern along the floor. For mixing ventilation and active displacement ventilation unsymmetrical flows can occur. Problems related to asymmetry for symmetric BC are also described by Etheridge and Sandberg [21]. Even for experts problems regarding grid dependency and poor convergence may arise, and it is suggested to have prior knowledge of the flow that is under investigation. This asymmetric behavior for symmetric BC has also been observed experimentally [93]. In modeling of simple cases of active displacement ventilation, it is tempting to use symmetric BC. If this is done, the person performing simulations must be aware of the chance of unsymmetrical flow when evaluating the results.

Hussain and Oosthuizen [83] performed in 2011 a study where different RANS based turbulence models were validated and compared to experimental results for an atrium with hybrid ventilation. This case is relevant for room simulations, and details near walls, close to inlets and outlets were not studied. One of the conclusions is that all the turbulence models studied, which was SKE, RNG $k-\epsilon$, RKE and $k-\omega$ SST, gave results that agreed well with the experimental results. CFD simulations of natural convection, conduction and radiation prove to give reliable results for the turbulence models studied. Stamou and Katsiris [81] did a similar study where different models were compared for indoor airflow. The conclusion coincides with the conclusion of Hussain and Oosthuizen [83]: "Calculations show that all the tested models predict satisfactorily the main quantitative features of the flow and the layers type of temperature fields. Thus, all these models (SST $k-\omega$, RNG $k-\epsilon$ and SKE) can be used for practical purposes".

In 2005 Ji et al. [47] published an article on CFD modeling of natural displacement ventilation in an enclosure connected to an atrium. See figure 2.21. The supply air is a top-down chimney (TDC), and is similar to the supply technique used in active displacement ventilation except that the old air is not entrained. A point source on the floor generates a plume that causes the air to flow through the storey outlet and out through the atrium outlet. The RNG model was used together with the central difference scheme for the

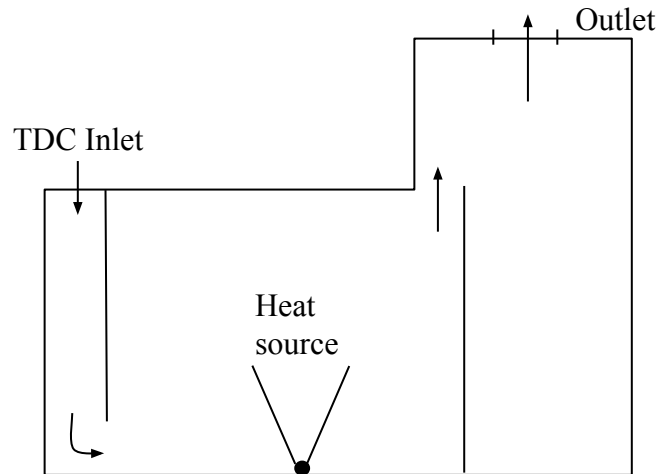


Figure 2.21: Figure of CFD simulation of displacement ventilation adapted from Ji et al. [47]

momentum and QUICK for the rest. For the velocity-pressure coupling, SIMPLEC was used. An interesting thing about the simulations is that convergence was not achieved without using false time steps as mentioned in section 2.6.5.1. The default under-relaxation factors were not sufficient to reach convergence.

Another study where CFD is used in room simulation is done by Gilani et al. [49] where displacement ventilation in a room with one heat source was investigated. The study claims, as many other studies do, that the turbulence model has a large impact on the results. The conclusion is that the $k-\omega$ model is the best for buoyant flows over a heat source, while the impact on the discretization scheme is minor and that numerical diffusion does not influence affect the results. The setup for this simulation is similar to the one in figure 2.20 except that there is no heated equipment on a desk.

The effect of the modeling of the occupants has still not been discussed. Typically, a cylinder or box can be used for the modeling where the area of the object equals the average area of a person. Deevy et al. [94] performed CFD simulations where the effect of an occupant were investigated, and he found that the flow around the body was unsteady. Modeling thermal radiation was found to be important to get an agreement with the experimental results. In addition, a realistic manikin geometry is required to give accurate heat transfer and contaminant predictions.

Today, CFD give us the opportunity to predict the thermal comfort and atmospheric environment in any point in space. Temperature, draught, turbulence intensity and concentration of contaminants are typical parameters for thermal and atmospheric comfort that can be predicted with CFD. The average age of a particle can also be included in the CFD model and is relevant when ventilation efficiency is evaluated [21].

Method

In this section two main questions will be answered: How was the data generated, and how was it analyzed. The first question will be answered by explaining how the CFD simulations are performed. This means presenting the geometrical model, boundary conditions, the meshing strategy, setup, solution method, and control setting. The second question is about how the results were analyzed. This includes both the analysis of the CFD results and the method used to predict the flow pattern using empirical relations.

3.1 Geometrical model and boundary conditions

Several geometrical models and boundary conditions are used in this thesis. The analysis of the isothermal and non-isothermal jets are performed with the same geometrical model, but for different BC. The geometrical model for active displacement ventilation and ordinary displacement ventilation are equal except for the inlet air device. Therefore, four different geometrical models will be presented in this section together with its BC.

3.1.1 Thermal and isothermal jets

Empirical relations developed for jets, as those developed by Skåret [1], are valid for certain conditions. The temperature around the jet is assumed constant, and the jets are supplied to an infinitely large room where the walls are not affecting the jet. An infinitely large room can of course not be simulated due to the limitation of computational power. Also, it can be hard to choose boundary conditions that fulfill the requirement of a uniform room air temperature.

For the CFD simulation of the thermal and isothermal jet a cubic room with side length 5 m is investigated. A circular inlet with a diameter of 0.2 m is placed in the center of the ceiling while two circular outlets are placed 4 m over the floor as seen in figure 3.1 (b). This is done to create a symmetrical problem where pressure differences will not affect the jet. It will reduce the chance of an unwanted unsteady solution and a jet that is not following a centerline located exactly in the middle of the room. This type of design makes it possible to have a double symmetric problem meaning that symmetrical BC can be chosen for two planes. This is illustrated in figure 3.1 (a) where the two white walls are symmetrical BC for

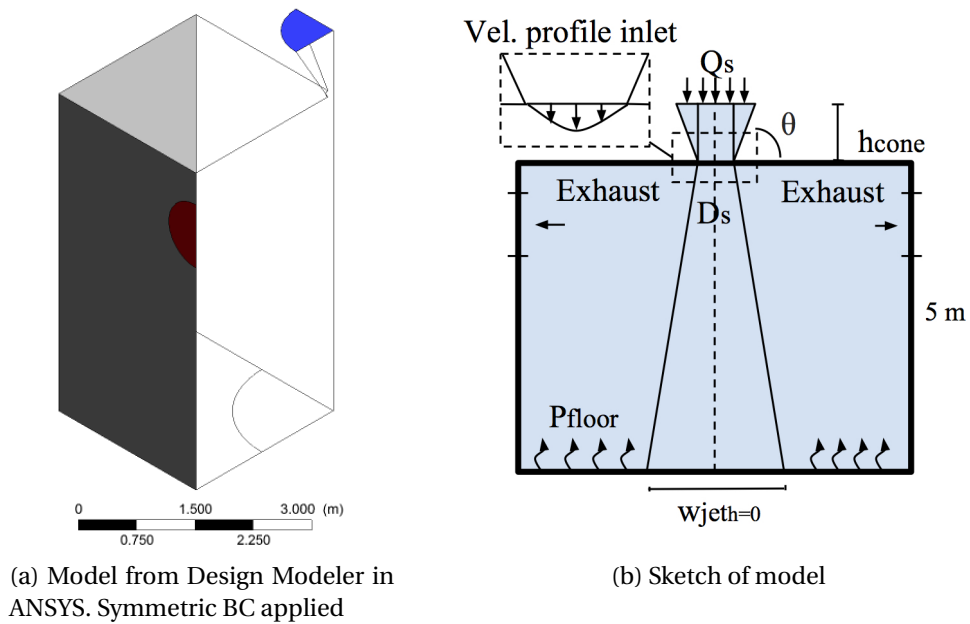


Figure 3.1: Geometrical model for modeling of buoyant jet. In figure (a) the white walls and the white surfaces in the inlet are symmetrical BC. The floor is not a symmetrical BC

the free jet. In addition, the two white surfaces in the inlet are symmetry BC.

The Inlet air terminal is modeled as a cone. The angle θ , indicated in figure 3.1(b), between the ceiling and cone wall, is 60° . The reason is that this is assumed to be a more realistic inlet air profile than with a uniform velocity at the inlet. Also, a low contraction coefficient is expected for such a geometry, and it is possible to create a similar case in a lab experiment if this is of interest later. Another benefit of modeling such a cone is that the temperature gradients at the inlet opening will be reduced since a more realistic temperature profile is expected at the inlet. This will also contribute to a lesser need for a high-resolution grid. Table 3.1 gives an overview of the geometry of the room.

Table 3.1: Boundary condition for simulation of thermal and isothermal free jets

Geometry	Value
Width room, w_{room}	5 m
Length room, l_{room}	5 m
Height room, h_{room}	5 m
Inlet diameter, D_s	0.2 m
Extract diameter, D_e	1 m
Cone height, h_{cone}	1 m
Cone angle, θ_{cone}	60°

For the wall jet, the room is cut in half as illustrated in figure 3.2 (b). The cone has symmetry BC to create a similar scenario as for the free jet and avoid increasing the contraction

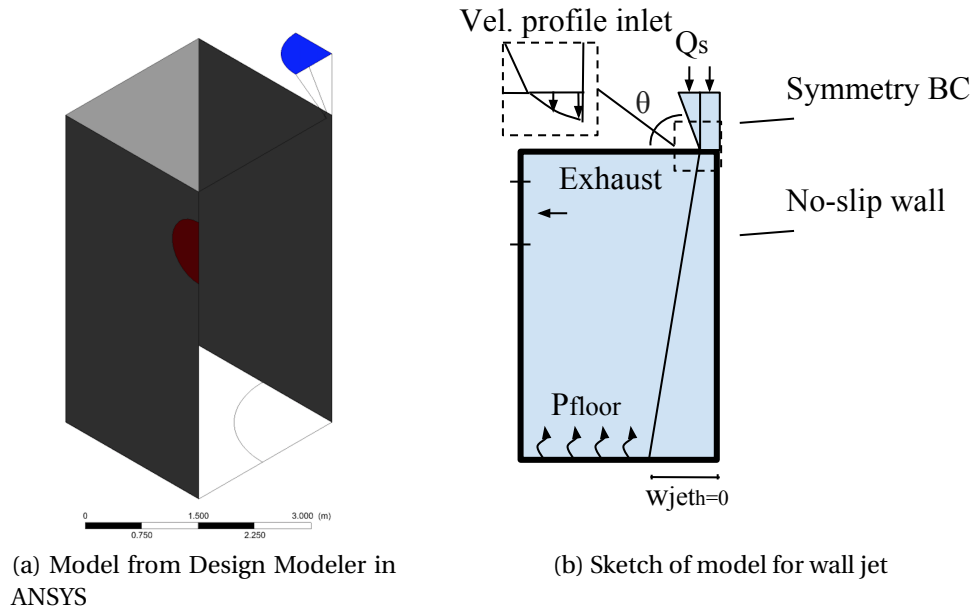


Figure 3.2: Geometrical model for simulation of wall jets

coefficient for the inlet. This kind of inlet will, therefore, be identical to half the inlet for the case of a free jet. In figure 3.2 one can see that one of the walls are gray compared to figure 3.1. This is now a wall and not a symmetry BC.

The inlet temperature is set to 12°C, and the floor is set to a constant temperature of 24°C. The quadrant illustrated on the floor in figure 3.1 (a) and 3.2 (a) is not heated to 24°C as the rest of the floor, but is rather chosen to be an adiabatic surface. The reason is that the jet very easily became unsteady due to convective flows from this area. By adding an adiabatic surface under the jet the vertical convection flow was avoided, and the flow became steady. It is also hard to achieve a room with a completely uniform room temperature, and a gradient is expected as for a real scenario with floor heating.

The Inlet air velocity in the cone is calculated so that the supply air velocity is approximately 0.2 m/s. The outlet boundary condition is a pressure outlet. Further, the turbulence intensity in the inlet is found from equation 2.40 and becomes

$$TI = 0.140 \left(\frac{U_0 D_0}{\nu} \right)^{-0.0790} \approx 0.075 = 7.5\% \quad (3.1)$$

Similarly, the outlet turbulence intensity can be calculated by performing a mass balance to estimate the outlet velocity. With $U_{out} = A_0 / A_{out} \cdot U_0$, the turbulence intensity becomes

$$TI = 0.140 \left(\frac{A_0 U_0 D_{out}}{\nu A_{out}} \right)^{-0.0790} \approx 0.090 = 9.0\% \quad (3.2)$$

Table 3.2: Boundary condition for simulation of thermal and isothermal jets

Boundary	Value	Comment
<i>Buoyant jet</i>		
Inlet air velocity, U_0	0.0044 m/s	$U \approx 0.2$ m/s at ceiling inlet
Supply air temperature buoyant jet, T_s	12°C	
Floor temperature, T_f (Dirichlet BC)	24°C	Except quadrant under jet
Remaining walls (Neuman BC)	$\frac{\partial T}{\partial x} = \frac{\partial T}{\partial y} = 0$	Included quadrant under jet
Outlet	Pressure outlet	
Inlet turbulent intensity, TI_{in}	7.5 %	
Outlet turbulent intensity, TI_{out}	9.0 %	
<i>Isothermal jet</i>		
Inlet air velocity, U_0	0.0044 m/s	$U \approx 0.2$ m/s at ceiling inlet
Inlet turbulent intensity, TI_{in}	7.5 %	
Outlet turbulent intensity, TI_{out}	9.0 %	

3.1.2 Active displacement ventilation

The geometrical model for the CFD simulations of active displacement ventilation is illustrated in figure 3.3, and the corresponding values are given in table 3.3. The BC is listed in table 3.4. A room with one inlet and one person is investigated. A simple design like this is convenient when comparing different ventilation methods. In the theory section we saw that simple geometrical models like this are normal when supply methods are investigated. For simplicity, the emissivity of all walls is set to 1 as suggested by Menchaca-Brandan et al. [54]. The CO_2 production and heat generation is taken for an adult at low activity work. The CO_2 production is modeled as a constant flow rate from a small circular opening with diameter d_{mouth} on the top of the cylinder. No heating is added for the simulations except for the heat generated by the cylinder representing a human. The inlet velocity and temperature will be varied to find the lowest possible airflow rate that satisfies the requirement for the thermal and atmospheric environment.

3.1. GEOMETRICAL MODEL AND BOUNDARY CONDITIONS

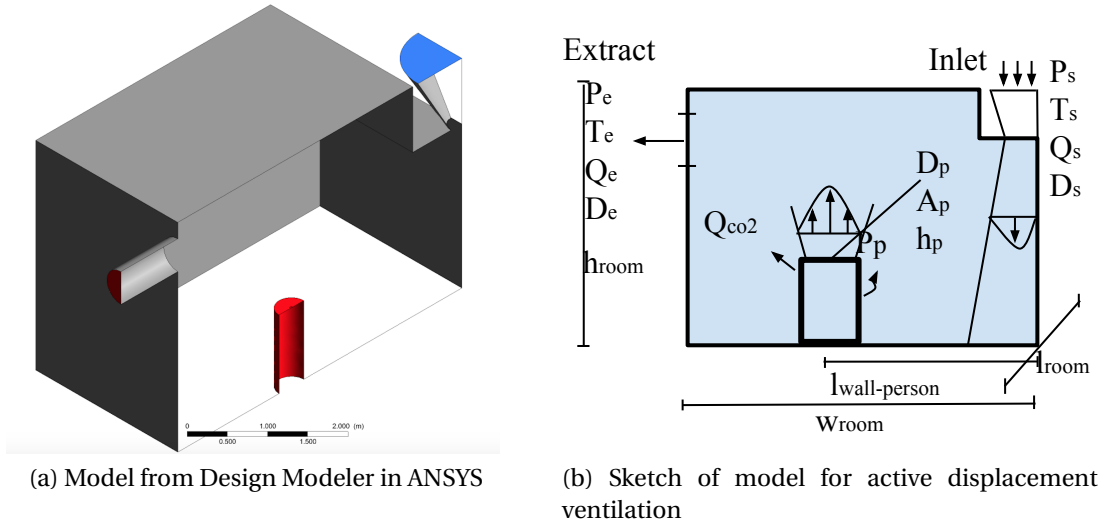


Figure 3.3: Geometrical model for simulation of active displacement ventilation

Table 3.3: Geometry for simulation of active displacement ventilation

Geometry	Value
Width room, w_{room}	5 m
Length room, l_{room}	5 m
Height room, h_{room}	5 m
Inlet radius, r_s	0.195 m
Extract diameter, D_e	1 m
Cone height, h_{cone}	1 m
Cone angle, θ_{cone}	60°
Area of person, A_p	1.8 m ²
Height person, h_p	1.2 m
Mouth opening, d_{mouth}	0.05 m
Length from wall to person, $l_{wall-person}$	3 m

Table 3.4: Boundary conditions for simulation of active displacement ventilation

Boundary condition	Value
<i>Inlet</i>	
Inlet airflow, Q_s	[5, 6, 7] l/s
Supply air velocity, V_s	[0.0833, 0.1, 0.1167] m/s
Supply air velocity cone, V_{cone}	[0.0053, 0.0064, 0.0075] m/s
Inlet air temperature, T_s	8-12°C
<i>Outlet</i>	
Outlet	Pressure outlet
Outlet hydraulic diameter	1 m
Outlet turbulent intensity	8.5 %
<i>Person</i>	
Total heat from person, P_p	100W = 55.55 W/m ²
Convective heat from person, P_{conv}	≈ 0.5 P_p = 50 W
Radiative heat from person, P_{rad}	50 W
CO ₂ production per person, Q_{CO_2}	0.02 m ³ /h
CO ₂ velocity, V_{mouth}	0.003 m/s
<i>Radiation</i>	
Emissivity for all surfaces	1

3.1.3 Model for ordinary displacement ventilation

In figure 3.4 (a) and (b) the geometrical model in Design Modeler and a sketch is presented. The geometry is similar as for active displacement ventilation except for the inlet. The boundary conditions are also the same except for the inlet. See table 3.5 and 3.6 for details of the geometry and boundary conditions.

Table 3.5: Geometry for simulation of ordinary displacement ventilation. The room geometry is as for active displacement ventilation

Geometry	Value
Height inlet, h_s	1 m
Width inlet, w_d	1 m
Area inlet, A_s	1 m ²
Room dimensions	See table 3.3
Outlet dimensions	See table 3.3
Person dimensions	See table 3.3

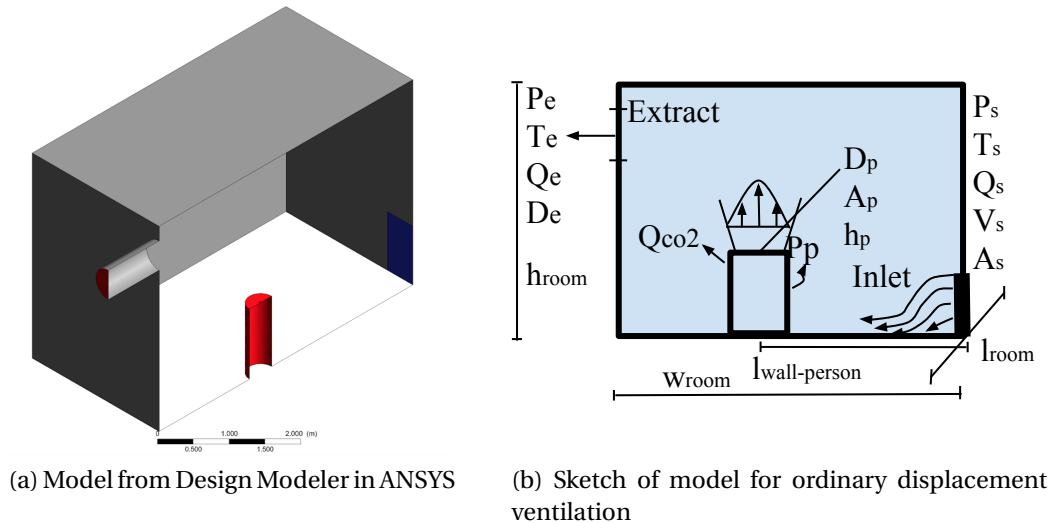


Figure 3.4: Geometrical model for simulation of displacement ventilation

Table 3.6: Boundary conditions for simulation of ordinary displacement ventilation

Boundary condition	Value
Supply air velocity, V_s	≈ 0.006 m/s
Inlet air temperature, T_s	18-19°C
Inlet airflow, Q_s	5-7 l/s
BC outlet	See table 3.4
BC person	See table 3.4
BC radiation	See table 3.4

3.2 Mesh

The mesh has been created and modified based on mesh quality indicators, inflation layer at walls (y^+ values), cell size and residuals. A refined grid has been chosen where large gradients are expected. The mesh for the jets and for active displacement ventilation can be seen in figure 3.5 (a) and (b). The mesh in figure 3.5 (a) is used both for the wall jet and for the free jet except for details near the wall.

The mesh quality indices are presented in table 3.7 and the values are within an acceptable range according to the ANSYS Theory manual [43]. The mesh for ordinary displacement ventilation is not included here, but are similar to the mesh in figure 3.5 (b) except for the inlet.

3.2. MESH

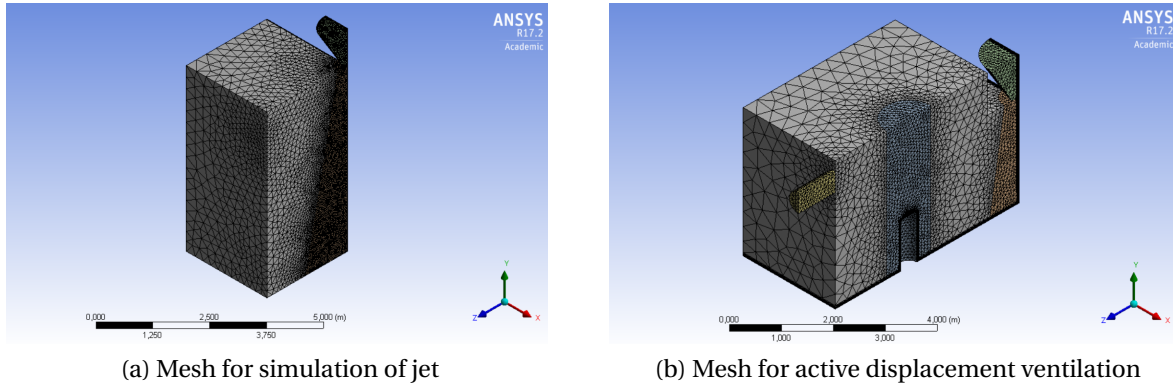


Figure 3.5: Mesh for simulation of jet and active displacement ventilation

Table 3.7: Boundary conditions for simulation of mixing ventilation

	Mesh for jet	Mesh for ADV
Orthogonal quality	0.27	0.23
Skewness	0.80	0.87

Based on equation 2.36 and 2.37 in section 2.6.3 y^+ can be estimated. The goal here is to find an estimate of the value of the first grid point to create a good inflation layer on the walls and floor where large gradients are expected. It is assumed that the velocity is approximately 0.1-0.3 m/s in the horizontal direction on the floor, and close to 0 m/s along the ceiling. The vertical velocity along the walls are also assumed to be close to 0 m/s. A velocity of 0.05 m/s is used in the calculations for the lowest velocity. For the wall jet, the velocity is approximately 0.6 m/s along the wall. The temperature is approximately 22°C, and the properties of air for this temperature is used. For the enhanced wall function, one does not need to be so accurate with the distance of the first node. However, the first node should ideally approximately correspond to $y^+ = 1$. Based on these approximations, the following first node values are calculated and presented in table 3.8.

Table 3.8: Distance of the first node for simulation of jet

	$y^+ = 1$
First layer thickness floor	0.0015 m
First layer thickness walls	0.0050 m
First layer thickness ceiling	0.0050 m
First layer thickness for wall jet	0.0006 m

The y^+ values at the wall at where the jet is are the most important. This wall will, therefore, be in focus when the y^+ values are checked in the next chapter.

When it comes to the element size, certain values were monitored as the grid was refined. For the jet, the sum of the velocity magnitude along the centerline from the inlet was used in the mesh independence test. The result is seen in figure 3.6. For the simulation, it was sufficient

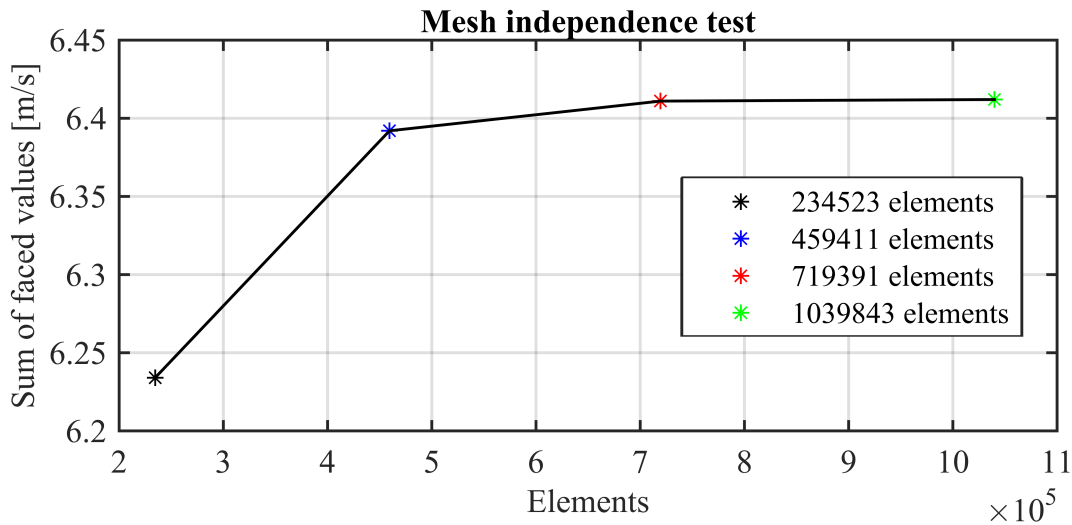


Figure 3.6: Mesh independence test for the simulation of the jet

with 719391 elements, and the solution converged after approximately 3000 iterations. This was the case for both the free jet and the wall jet.

For the simulation of active and ordinary displacement ventilation, the cell size had to be increased, and the number of elements decreased. The reason was very long computation time since both the equation for radiation and transportation of species were turned on. The domain was also twice as big since only one BC was symmetric. Ideally, symmetric BC should be avoided for this simulation as suggested by Nielsen [92]. More than 70,000 iterations were required for the monitored values to converge even for coarse grids, so the simulations had to be performed without a complete mesh independence test for this mesh due to the limitation of computational power and time. This is a weakness of the CFD simulations, and the consequences should be evaluated.

The requirement for the residuals for all simulations was that the value should be lower than $10E-03$, and for many cases they were less than $10E-04$. For the simulation of active displacement ventilation the solution did not converge with the SIMPLE Velocity-pressure coupling, so the Coupled pseudo-transient velocity-pressure coupling had to be used. This contributed in even longer computation time.

3.3 Setup

Two different turbulence models, the RNG $k-\epsilon$ and RKE, were investigated for the jet simulations. RNG $k-\epsilon$ was used for the simulation of active and ordinary displacement ventilation. The reason for using two models is that the literature study showed that these factors might have a large influence on the prediction of jet flows, and it was of the author's interest to examine in which degree this was true. Table 3.9 show the setup for the simulations done in this thesis.

Table 3.9: Setup for simulations

Setup	
<i>Simulation of jet</i>	
Energy equation	On for buoyant jet
Turbulence model	RNG/RKE
Wall function	Enhanced wall function
Pressure-velocity Coupling	SIMPLE
Density	Incompressible-ideal-gas for buoyant jet
Spatial discretization:	
Gradient	Least squares Cell Based
Pressure	Body Force Weighted
Momentum	Second order upwind
Turbulence Kinetic Energy	Second order upwind
Turbulent Dissipation Rate	Second order upwind
<i>Simulation of active and ordinary displacement ventilation</i>	
Energy equation	On for buoyant jet
Turbulence model	RNG $k - \epsilon$
Radiation	On
Transportation of species	On
Wall function	Enhanced wall function
Pressure velocity coupling	Coupled - Pseudo Transient
Density	Incompressible-ideal-gas
Spatial discretization:	Same as for jet simulations

3.4 Method for analyzing jets

Numerical results are extracted from ANSYS Fluent and analyzed further in Matlab. A research of the velocity profile, jet angle, similarity profile and pole distance is done for the jets. This is done by investigating cross-sectional lines of the jets. Only the velocity in y-direction will be investigated since empirical relations assumes that the flow is only in this direction. 20 horizontal lines will be used to find the similarity profile, jet angle, and pole distance. The horizontal lines are located from 2.0 m to 4.0 m from the inlet. The jet is assumed developed at 2.0 m since Skåret [1] suggested that the jet is developed after $6d_0$ to $10d_0$.

To calculate the similarity profile at these 20 distances the distance from the centerline at which the velocity has reached $U_{0.5} = U_{max}/2$ must be found. Then, the similarity profile and end point of the jet can be found from equation 2.4 by Abramovich [27].

The method used is to search through the velocity vector and find the two points U_i and U_{i+1}

3.5. METHOD FOR DESIGN OF ACTIVE DISPLACEMENT VENTILATION USING EMPIRICAL RELATIONS

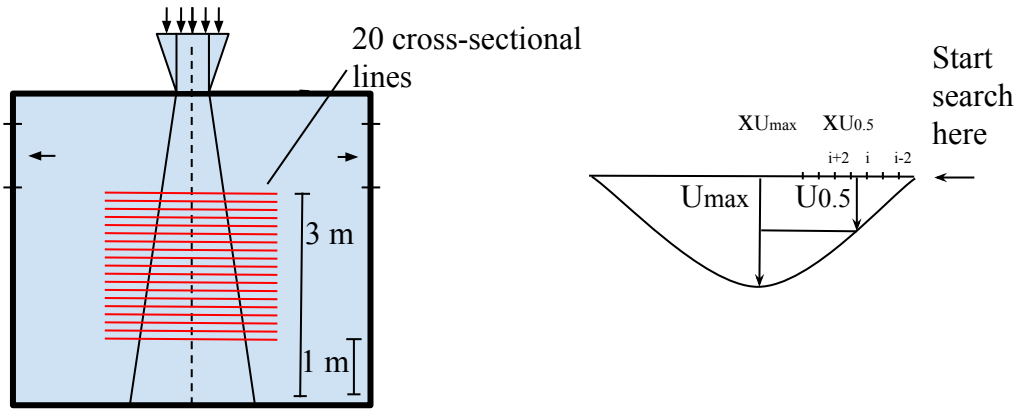


Figure 3.7: Illustration of method of analyzing jets

that satisfies $U_i < U_{0.5} < U_{i+1}$. By linear interpolation $x_{U_{0.5}}$ can be found from the equation

$$x_{U_{0.5}} = x_i + (U_{0.5} - U_i) \frac{x_{i+1} - x_i}{U_{i+1} - U_i} \quad (3.3)$$

Equation 2.4 can then be applied to calculate the width of the jet. Further, the angle of the jet can be calculated by linear regression using the built-in function *polyfit* in Matlab. The jet angle and pole distance is found from this regression line. The angle is expected to be between approximately 20° and 25° .

The local Archimedes number is simply calculated using the regression lines and the local temperature- and velocity difference.

3.5 Method for design of active displacement ventilation using empirical relations

In this section methods for the design of active displacement ventilation will be presented since cases of active displacement ventilation calculated from empirical relations, mass balance and heat balance will be compared to results from CFD simulations. The heat and mass balance for a room with active displacement ventilation give the following equations for calculating T_2 , $[CO_2]_2$ and $[CO_2]_1$:

$$T_2 = T_s + \frac{P_p}{\rho c_p Q_i} \quad (3.4)$$

$$[CO_2]_2 = [CO_2]_o + \frac{CO_2 \text{ production}}{\rho_{CO_2} Q_i} 10^6 \quad (3.5)$$

$$[CO_2]_1 = \frac{(Q_{strat} - Q_i)[CO_2]_2 + Q_i [CO_2]_o}{Q_{strat}} \quad (3.6)$$

3.6. METHOD FOR DESIGN OF DISPLACEMENT VENTILATION USING EMPIRICAL RELATIONS

All the walls are assumed insulated. T_s is the supply temperature, T_e is the exhaust temperature and equals the temperature T_2 in the upper zone, P_p is the power generated from the person in the room and Q_{strat} is the flow at the stratification line. The indices o , i and 2 stands for outside, inlet and upper zone.

Q_{strat} will depend on the supply airflow Q_i , the height of the diffusers, the number of diffusers and the convective plumes from the occupant. It is important that the inlet airflow rate ensures an acceptable concentration of CO_2 in the zone of occupancy. The height of the diffusers affects the degree of mixing with old air, the air velocity in the occupancy zone as well as the temperature and CO_2 concentration.

Q_{strat} is calculated by finding the height at where the flow in the positive vertical direction equals the flow in the negative vertical direction. The flow in the positive vertical direction is flow due to heat sources as persons, convectors, office equipment and other warm objects. The flow in the negative vertical direction is due to the buoyant jet from the supply air.

Appendix A.4 shows a simplified version of the main script of the Matlab program used for calculation of active displacement ventilation. The program is included to explain how the procedure of the design is done.

3.6 Method for design of displacement ventilation using empirical relations

Calculations for the design of displacement ventilation can be done with mass- and energy conservation of the lower and upper zone when the two zone model is applied. The supply airflow decides the height of the stratification line.

The concentration of CO_2 in the breathing zone sets the limitation for the airflow rate, and requirements for thermal comfort sets the limit for the inlet air temperature. The relations become

$$T_1 = T_0 \quad (3.7)$$

$$T_2 = T_s + \frac{P_{per}}{c_p \cdot \rho \cdot Q_i} \quad (3.8)$$

$$[CO_2]_1 = [CO_2]_o \quad (3.9)$$

$$[CO_2]_2 = [CO_2]_1 + \frac{[CO_2]_{prod}}{\rho_{CO_2} Q_i} 10^6 \quad (3.10)$$

P_{per} is heat from the occupants. Floor heating is not necessary if the heat from occupants cover the heating demand. The outside air temperature T_o will for winter conditions be low, and preheating of the air is essential. Typically the inlet air temperature for displacement ventilation is 17–19°C. The reason that the temperature can not be much lower is discomfort due to cold draught at ankles and low temperatures in the lower zone.

The CO_2 -concentration in the lower zone is the same as for the inlet air according to the two

zone model. The height of the stratification line must be decided and is important to discuss for the design of displacement ventilation.

The stratification line will always be at the height at where the flow leaving the control volume equals the inlet airflow. This means that

$$Q_i = \sum_1^n Q_{zone n} \quad (3.11)$$

where Q_{zone} is the airflow in/out of the upper surface of the control volume, and n is the number of flow elements, except from the inlet air, interacting with the control volume. This means that one is dependent on knowing the distribution of the sum of the airflows from the flow elements in the room. In the case where only one person is in the room, this will be the only flow element.

Immediately one will believe that the height of the head is a good height for the stratification level since one want fresh and tempered air in the breathing zone, but as we saw in section 2.2.1.2 and 2.2.1.3 a stratification line placed at a lower height is acceptable since fresh and tempered air is transported along the body and to the breathing zone. The following table is adapted from figure 2.3 by Sandberg [8].

Table 3.10: Ratio between concentration in the breathing zone and in the ambient at the same height adapted from figure 2.3 by Sandberg [8]

Airflow per person $\frac{\text{liter/s}}{\text{person}}$	Air change rate $\frac{\text{roomvol}}{h}$	$\frac{\text{concentration in the breathing zone}}{\text{concentration in the ambient}}$
5	0.9	0.5
6	1.1	0.44
8	1.5	0.32
10	1.8	0.24
12	2.2	0.2

If we take the inlet airflow 10 l/(s·person) as an example, we see that the concentration in the breathing zone is 0.24 times the concentration in the ambient. This means that one can accept the CO_2 -concentration in the ambient to be approximately 4 times higher than the requirement for CO_2 -concentration.

The temperature of the air in the breathing zone and along the body will be lower than the ambient of the same reason.

3.7 Method for design of complete mixing ventilation

In the designing of mixing ventilation one can either design with respect to IAQ or with respect to the thermal environment. Both airflows are calculated, and the highest airflow must be chosen for the design. In the case where the ventilation is not the only cooling or heating source, additional heating or cooling devices must be installed. A mass balance for

3.7. METHOD FOR DESIGN OF COMPLETE MIXING VENTILATION

CO_2 , and energy balance for the temperature gives:

$$[CO_2] = [CO_2]_o + \frac{[CO_2]_{prod}}{\rho_{CO_2} Q_s} 10^6 \quad (3.12)$$

$$T_{room} = T_s + \frac{P_{per} + P_{heat}}{c_p \rho Q_s} \quad (3.13)$$

where one solve the equations for Q_s to find the supply airflow. $[CO_2]$, $[CO_2]_o$ and $[CO_2]_{prod}$ are concentration of CO_2 outside [ppm], inside [ppm] and indoor production rate [kg/s]. The diffusers must be designed to ensure complete mixing, and the air entering the occupancy zone must have velocities and temperature within the requirements for draught. To ensure sufficient temperatures and avoid draught, a certain amount of air should be entrained before it reaches the zone of occupancy.

Results and discussion

The results will be presented in this section and discussed continuously. First, the results from the simulations of the buoyant and isothermal jets will be presented. Then, some cases of active displacement ventilation will be presented and compared to cases where empirical relations are used for the design. As a final discussion pros and cons of active displacement ventilation be discussed. The focus will be energy use, comparison with other supply methods, and suggestions on how the results in the thesis can be applied. The results will be presented in the following order:

- Simulation of buoyant jets
- Simulation of buoyant wall jets
- Simulation of isothermal jets
- Simulation of isothermal wall jets
- Simulation of active displacement ventilation
- Discussion and application of active displacement ventilation

4.1 Simulation of buoyant jet

In this section the simulation of a buoyant jet is compared to empirical relations and existing jet theory. Several aspects will be discussed, such as the similarity profile, jet angle, pole distance, velocity- and temperature distribution along the centerline and the Archimedes number. In addition, two different turbulence models, the RNG $k-\epsilon$ and RKE model, will be investigated since it is not clear from the literature study which method is best for ventilation applications and simulation of low-velocity air jets. The $k-\omega$ model will not be investigated further in this thesis even though this model also is popular for HVAC design.

4.1.1 Initial discussion of the simulations

Before comparing the result with empirical relations, an initial consideration of the results is done to adapt the empirical relations to the problem in the best way possible. Another reason for the initial consideration is to discuss whether the results are reasonable or not.

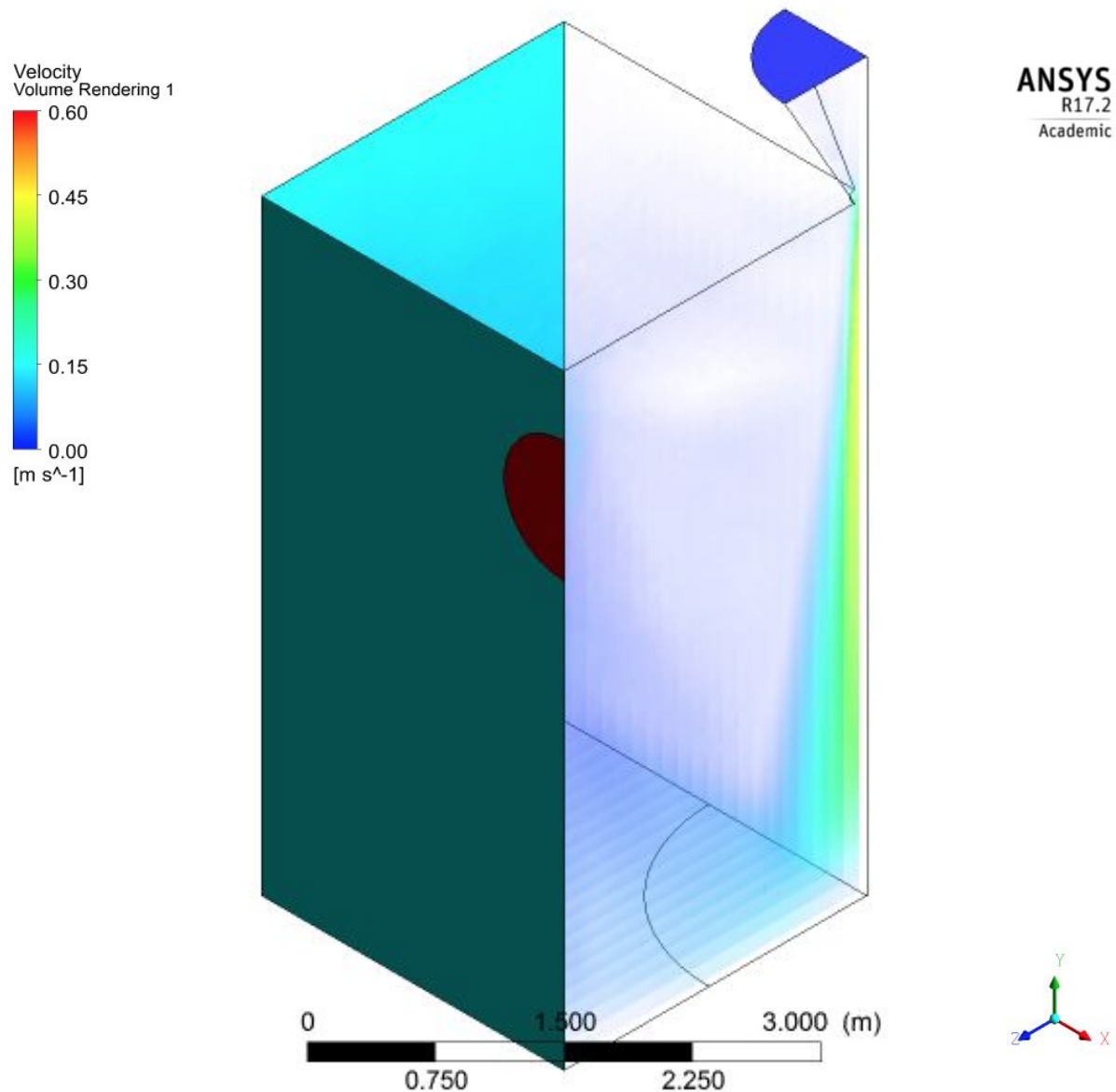


Figure 4.1: Contour of velocity magnitude (air speed) for a free buoyant jet. The light blue areas are walls, while the blank walls are symmetry surfaces

Figure 4.1 shows the rendering of the velocity for the simulation with the RKE model. This is a free buoyant jet, and the blank vertical walls are symmetry BC and not walls. The maximum velocity is almost 0.6 m/s, and the flow pattern is logical since the jet width increases and the maximum velocity seem to be in the middle of the jet and decreasing with the distance from the inlet. The width increases due to entrained air from the ambient. The contour plot of the velocity is presented in figure 4.2. The contour plot is taken from the simulation where the RKE model was used. We see how the jet accelerates the first meter along the centerline due to the buoyant forces before it slowly decelerates as it develops further. The velocity enters the room at approximately 0.2 m/s. This was the goal when the geometry and inlet BC was chosen for the cone. As the jet approaches the floor it spreads horizontally as expected.

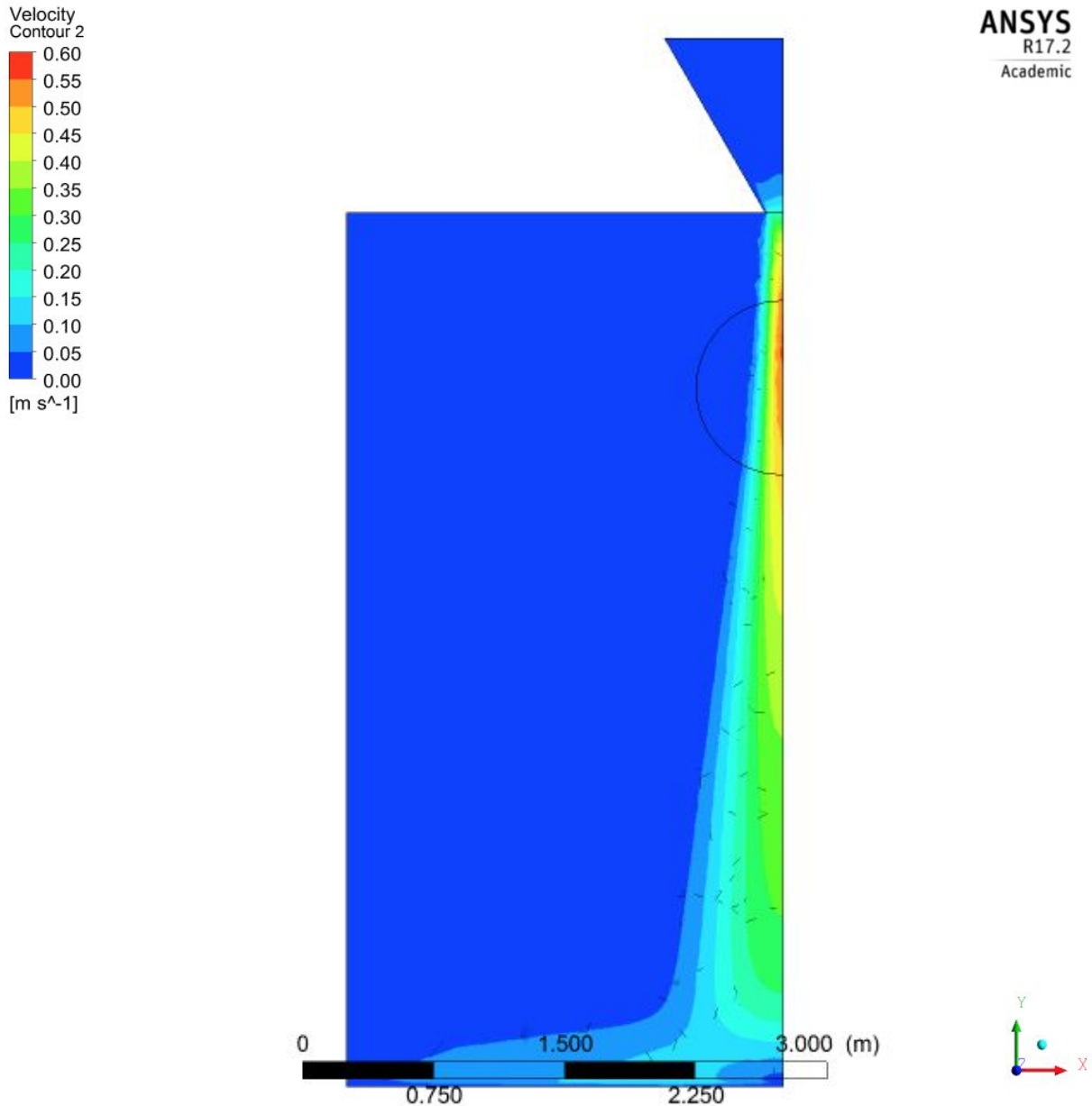


Figure 4.2: Contour of velocity magnitude (air speed) for free buoyant jet with RKE model in the plane $z = 0$

The temperature contour in figure 4.3 shows how the temperature of the center of the jet increases as it approaches the floor due to entrained air. The temperature in the ambient experience a sudden jump from 22.5°C to 23.5°C approximately 4 m over the floor. This is assumed to be the height of where the stratification line is, i.e., the flow rate in the negative direction equals the flow rate in the positive direction at this height. Since the radiation model is turned off in these simulations, a sudden temperature jump occurs as discussed in section 2.2.1.3. For the case with the radiation model turned on, a slower temperature increase is expected. Also, the temperature is unchanged through the cone, so choosing $T_0 = 12^{\circ}\text{C}$ for the empirical relations is reasonable.

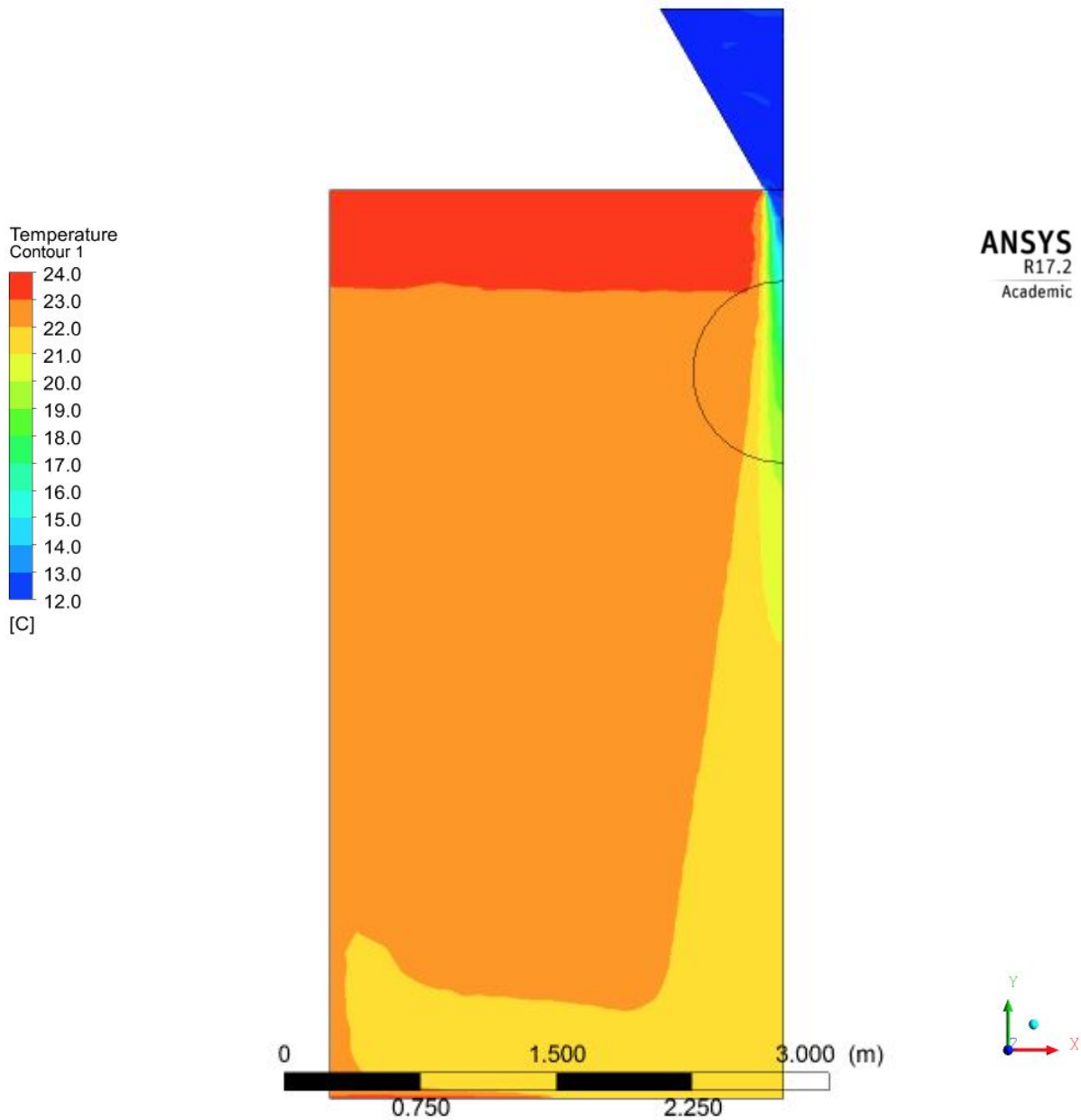


Figure 4.3: Contour of air temperature distribution for free buoyant jet with RKE model in the plane $z = 0$

Figure 4.5 show the temperature stratification in the room and show the same sudden jump at 4 m over the floor. The measurement is done between the jet centerline and the wall as indicated on the figure in the bottom right corner of the figure. It is assumed that the jet is not directly influencing the temperature on this line and that this can be considered as the ambient temperature. We see that the room temperature is approximately 22.5°C between 0.5 m and 4 m over the floor. This temperature will, therefore, be used when comparing the simulation to empirical relations.

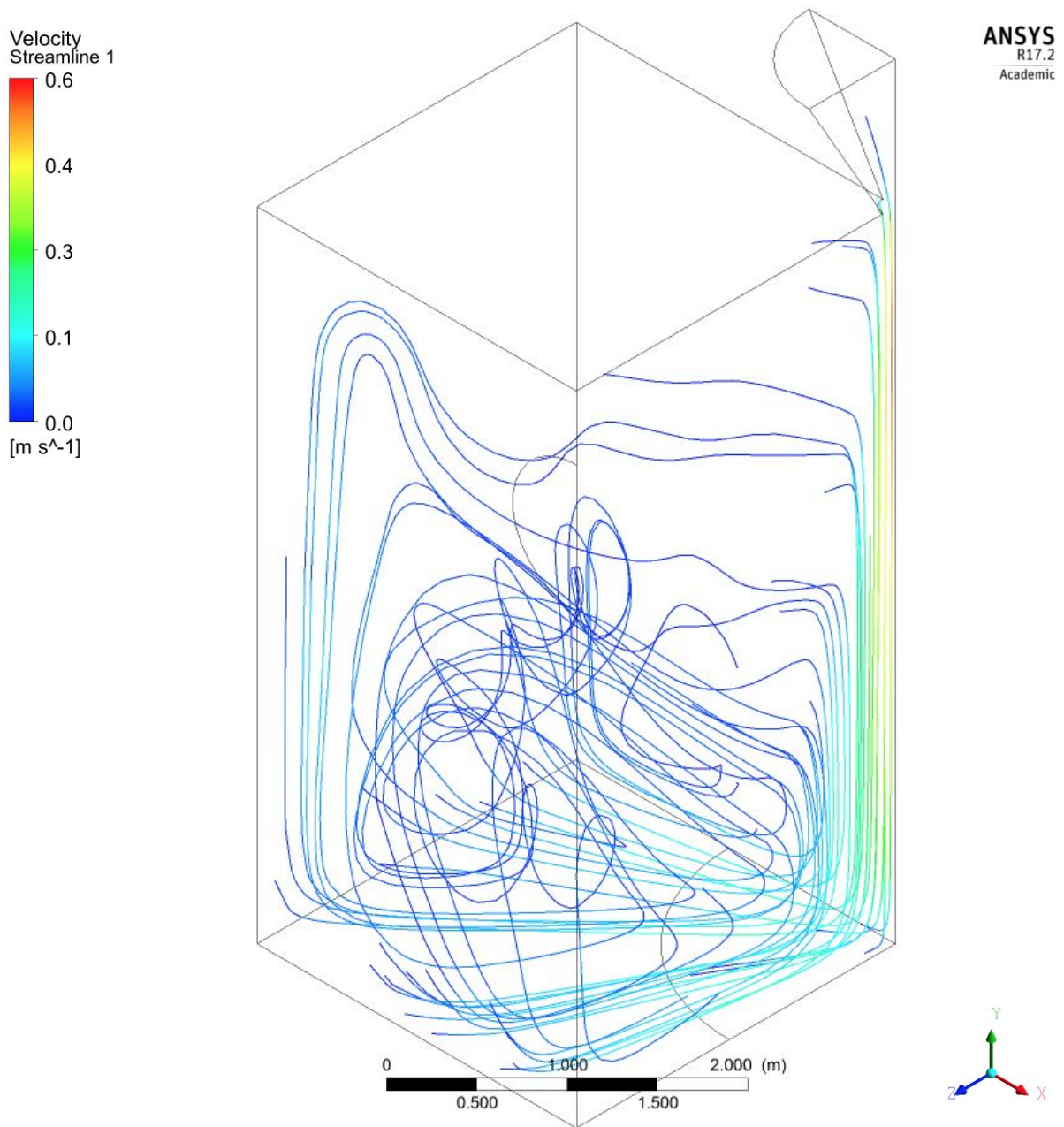


Figure 4.4: Plot of streamlines for buoyant jet

In figure 4.4 streamlines are illustrating the flow pattern in the room. We see how the air circulates, and that even though the room has a length of 5 m, air particles are in movement in the entire room. The room should ideally be even larger if the idealized situation for the empirical relations should be constructed. From the streamlines, it is obvious that air is entrained as the jet approaches the floor.

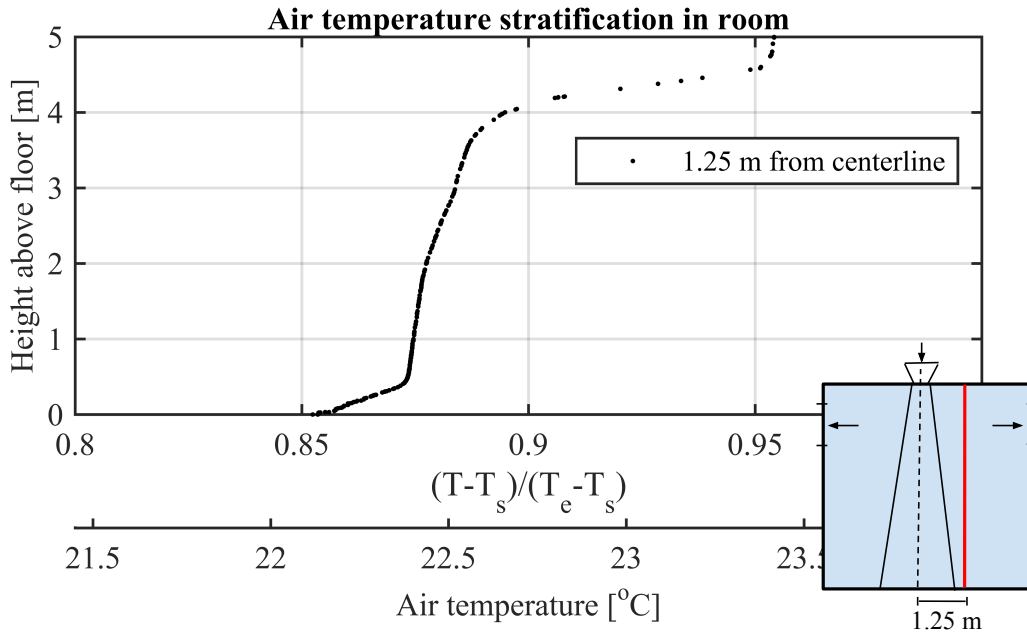


Figure 4.5: Vertical temperature stratification 1.25 m from jet centerline

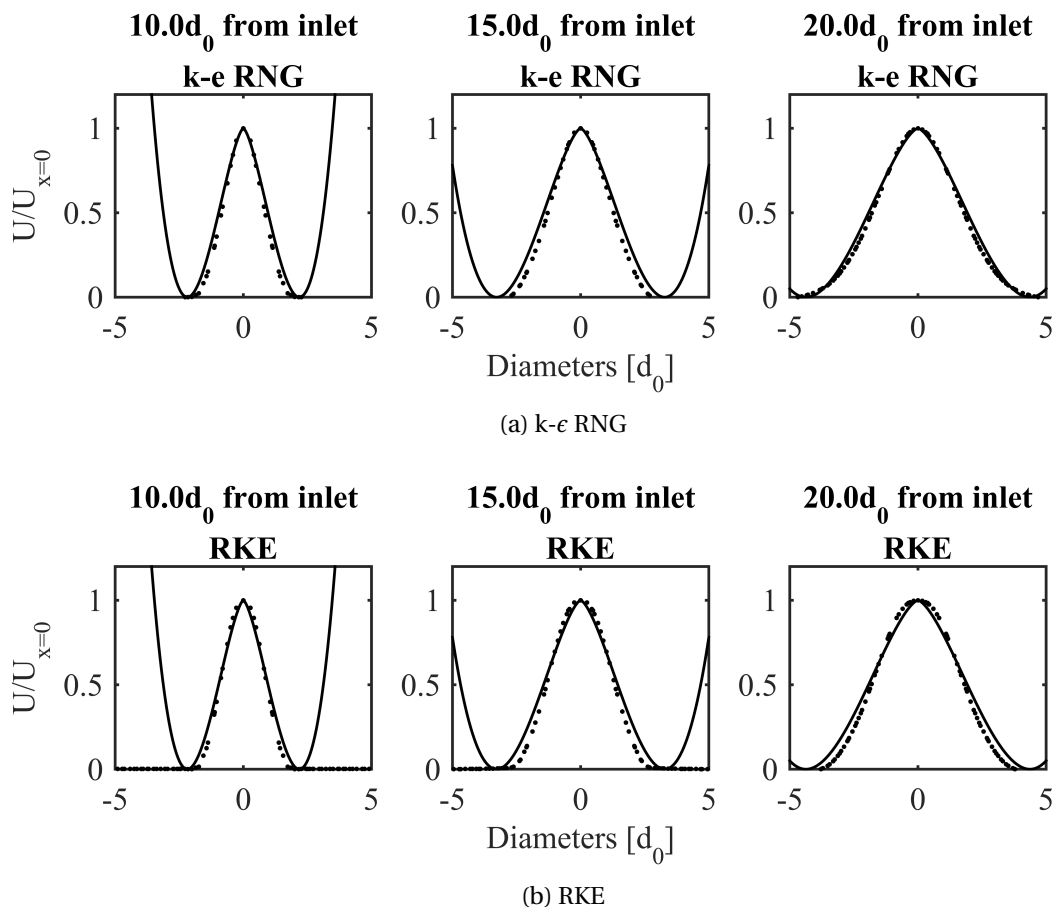


Figure 4.6: Analysis of spreading of buoyant horizontal jet for two different $k-\epsilon$ turbulence models. Dotted lines are from CFD simulations, while the solid lines are equation by Abramovich [27]

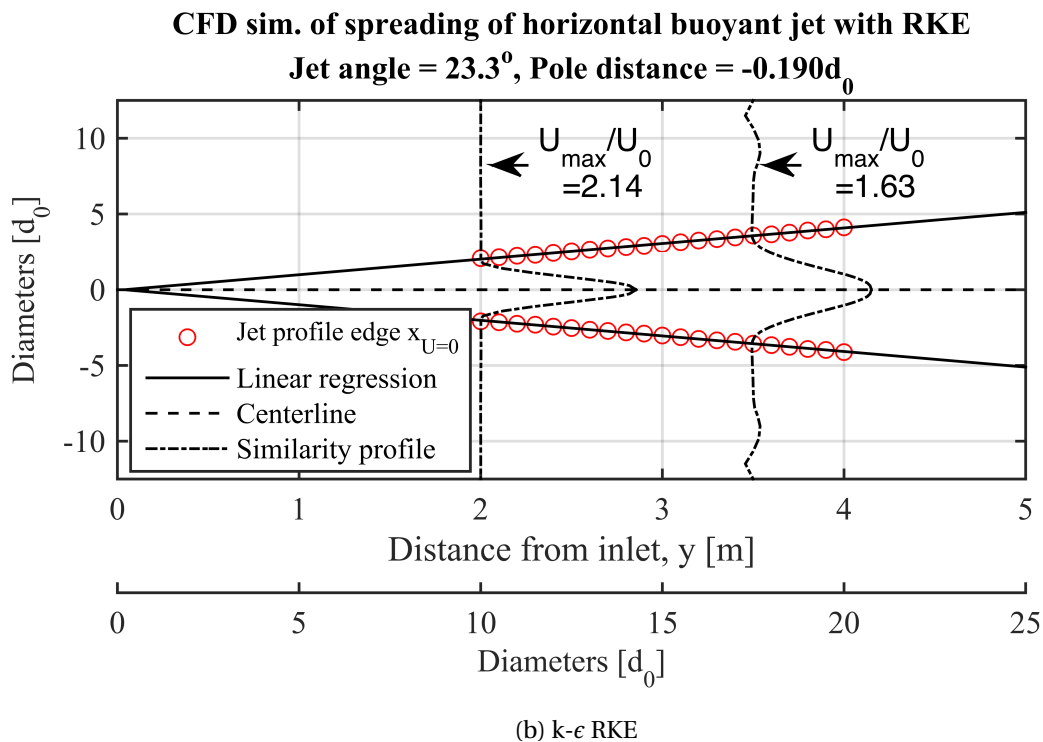
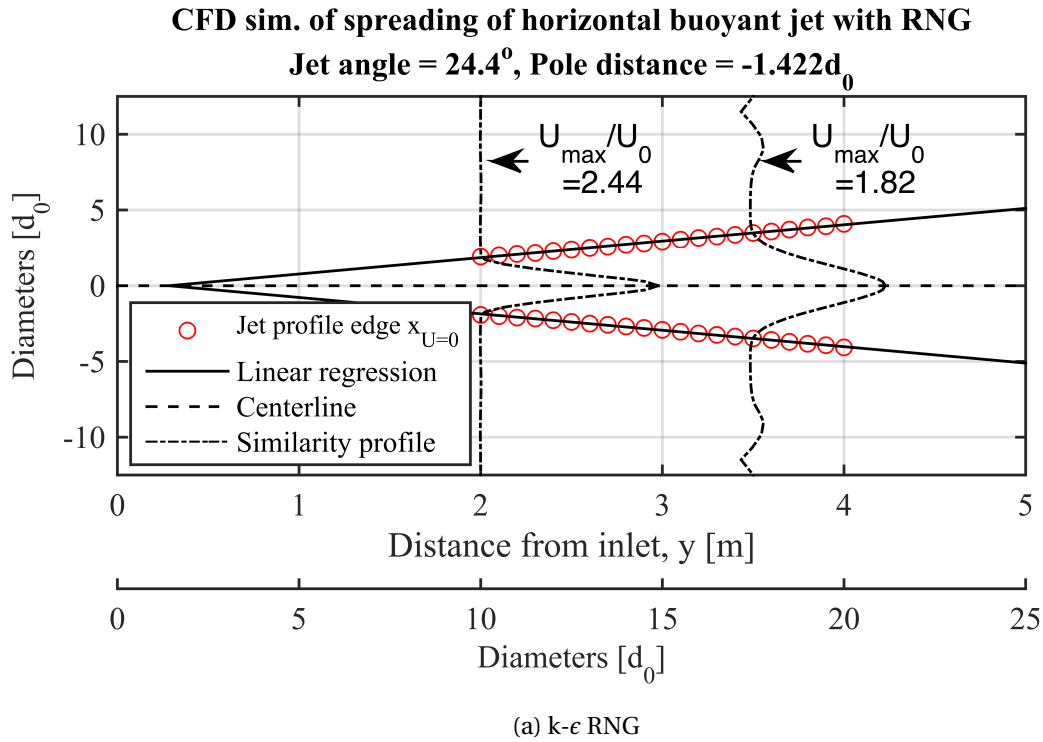


Figure 4.7: Analysis of spreading of buoyant horizontal jet for two different k- ϵ turbulence models

4.1.2 Similarity profile, jet angle and pole distance

So far the inlet velocity, inlet temperature, and the ambient temperature is found for the simulations and will be used for the empirical relations. One also need information about the pole distance, jet angle and similarity profile to know how to adapt the empirical relation to the CFD simulations.

The similarity profiles from the simulations are plotted together with the relation for similarity profile developed by Abramovich [27] in figure 4.6 (a) and (b) for $y=10d_0$, $15d_0$ and $20d_0$. Both the RNG $k-\epsilon$ and RKE model coincide very well with this equation, and it is hard to say which method is the most equal to the relation for the similarity region. It is clear that the jet is fully developed at these distances from the jet inlet. In some of the plots in figure 4.6 the velocity profile developed by Abramovich seem to go towards infinity when the width goes to $\pm 5d_0$. This area is not valid for the equation, and should not be used for the comparison.

Figure 4.7 show a graphical illustration of the spreading of the jet where 4.7 (a) is for the RNG $k-\epsilon$ model and 4.7 (b) is for the RKE-model. Horizontal lines between $20d_0$ and $40d_0$ are used for the analysis. See section 3.4 for the description of the analysis method. In the graphical illustration, the red circles are calculated values of the jet edge for 20 distances from the inlet. By linear regression, the jet angle and pole distance are found. The calculated jet angle and pole distance are stated in the figure title.

Both turbulence models give reasonable results when it comes to the jet angle since an angle between 20° and 25° where expected (half angle ca. $10-12.5^\circ$). The pole distance is somewhat lower than expected. In the theory section we saw that the pole distance was assumed to be between $0.7d_0$ and $2.25d_0$. For these simulations, the pole distance is $\approx -0.2d_0$ for the RKE-model and $\approx -1.4d_0$ for the RNG-model. The reason could be that inlet design is causing the flow to use more time than expected to develop, and therefore decreasing the pole distance. From both the figures we see that $U_{max}(y)/U_0$ decreases from $10d_0$ to $17d_0$ while the jet width increases. The maximum velocity $U_{max}(y)/U_0$ is slightly larger for the RNG $k-\epsilon$ model than the RKE model. For these simulations, the only difference in the setup is the turbulence model, and the same mesh is used.

Table 4.1: Values inserted in empirical relations

Inlet temperature	$12^\circ C$
Ambient temperature	$22.5^\circ C$
Inlet velocity	0.2 m/s
Pole distance	$0d_0$
Jet angle	12.5°

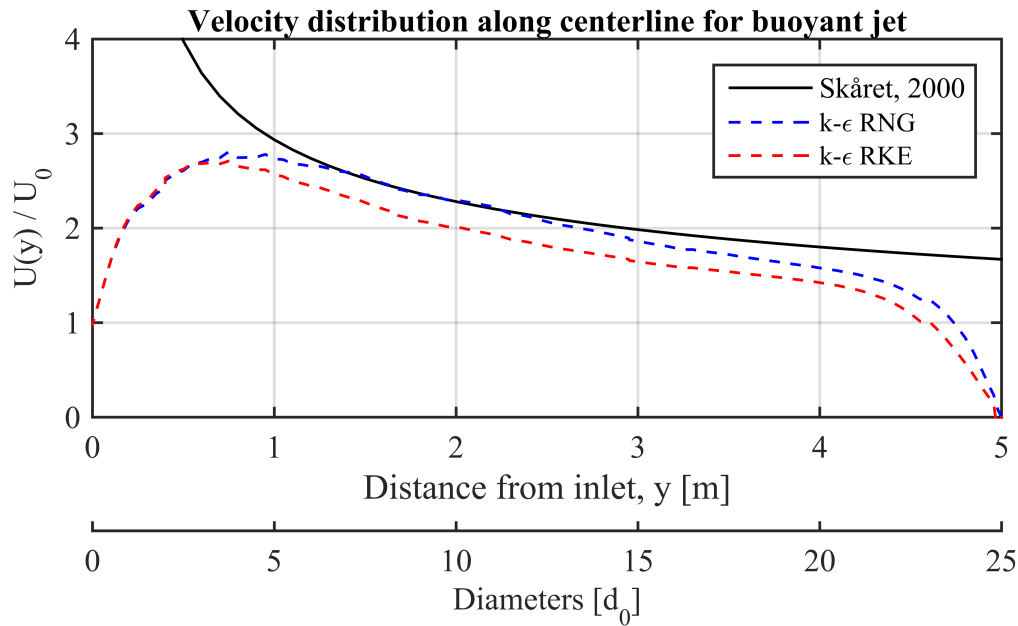


Figure 4.8: Velocity in horizontal direction along centerline for free buoyant jet

4.1.3 Centerline distribution

The y-velocity along the centerline for the RNG k- ϵ and RKE model is plotted together with the empirical relation for buoyant jets developed by Skåret [1] in figure 4.8 where the x-axis show both diameters and meters from the inlet plotted against U/U_0 . Table 4.1 shows which parameters that are used for the empirical relations. The RNG k- ϵ model shows a slightly better match than the RKE model with this empirical relation which seems to underpredict the velocity. As the jet approaches the floor, the velocity decreases and reaches 0 at the floor as expected. According to this simulation, the main effect of the floor starts approximately 0.5 m over the floor.

Figure 4.9 show the relative temperature along the centerline for the two turbulence models. Both the RNG k- ϵ and RKE model seem to give the same result as the empirical relation when the pole distance is $0d_0$. For both the velocity and temperature the empirical relation is valid after approximately 5-6 diameters from the inlet. Skåret [1] suggested that the jet was developed after 6-10 diameters, so the CFD simulations coincide with the literature.

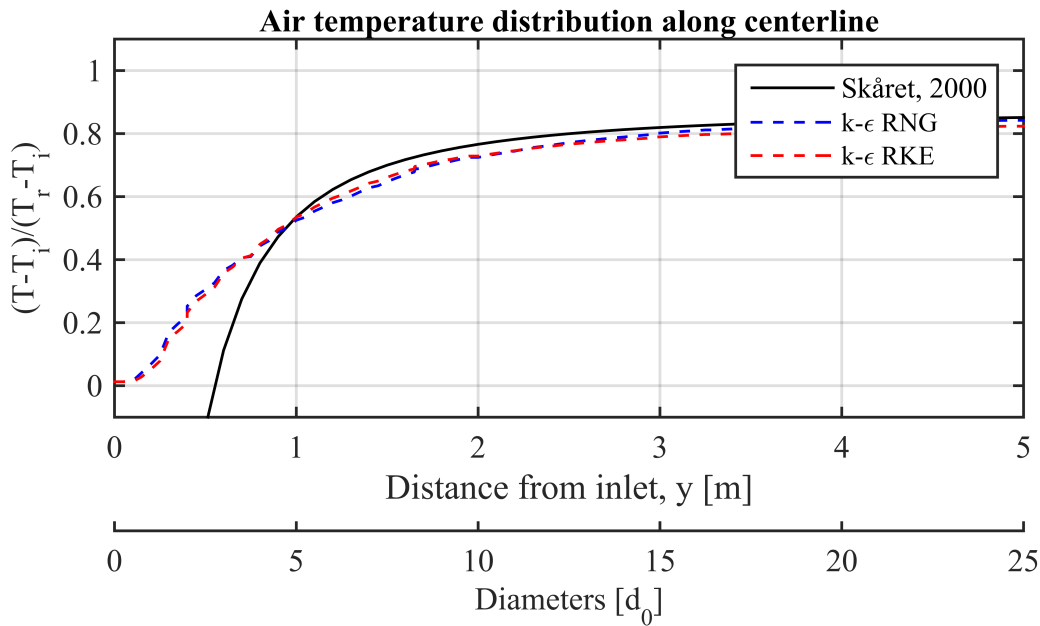


Figure 4.9: Temperature distribution along centerline for free buoyant jet

4.1.4 Local Archimedes number

The local Archimedes number is plotted for the centerline. Equations from section 2.5.1 are used. From figure 4.10 we see how the local Archimedes number for the vertical buoyant jet changes with the distance from the inlet. The jet width is calculated from the results in section 4.1.2 and the width b_x is defined as $b_x = \max(d_0, b_x)$ to avoid negative Archimedes numbers in the core region. As the relative change in the velocity is larger than the relative change in temperature for the first diameters the local Archimedes number will decrease. After approximately 5 diameters the Archimedes is close to 0.2, and it increases slowly as the jet approaches the floor. When the jet reaches the floor, the velocity is decreasing rapidly, while the temperature is unchanged. This causes the Archimedes number to go towards infinity.

The local Archimedes number calculated from empirical relations is also shown in the figure. The region between approximately 5 diameters and 20 diameters are of interest when the plots are compared since this area is not affected by the core region or the floor. The empirical relations give slightly lower values. From figure 4.8 and 4.9 it is clear that the difference in the centerline velocity is the reason. Since U_m is squared in the relation for the Archimedes number, small differences as in figure 4.8 have a large impact on the result.

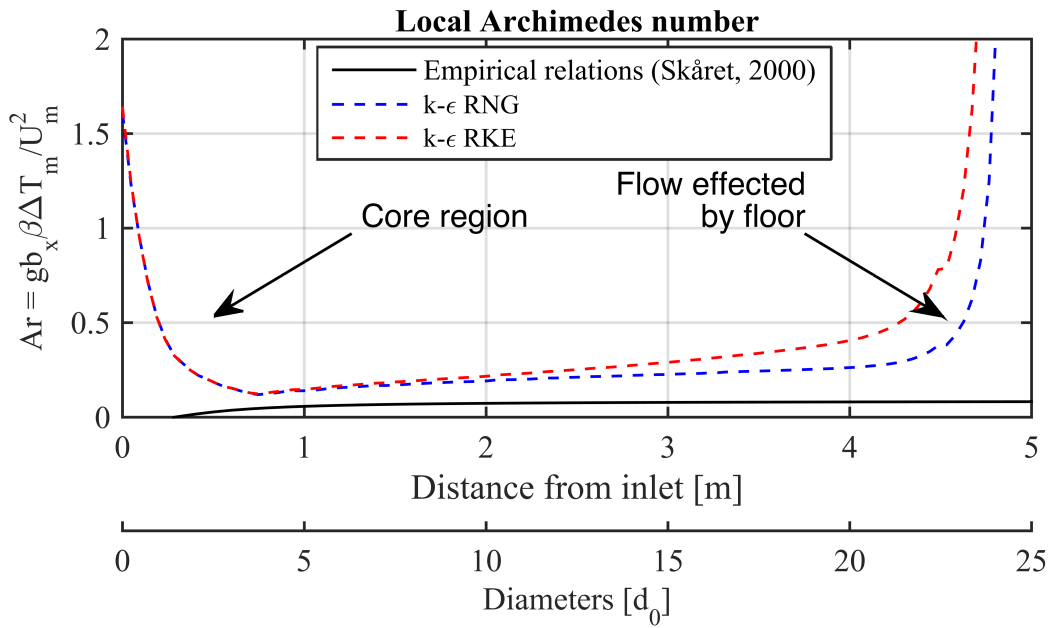


Figure 4.10: Local Archimedes number for buoyant jets

4.2 Simulation of buoyant wall jet

In this section we will look at a situation where the buoyant jet is placed next to a wall. All other conditions, geometrical and BC, are the same. The simulations will hopefully reveal how the wall will affect such a flow. The RNG $k-\epsilon$ model will be used for the simulations.

4.2.1 Validation of mesh

Before investigating the results, the y^+ -value for the wall is checked. Figure 4.11 show that y^+ is between approximately 0.8 and 1.5 in the jet region. These values are within the recommended range for the enhanced wall function, and the values coincide with studied literature.

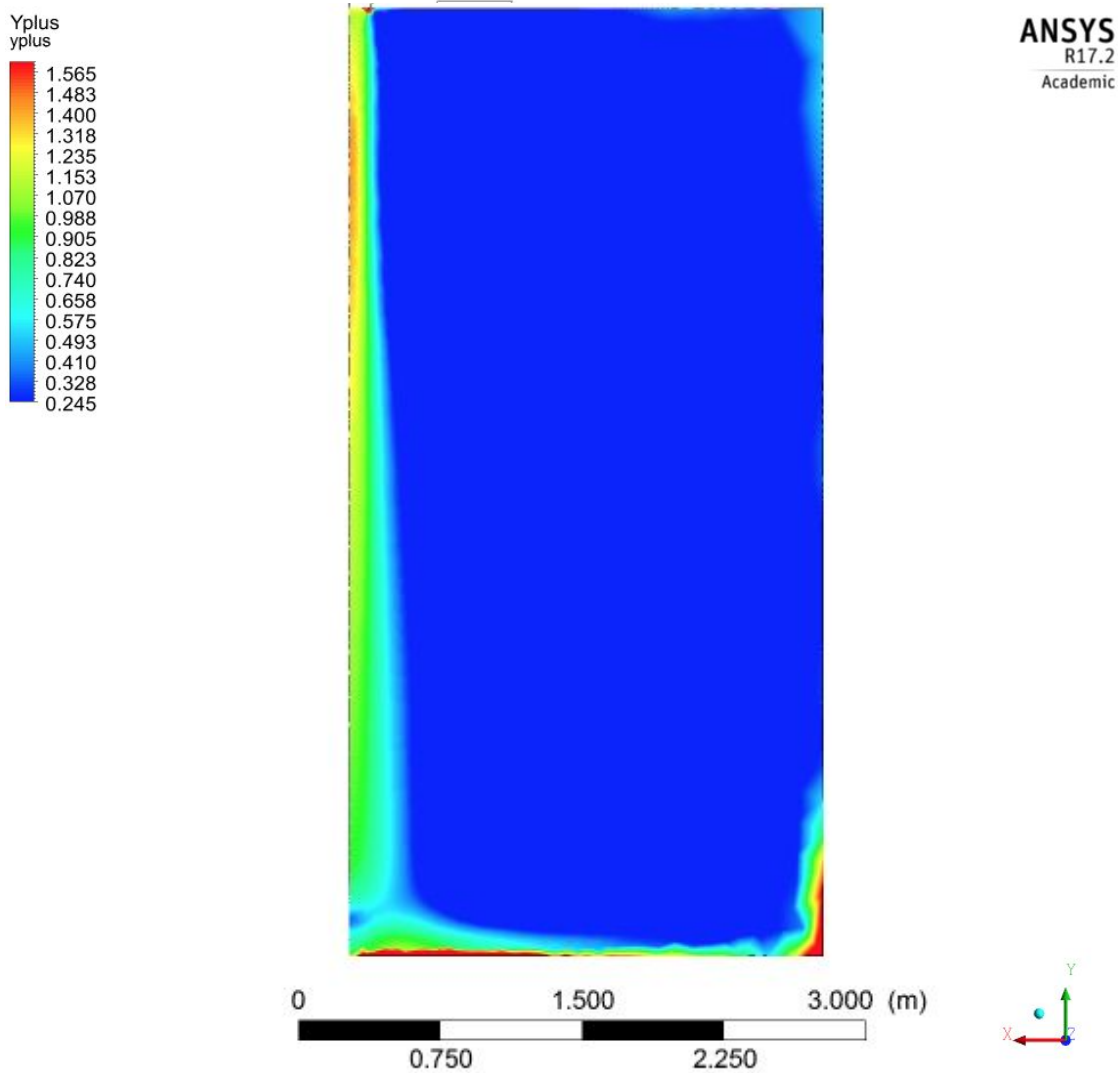


Figure 4.11: Contour of y^+ for the buoyant wall jets

4.2.2 Comparison of buoyant wall jet and free buoyant jet

The simulation of the wall jet is compared to simulations without wall and the empirical relation for positive buoyant jet velocity by Skåret [1]. For the empirical relations, the friction is neglected, and the relations are used as for free jets. The velocity of the wall jet is taken from where the maximum velocity is which is approximately 1.5 cm from the wall. Surprisingly, the simulation of the wall jet shows higher maximum velocity than the simulation without a wall. Due to wall friction, one would expect the wall jet to have a slightly lower velocity. Figure 4.12 shows how the wall jet is approximately $0.5U/U_0$ larger than the free jet between 10 and $25d_0$ from the inlet.

The plot of the temperature distribution in figure 4.13 for the free jet and wall jet show the same problem. The temperature for the wall jet is lower. It makes sense that the temperature is lower for the jet with the highest velocity since it is the buoyant forces that cause the

velocity, but the fact that it is the wall jet that has the highest velocity seems incorrect.

The results are investigated further. To see whether the mass balance seems correct, the velocity in y-direction 2.5m over the floor is plotted against the distance from the wall. This is illustrated in figure 4.14. We see how $U(y)/U_0$ is negative after 0.4 m from the wall, and that $U(y)/U_0$ is 0 both at 0m and 2.5 m from the wall. The plot is very steep at the wall which makes it hard to see that $U(y)/U_0$ is 0 at 0m from the wall. This plot indicates that the air circulates back up to the exhaust after it has reached the floor which is the behavior one would expect for a wall jet.

When air flows along a wall the displacement thickness increases as the distance from the inlet increases. Also, the boundary layer thickness increases. Figure 4.15 shows how the distance between the wall and the line of maximum velocity increases with the distance from the jet inlet. This coincides with the theory about displacement thickness since the flow is deflecting. The displacement thickness is not assumed to play any role in the explanation of the error in the velocity and temperature distribution. The line of U_{max} is calculated from 20 cross section lines between 10 and 20 diameters from the inlet. The line is extended giving a distance between the line of maximum velocity and the wall 1.17 cm at $y = 0$ m, and a width 1.88 cm at the floor.

Figure 4.16 show the similarity profile of the wall jet and half the similarity profile of the free jet. The profiles are taken 10, 15 and 20 diameters from the inlet. We see how the maximum velocity is higher for the wall jet, and that the difference decreases as we approach the edge of the jet. This can indicate that the mass balance still yields for the simulation.

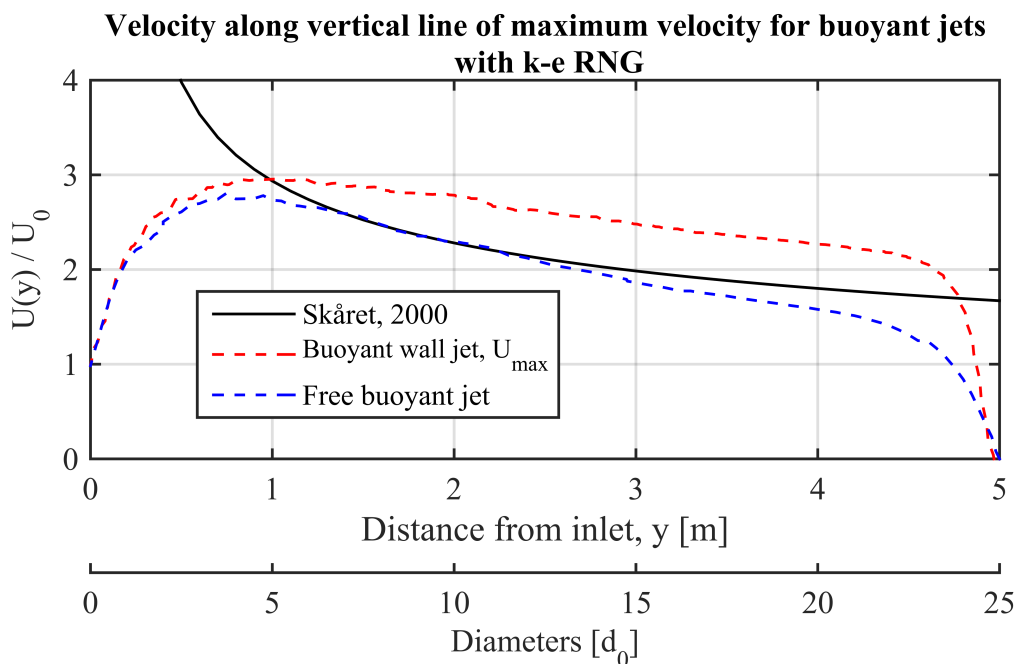


Figure 4.12: CFD simulation of free buoyant jet and buoyant jet along wall compared to empirical relation by Skåret [1]

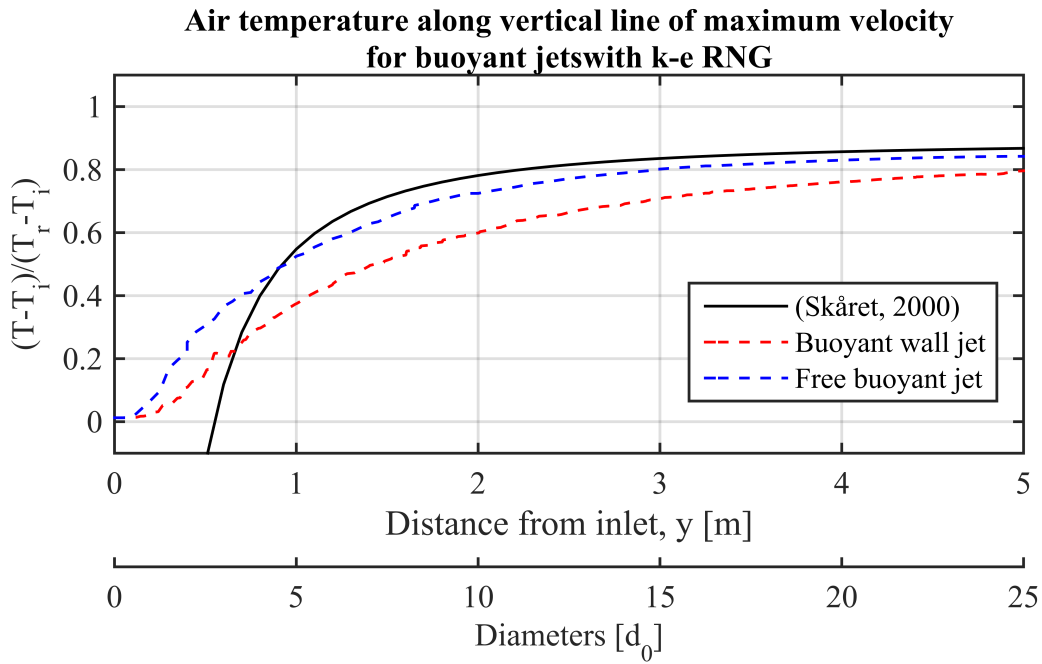


Figure 4.13: CFD simulation of free buoyant jet and buoyant jet along wall compared to empirical relation by Skåret [1]

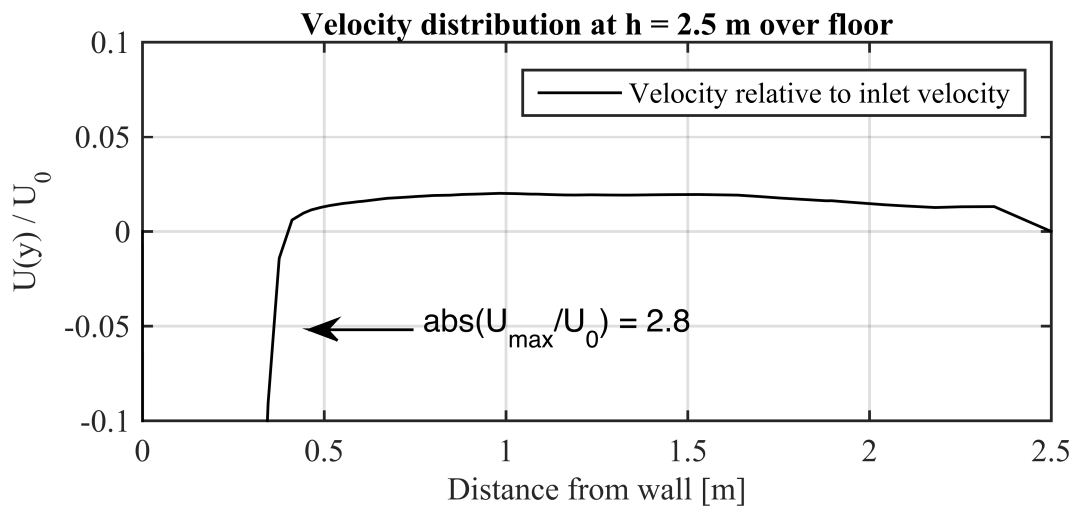


Figure 4.14: Relative velocity in y-direction 2.5m over the floor

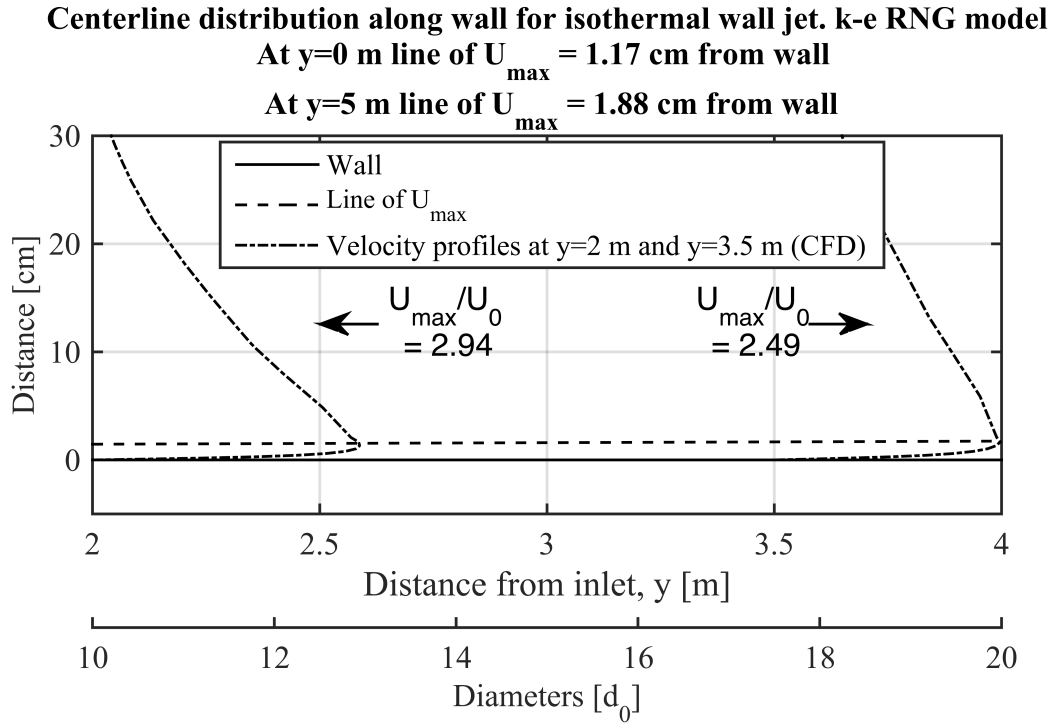


Figure 4.15: Shifting of centerline for isothermal wall jets

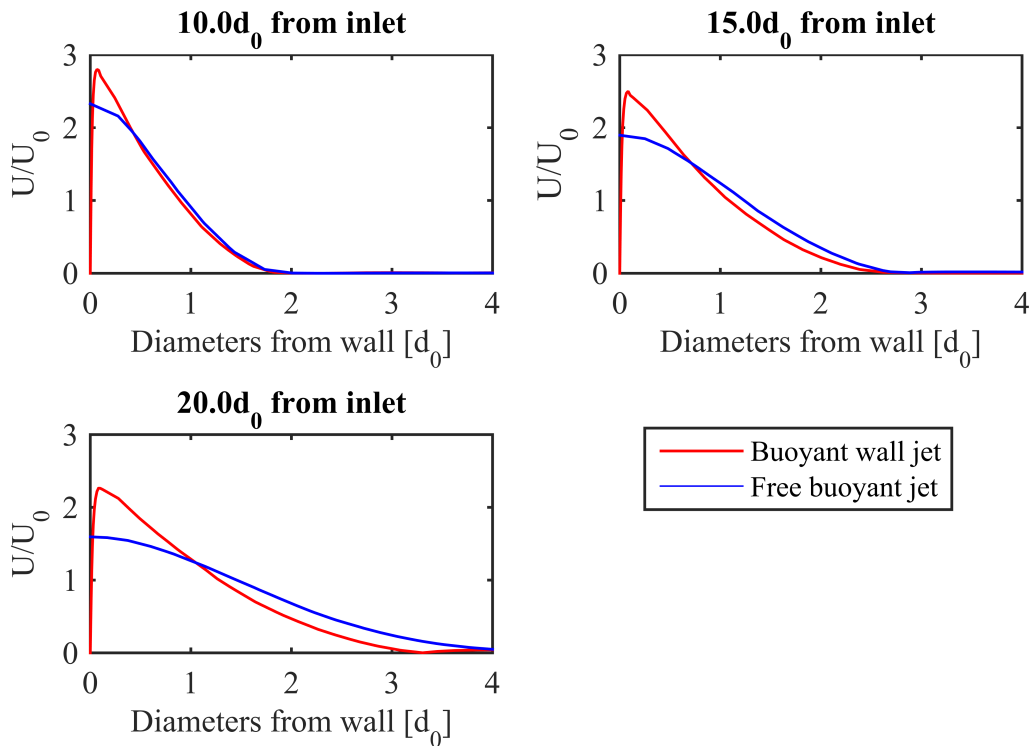


Figure 4.16: Velocity profile for free buoyant jet and buoyant wall jet

4.2.3 Discussion of errors

It is not clear to the author why the velocity is larger, and the temperature is lower at the line of maximum velocity for the buoyant wall jet compared to the free buoyant jet. From the comparison of the velocity in figure 4.12 and temperature in figure 4.13 one see how the velocities and temperatures are equal for the first diameters from the inlet. This indicates that it is not the inlet geometry or inlet BC that causes the error, but rather factors such as a mesh with poor quality, wrong choice of settings and/or wrong choice of turbulence model. Since the results obtained in this section does not correspond to what is expected from a real scenario, the problem is assumed to come from inaccurate/ failed CFD simulations and not from the physical behavior of the flow. The free buoyant jet coincided well with the empirical relations, so the error is assumed to lie on the simulation of the wall jet.

Since the temperature is lower for the buoyant wall jet after approximately 4 diameters, it is assumed that the choice of turbulence model or other solver settings contribute to errors in the heat transfer from the ambient to the jet. It is assumed that it is the heat transfer due to diffusion that is the main problem since this is the major heat transfer for such a jet. If there is a too little amount of entrained air, the velocity will increase as the jet is approaching the floor since the temperature is lower and the buoyant forces are larger. The error will then increase with the distance from the jet as figure 4.12 and 4.13 show. It is the turbulence model that is responsible for calculating the air entrainment close to the wall. In the literature study in section 2.7.3, we saw that it had been problems with the k- ϵ -model for wall jets in other CFD studies. This is so far the main hypothesis for the error. As we will see in the next section it is assumed to be other errors than the heat transfer in the calculation of wall jets since problems also occur for isothermal jets.

4.3 Simulation of isothermal jets

In this section, both free isothermal jets and isothermal wall jets will be investigated. Figure 4.17 show the velocity along the centerline for the CFD simulation compared to the empirical relation in equation 2.7. The plots are coincidental with one other, and it is hard to tell whether the RNG k- ϵ or RKE model is recommended for simulation of such jets. The jet angle and pole distance for the RNG-model are calculated and illustrated in figure 4.18. The jet angle is 23.9° , and the pole distance is $5.672d_0$. The jet angle is as expected, while the pole distance is higher than for the buoyant jet. From figure 4.17 we also see that the empirical relation yield after approximately $3-5d_0$. This is less than for the buoyant jet. For isothermal jets, the momentum is preserved along the jet. Figure 4.18 indicate this since $U_{max}(y)/U_0$ decreases as the jet area increases.

A wall jet is also investigated for isothermal flow. Also here the line of maximum velocity is shifted away from the wall due to the increasing displacement thickness as illustrated in figure 4.19. At $y=0$ m the distance between velocity maximum and the wall is 3.43 cm, while at $y=5$ m the distance is 7.05 cm. The values are calculated in the same way as for the buoyant wall jet, i.e. from 20 horizontal lines between $10d_0$ and $20d_0$ are used to calculate the values.

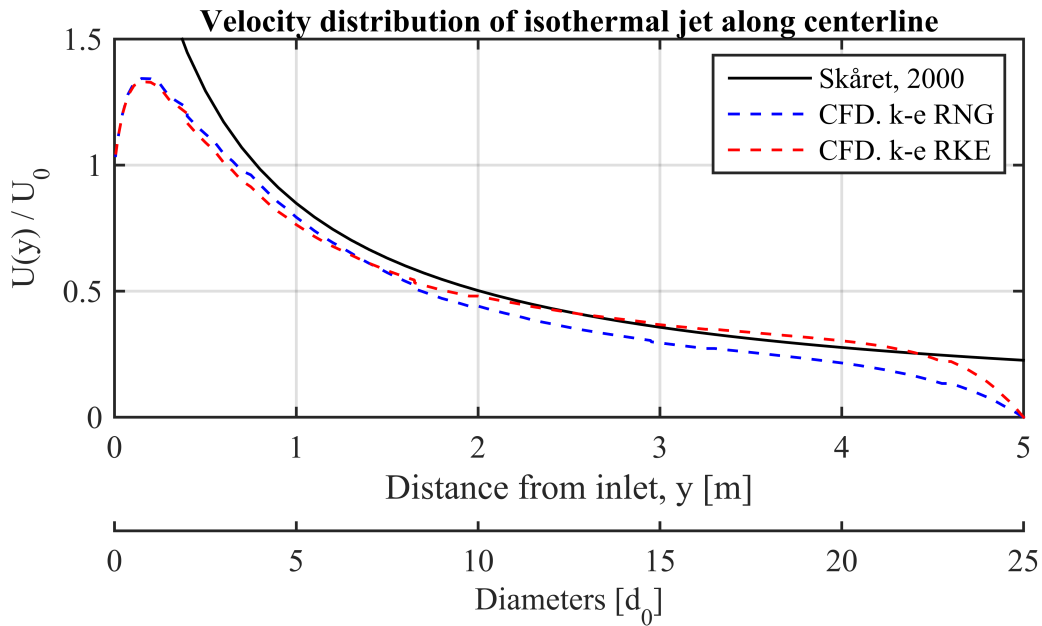


Figure 4.17: CFD simulation of free isothermal jet and isothermal jet along wall compared to empirical relation by Skåret [1]

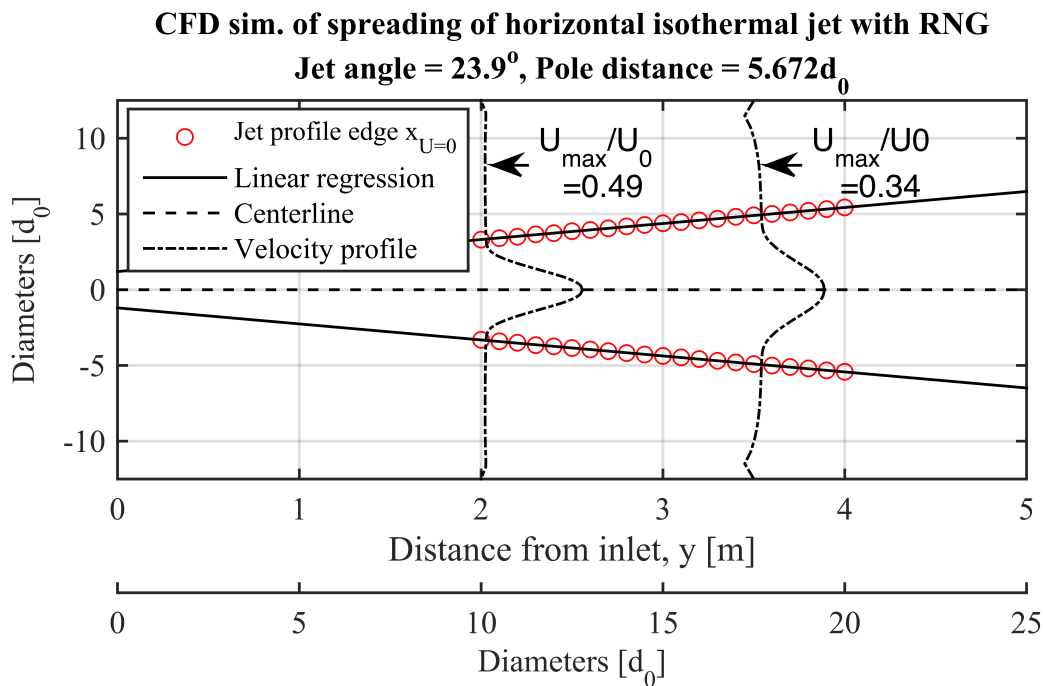


Figure 4.18: CFD simulation and analysis of the velocity profile development of an isothermal free jet with k- ϵ RNG model

The wall jet for the isothermal jet has the same tendency as the buoyant wall jet, namely that the wall jet has a higher velocity than the free jet. See figure 4.20. The difference is not as big as for the buoyant jet, but big enough to conclude that something is wrong with

4.3. SIMULATION OF ISOTHERMAL JETS

the numerical solution. The same mesh is used for the buoyant and isothermal wall jet, and the only difference in the setup it that the energy equation and the incompressible ideal gas law for the density is turned off. The fact that the error is decreased when the jet isothermal strengthens the assumption that the heat transfer in the buoyant jet is not calculated correctly.

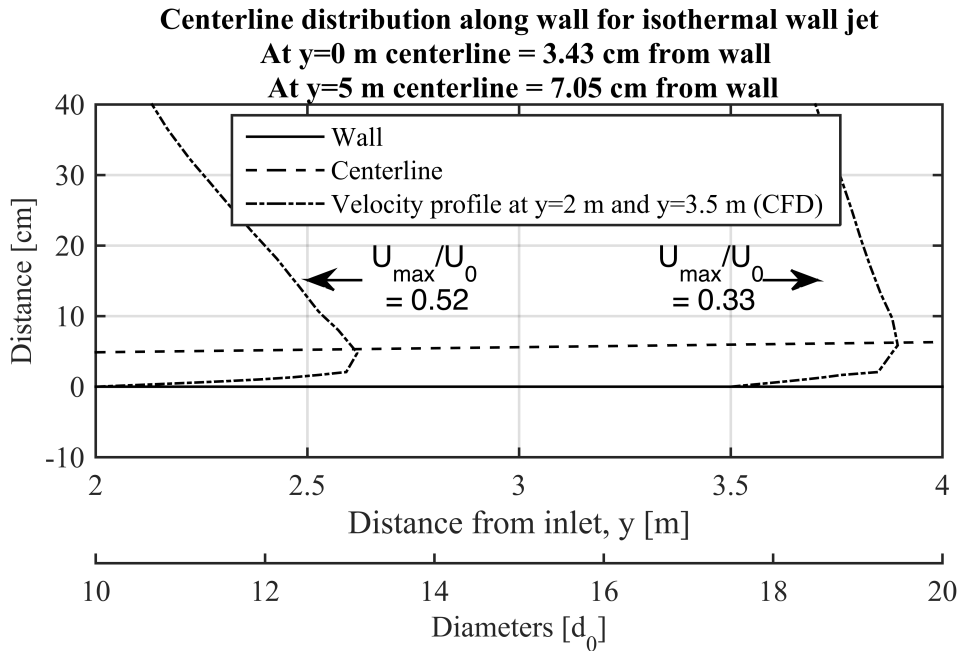


Figure 4.19: Shifting of line of maximum velocity for isothermal wall jets

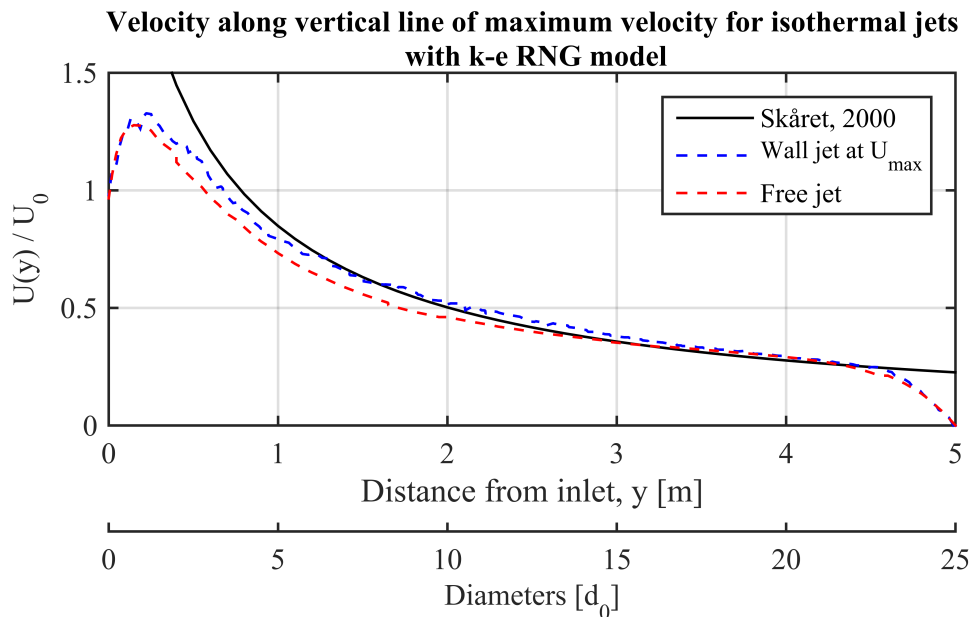


Figure 4.20: CFD simulation of free isothermal jet and isothermal jet along wall compared to empirical relation by Skåret [1]

4.4 Simulation of active displacement ventilation

Different cases of active displacement ventilation will be examined. Even though it is assumed some error in the calculation of the velocity and temperature profile for the buoyant wall jet, the mass balance and heat balance is still assumed to be satisfied, and the simulation is assumed to give realistic results on a global level. Placing the diffuser 2.5 m over the floor gave the best results in the project thesis in the fall 2016 where only empirical relations were used for the design. The reason was that placing the diffuser higher caused too much polluted air to be entrained, resulting in a high CO_2 -concentration in the lower zone that exceeded the upper requirement. Placing the inlet at this height is therefore done for the investigation of active displacement ventilation where CFD is used. The ceiling height is set to 3.5 m since a high upper zone is recommended. In the project thesis, it was not clear whether the inlet airflow rate should be 6 l/s or higher, so several scenarios will be investigated. For the plots where the CO_2 - and temperature distribution are illustrated as a function of the height, it is the temperature and CO_2 -concentration on the red line 1 m from the cylinder (2 m from the wall) as indicated in figure 4.21 we are looking on.

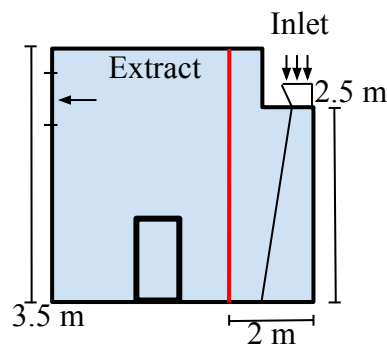


Figure 4.21: Red line indicating where the vertical CO_2 - concentration and temperature are studied

4.4.1 Inlet airflow rate 6 l/s for active displacement ventilation

The first case that will be investigated is the case where the inlet airflow rate is 6 l/s. The thermal and atmospheric environment will be compared to the results generated from empirical relations.

4.4.1.1 Empirical relations

The Matlab program used in the project thesis is modified to fit the geometrical model used for the CFD simulations. Empirical relations, in addition to heat and mass balance for the room, give the air flow pattern shown in figure 4.22. The CO_2 -concentration in the upper and lower zone in addition to the temperature in the upper zone are given in the title of the figure. In the jet calculations, it is assumed a constant room temperature $1^\circ C$ lower than the

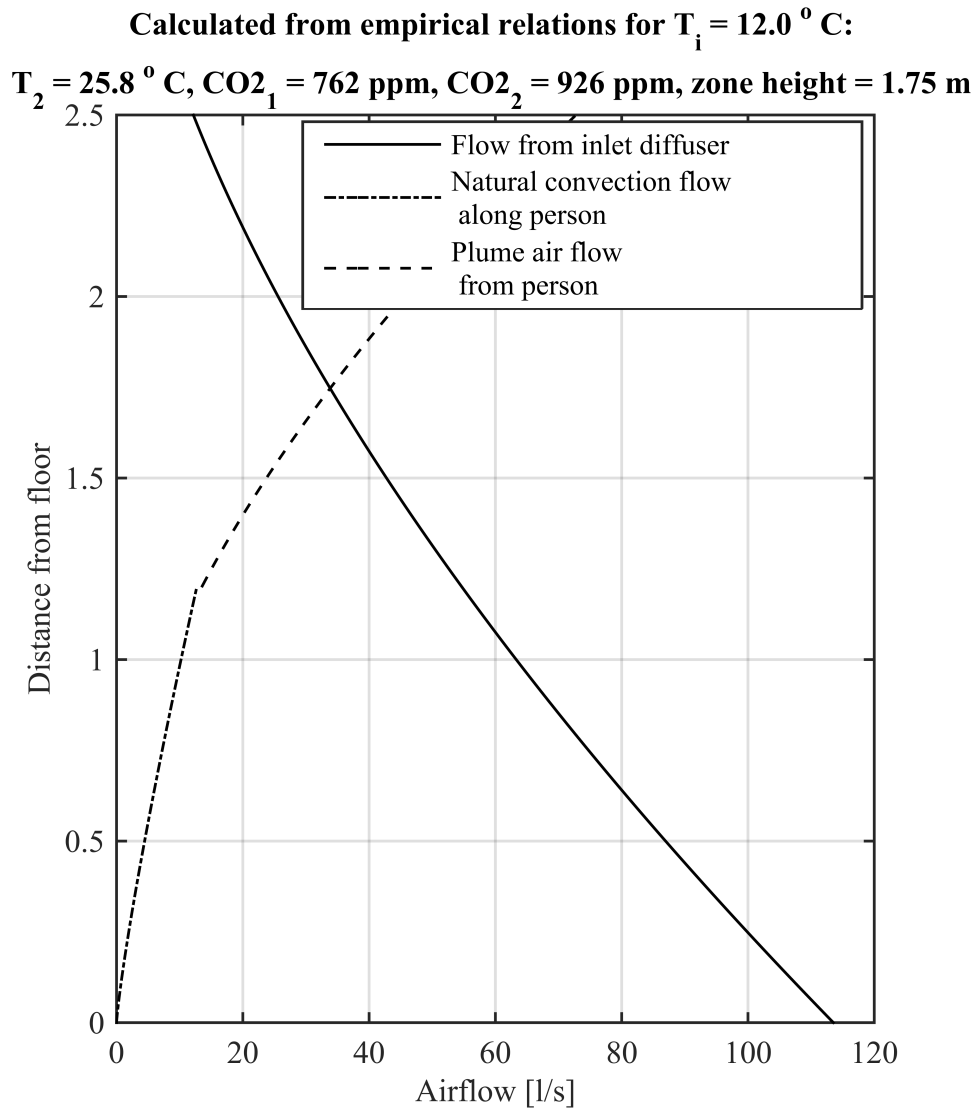


Figure 4.22: Flow pattern calculated from empirical relations. $Q_i=6 \text{ l/s}$, $T_i = 12^\circ \text{C}$ and $H_{diffuser}=2.5 \text{ m}$

temperature in the exhaust. We see how the convective plume from the person increases as the distance from the floor increases, and that the flow from the inlet increases as the jet approaches the floor. This makes sense since air is entrained in both cases. The plume from the person is divided in two since the first part is a natural convection flow, and the second is calculated from a point source. An inlet airflow rate of 6 l/s seems to give too high CO_2 -concentrations in the lower zone indicated as CO_2_1 at the top of the figure. The concentration should ideally be 600 ppm or less to fulfill the requirement for the atmospheric environment. We see that the zone height, which is the height at which the graphs cross, is 1.75 m over the floor. This height is also calculated and is shown in the title of the figure.

4.4.1.2 CFD-simulation

The CFD simulation done for the same geometry give similar results. See figure 4.23 for CO_2 - and temperature distribution, and figure 4.24 and 4.25 for contour plot of the CO_2 -concentration and temperature respectively. The CO_2 -concentration in the lower zone is approximately 760 ppm, while it is approximately 900 ppm in the upper zone. These results are almost identical to the results generated from the empirical relations and are higher than the requirement for CO_2 -concentration recommended for classrooms. The temperature distribution shows that a temperature of approximately $25.2^\circ C$ is to be expected in the upper zone. We also clearly see the effect of radiation when we compare the shape of the CO_2 - and temperature distribution in figure 4.23 as discussed in section 2.2.1.3. Table 4.2 summarize and compare the key-values of the results generated from empirical relations and CFD-simulations.

The efficiency indices are also shown in table 4.2. These are directly dependent on the other values in the table, and it is no surprise that also these values also coinciding.

Changing the inlet temperature will not have a large effect on the atmospheric environment since the relative temperature differences in the room will be the same resulting in an almost identical flow pattern. It is therefore concluded that the inlet airflow rate must be increased to reach the required air quality. In a scenario where there were floor heating or other heating equipment that ensured a constant room temperature, changing the inlet temperature would have an impact on the flow pattern since the buoyant forces would be higher.

In this case, we have one person and one inlet diffuser. Having one air inlet device per person is not often practiced in buildings, especially not in classrooms. One important discussion is therefore what happens if the number of occupants are increased while we still only have one inlet diffuser. This means that the area of the inlet would have to be increased if the inlet velocity were held constant at approximately 0.2 m/s. It is suggested to keep the inlet velocity at a minimum to reduce the pressure losses in the system. For a larger inlet area, the relative quantity of entrained air will decrease since the jet surface relative to the airflow will decrease. This can also be seen from the empirical relations of the buoyant jets in section 2.5.3.2 if they are plotted for different ratios of Q_i and A_0 . Less air is thus entrained per liter inlet airflow. This means that the CO_2 -concentration and temperature in the lower zone will decrease, and it would maybe be possible to achieve acceptable indoor air quality with an inlet airflow of 6 l/s. Problems with cold draught could, on the other hand, be a problem since less warm air is entrained and the velocities are increased due to higher buoyant forces.

In figure 4.24 we see how the clean air is polluted on its way down to the floor. When it enters the floor and start spreading along the floor, it is between 600 ppm and 700 ppm. On its way up to the breathing zone, more air is entrained, and the concentration approaches 750 ppm. Figure 4.25 show that heat from the upper zone is entrained. The temperature in the zone of occupancy is between $24^\circ C$ and $25^\circ C$ which is too high according to Norwegian standards.

4.4. SIMULATION OF ACTIVE DISPLACEMENT VENTILATION

Table 4.2: Summary of comparison of results from empirical relations and CFD simulations for active displacement ventilation with $Q_i = 6\text{ l/s}$

	Empirical relations	CFD simulation
$[CO_2]_1$	762 ppm	760 ppm
$[CO_2]_2$	926 ppm	900 ppm
T_1	$\approx 24.8^\circ\text{C}$	$\approx 24.5^\circ\text{C}$
T_2	25.8°C	25.2°C
Zone height	1.75 m	≈ 1.4 m
Contaminant removal efficiency	1.21	1.23
Temperature effectiveness	1.05	1.04

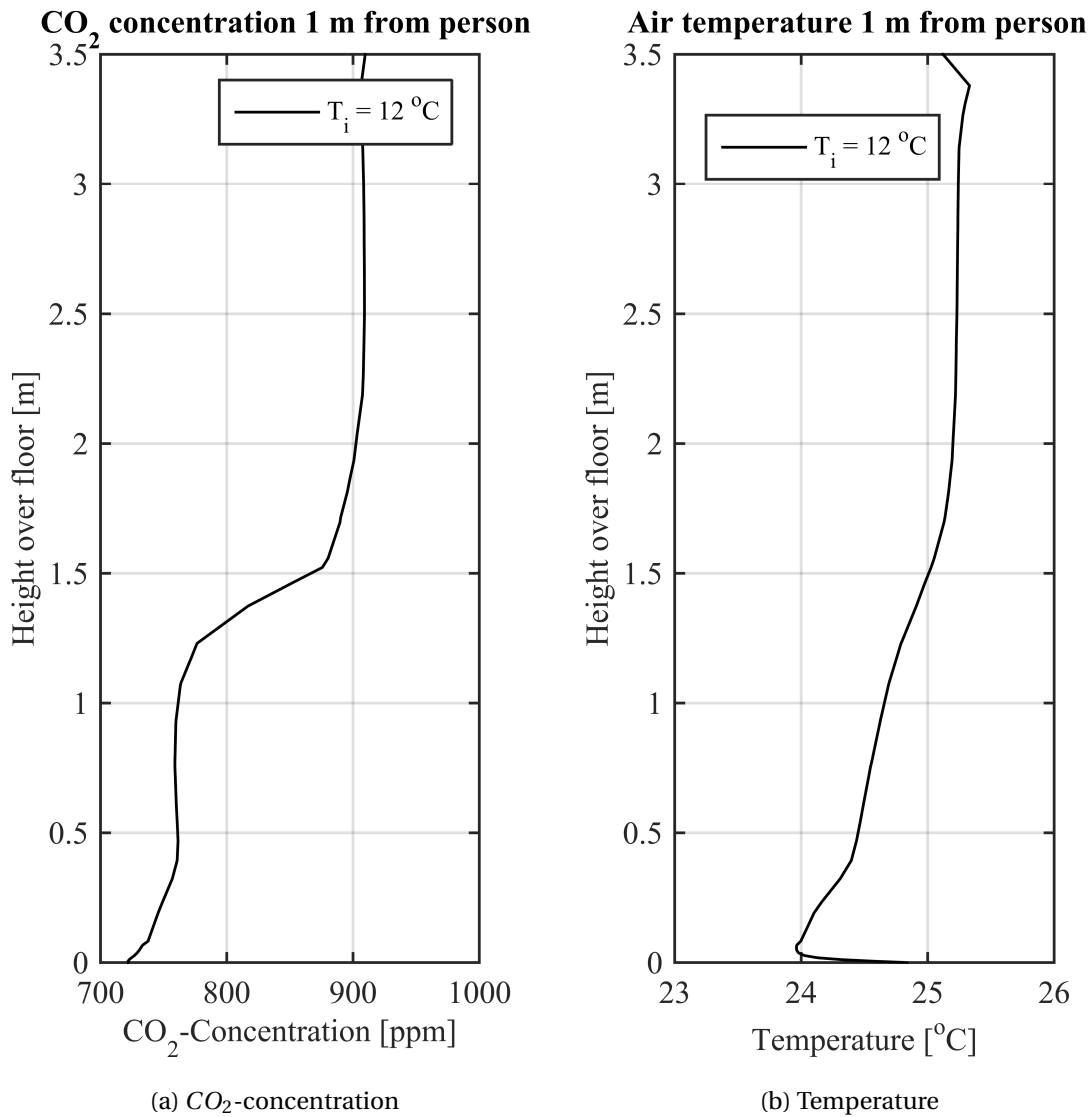


Figure 4.23: CO_2 concentration from floor to ceiling. $Q_i = 6\text{ l/s}$, $T_{in} = 12^\circ\text{C}$ and $H_{diffuser} = 2.5$ m. Plot taken from red line indicated in figure in the right bottom corner

4.4. SIMULATION OF ACTIVE DISPLACEMENT VENTILATION

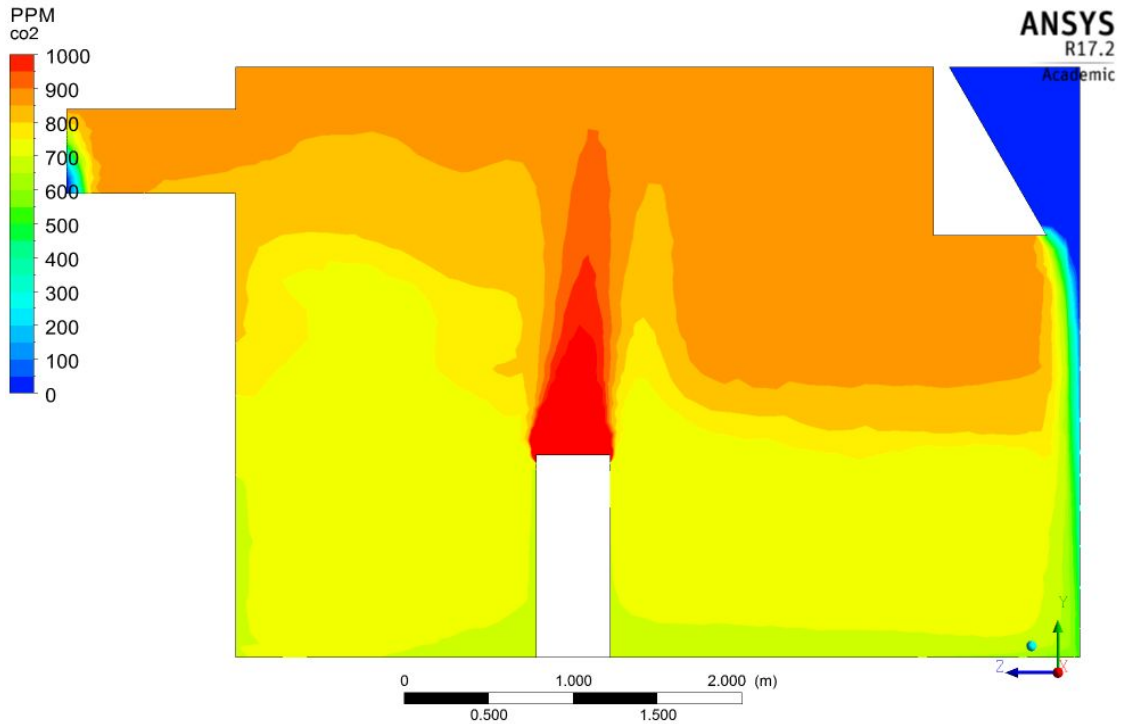


Figure 4.24: Contour of concentration of CO_2 for active displacement ventilation. $T_{in} = 12^\circ C$, $Q_i = 61/s$ and $H_{inlet}=2.5$ m

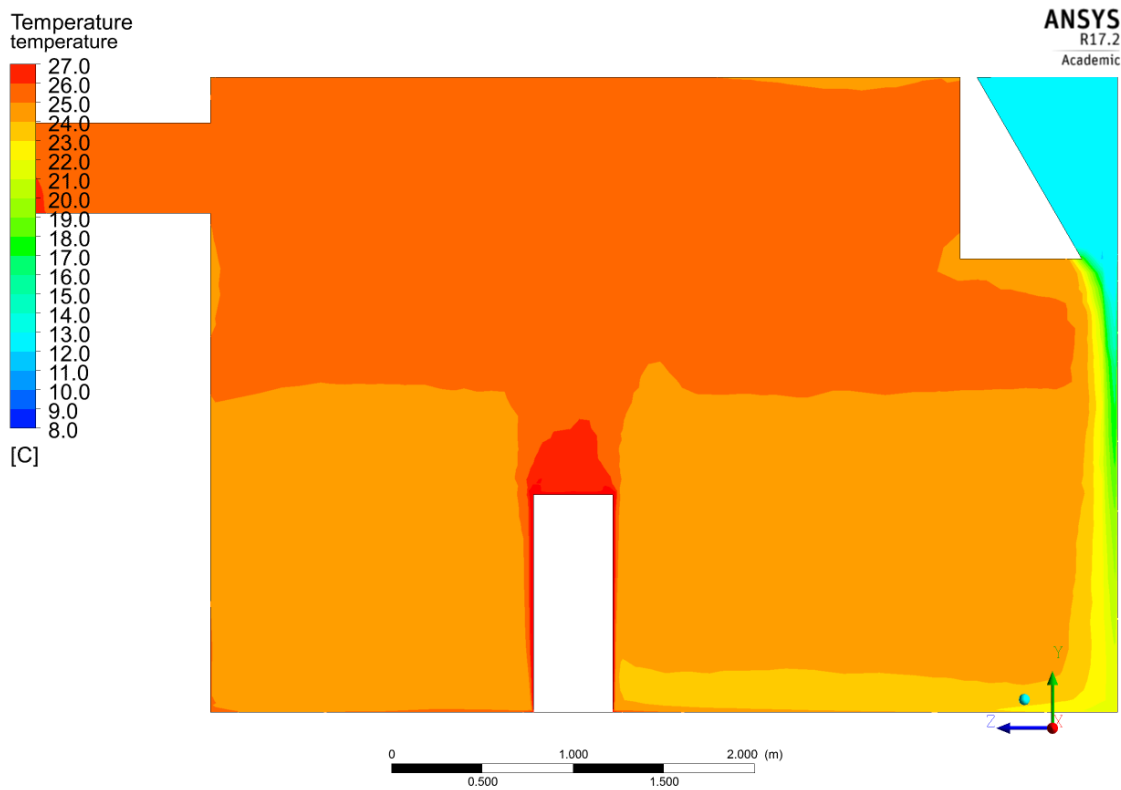


Figure 4.25: Contour of air temperature for active displacement ventilation. $T_{in} = 12^\circ C$, $Q_i = 61/s$ and $H_{inlet}=2.5$ m

4.4.2 Inlet airflow 7 l/s for active displacement ventilation

The inlet airflow is increased to see if the indoor air quality and thermal environment can be satisfied. Different inlet temperatures are investigated to see how low the temperature can be before the room is dependent on more heating than from the person.

4.4.2.1 Empirical relations

The results from the empirical relations are here presented in table 4.3. We see how the CO_2 -concentration is unchanged for the different scenarios, while the temperature in the upper zone, equivalent to the temperature in the exhaust, changes with the inlet temperature. This time we are close to satisfying the requirement for indoor air quality according to the calculations based on empirical relations and the temperature in the occupancy zone is satisfactory for inlet temperature $T_i = 10^\circ C$ and $T_i = 12^\circ C$. If the inlet temperature is decreased further, additional heating is required to satisfy the thermal environment in the room. The only heat loss is through the ventilation duct. The contaminant removal efficiencies and temperature effectiveness are also calculated and presented in the table.

Table 4.3: Key values from the calculation of active displacement ventilation based on empirical relations for $Q_s=7$ l/s. Index 1,2 and r stands for lower zone, upper zone, and average room temperature respectively

	8°C	10°C	12°C
$[CO_2]_1$	645 ppm	645 ppm	645 ppm
$[CO_2]_2$	794 ppm	794 ppm	794 ppm
T_r used for calculations of jets	18.8°C	20.8°C	22.8°C
T_2	19.8°C	21.8°C	23.8°C
Zone height	1.75 m	1.75 m	1.75 m
Contaminant removal efficiency	1.23	1.23	1.23
Temperature effectiveness	1.05	1.05	1.04

4.4.2.2 CFD-simulation

The CFD-simulations confirm that the calculations performed with empirical relations are realistic. The CO_2 -concentration is approximately 620 ppm in the lower zone, and 775 ppm in the upper zone. This is slightly lower than the results generated from empirical relations. We see from figure 4.26 (a) that the CO_2 -concentration is unaffected by the inlet air temperature. The reason is, as already mentioned, that the relative temperature difference between the jet and ambient air is the same for different inlet air temperatures. This causes the airflow rate and amount of entrained air to be the same. The temperature in the room is 18-19°C for $T_i = 8^\circ C$, and room heating is recommended for this temperature and lower temperatures. If the temperature exceeds 12°C it might be a need for cooling for rooms with nearly no heat loss through windows and walls. The height of the stratification line, referred

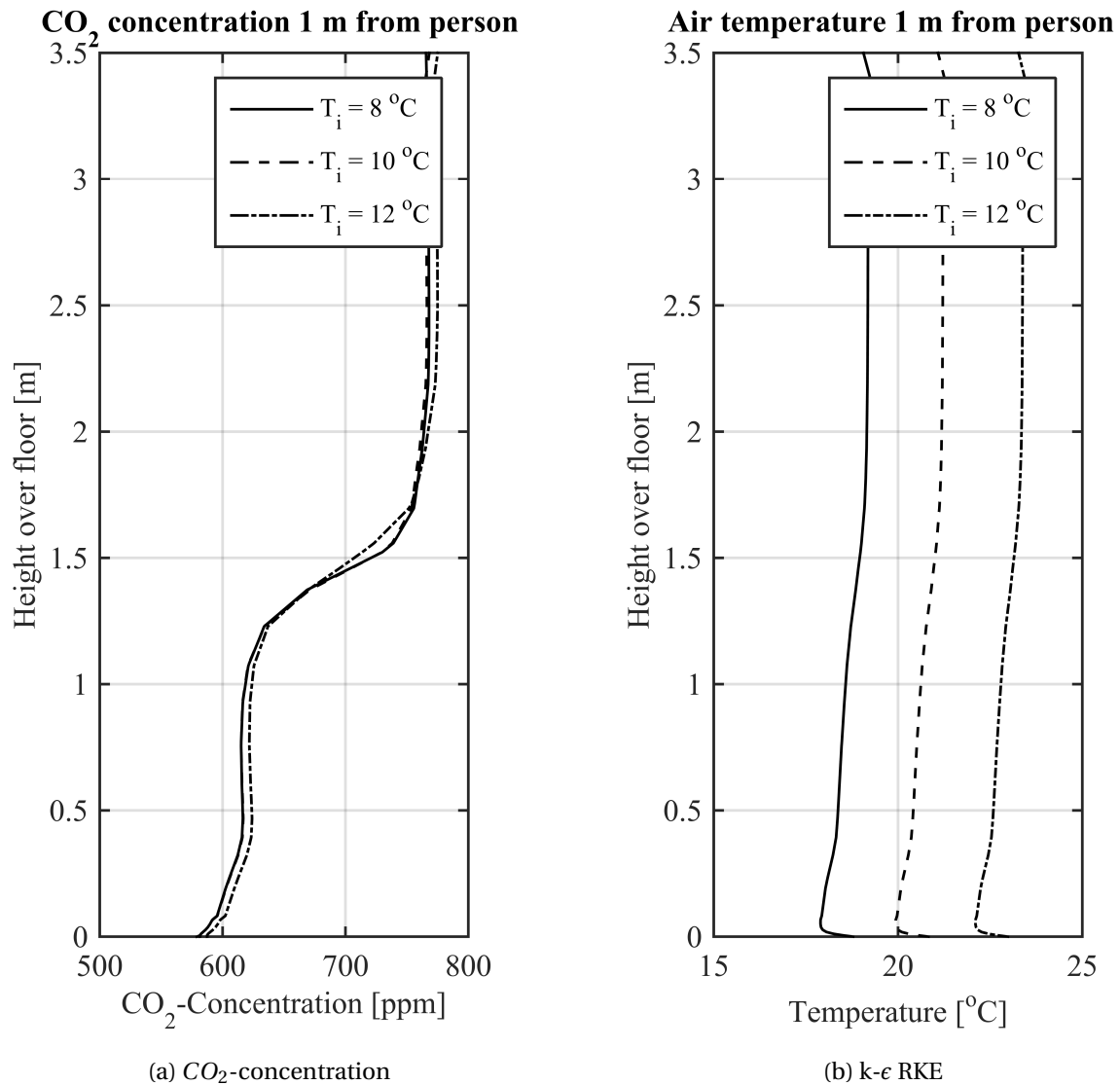


Figure 4.26: CO_2 concentration from floor to ceiling. $Q_i=7$ l/s, $T_{in} = 8 - 12^\circ\text{C}$ and $H_{diffuser}=2.5$ m

to as the zone height in table 4.3, is approximately 1.4 m for the CFD-simulations. This is seen for from figure 4.26 (a) where the CO_2 -concentration is suddenly changing.

The contaminant removal efficiency and temperature effectiveness are found for the simulations. The efficiencies are the same for different values of T_i . We see how the contaminant removal efficiency is approximately the same as for the calculations with empirical relations. For a situation of complete mixing, the efficiency indices are 1.

4.4. SIMULATION OF ACTIVE DISPLACEMENT VENTILATION

Table 4.4: Efficiency indices for active displacement ventilation. Results are valid for $T_i=8^\circ\text{C}$, 10°C and 12°C with $Q_i = 7\text{l/s}$

Index	Value
Contaminant removal efficiency	1.25
Temperature effectiveness	1.05

Figure 4.27 show the contour plot of the CO_2 -concentration for $T_i = 8^\circ\text{C}$. The contour plot for $T_i = 10^\circ\text{C}$ and $T_i = 12^\circ\text{C}$ will look almost identical as we saw in figure 4.26. The atmospheric environment in the lower zone is satisfactory while the upper zone is more polluted. Figure 4.28 and 4.29 show the contour plot of temperature for $T_i = 8^\circ\text{C}$ and $T_i = 12^\circ\text{C}$ respectively. It is clear that heat is transported from the heated cylinder to the upper zone and that heat is mixed into the clean cold air from the inlet.

Table 4.5 summarize the key values from the results from the empirical relations and CFD simulations for different inlet temperatures. As for the case with inlet airflow rate 6 l/s the results are very similar to each other. Also here it is assumed that the temperature in the lower zone is approximately 1°C lower than the exhaust for the empirical relations.

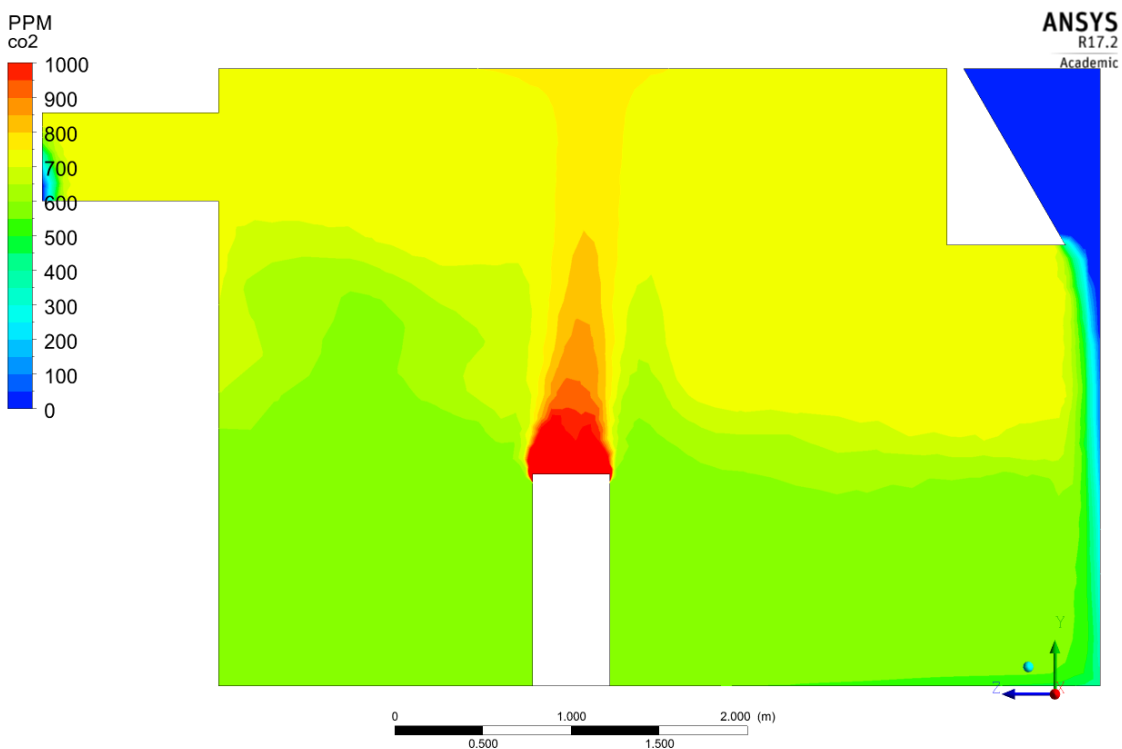


Figure 4.27: Contour of concentration of CO_2 for active displacement ventilation. $T_i = 8^\circ\text{C}$, $Q_i = 7\text{ l/s}$ and $H_{inlet}=2.5\text{ m}$

4.4. SIMULATION OF ACTIVE DISPLACEMENT VENTILATION

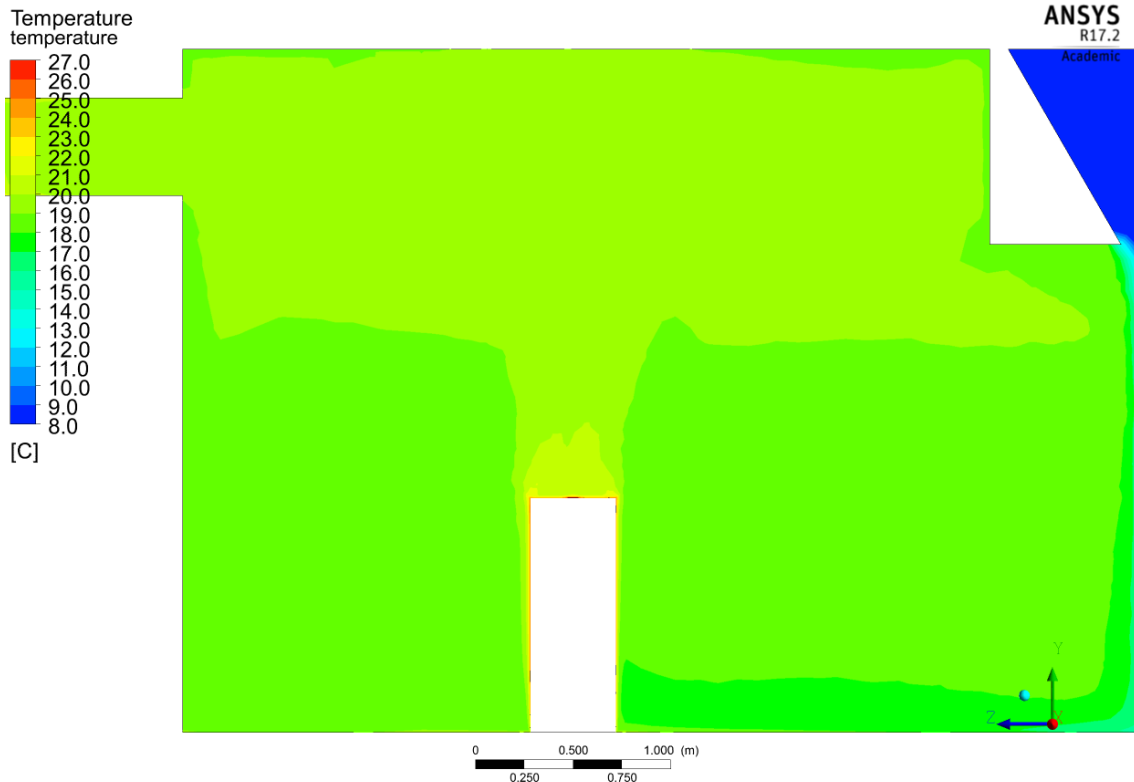


Figure 4.28: Air temperature for active displacement ventilation. $T_i = 8^\circ\text{C}$, $Q_i = 7\text{ l/s}$

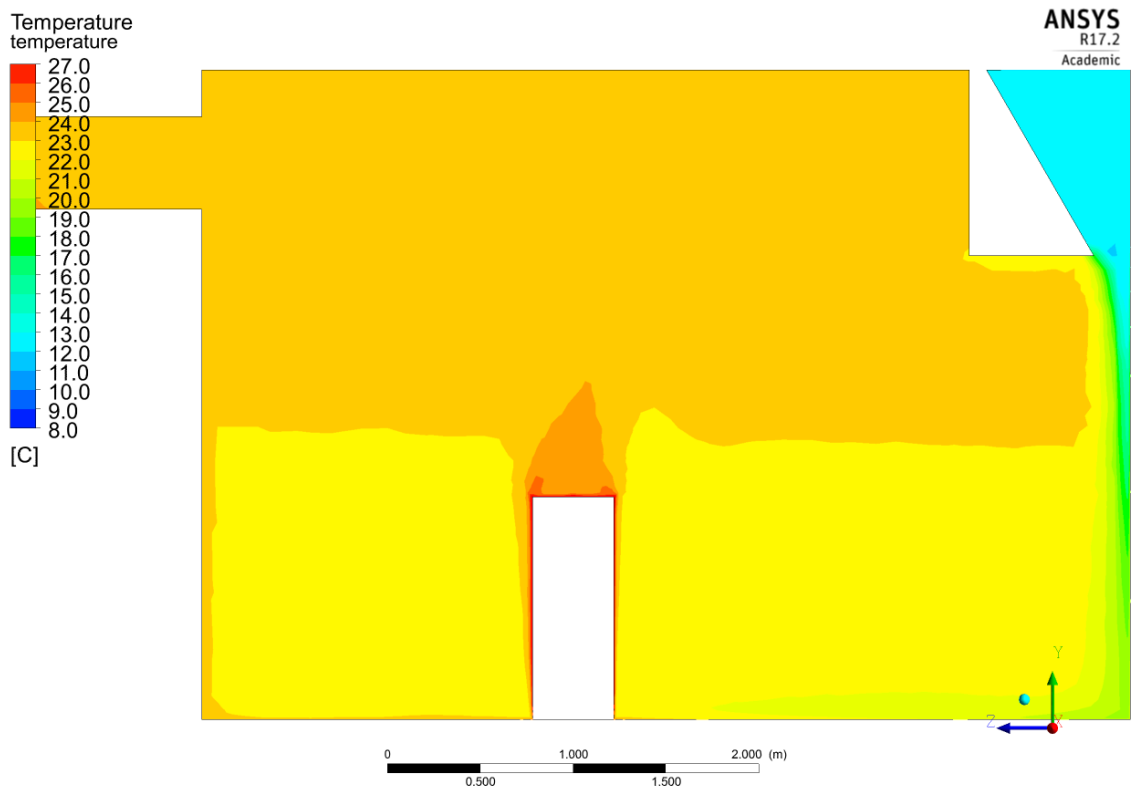


Figure 4.29: Contour of air temperature for active displacement ventilation. $T_i = 12^\circ\text{C}$, $Q_i = 7\text{ l/s}$

4.4. SIMULATION OF ACTIVE DISPLACEMENT VENTILATION

Table 4.5: Summary of comparison of results from empirical relations and CFD simulations for active displacement ventilation with $Q_i=7\text{ l/s}$. Index 1,2 and r stands for lower zone, upper zone and average room temperature respectively

$T_i = 8^\circ\text{C}$	Empirical relations	CFD simulation
$[CO_2]_1$	645 ppm	620 ppm
$[CO_2]_2$	794 ppm	780 ppm
T_1	$\approx 19.8^\circ\text{C}$	$\approx 18^\circ\text{C}$
T_2	19.8°C	19°C
Zone height	1.75 m	$\approx 1.4\text{ m}$
Contaminant removal efficiency	1.23	1.25
Temperature effectiveness	1.05	1.05
$T_i = 10^\circ\text{C}$		
$[CO_2]_1$	645 ppm	620 ppm
$[CO_2]_2$	794 ppm	780 ppm
T_1	$\approx 20.8^\circ\text{C}$	$\approx 20.5^\circ\text{C}$
T_2	21.8°C	19°C
Zone height	1.75 m	$\approx 1.4\text{ m}$
Contaminant removal efficiency	1.23	1.25
Temperature effectiveness	1.05	1.05
$T_i = 12^\circ\text{C}$		
$[CO_2]_1$	645 ppm	620 ppm
$[CO_2]_2$	794 ppm	780 ppm
T_1	$\approx 22.8^\circ\text{C}$	$\approx 22.5^\circ\text{C}$
T_2	23.8°C	19°C
Zone height	1.75 m	$\approx 1.4\text{ m}$
Contaminant removal efficiency	1.23	1.25
Temperature effectiveness	1.05	1.05

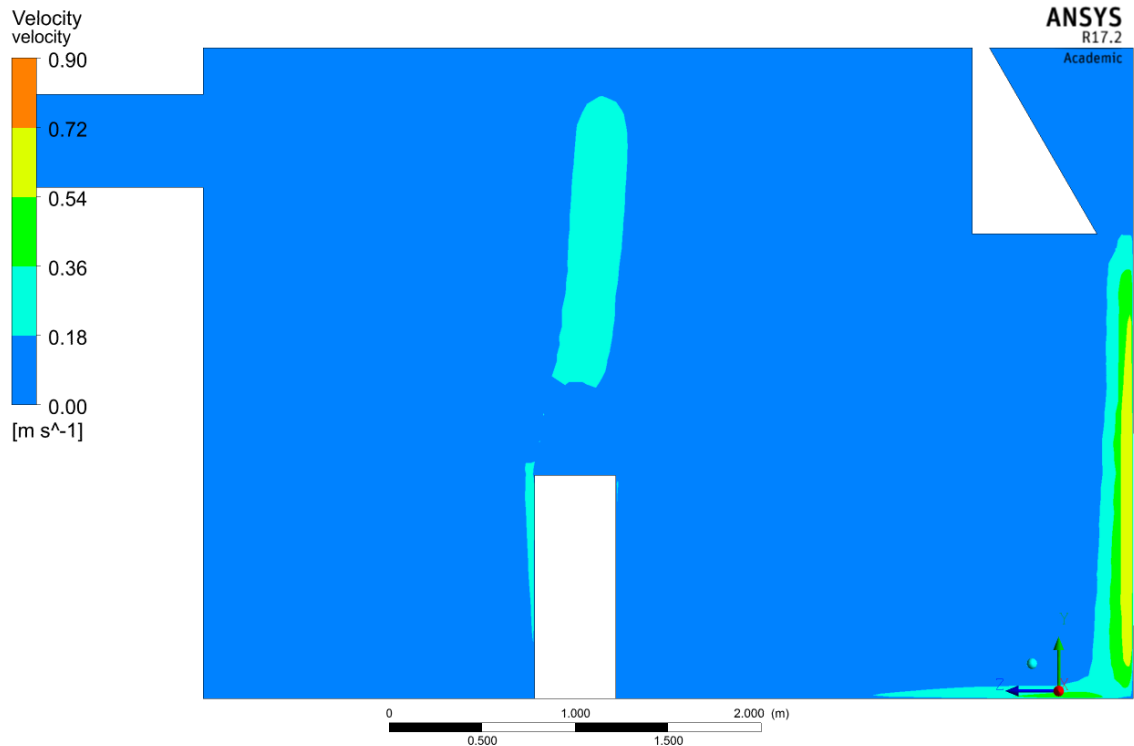


Figure 4.30: Contour of air speed (velocity magnitude) for active displacement ventilation. $T_i = 8^\circ\text{C}$, $Q_i = 71 \text{ l/s}$ and $H_{inlet}=2.5 \text{ m}$

Figure 4.30 shows the air speed in the room for $T_i = 8^\circ\text{C}$. A similar velocity pattern will yield for $T_i = 10^\circ\text{C}$ and $T_i = 12^\circ\text{C}$. All areas in dark blue are areas where the air velocity is within the requirement for classrooms at winter conditions, i.e. the air speed is less than 0.18 m/s . We see how the air spread horizontally under the inlet as the air approaches the floor, and that draught can be felt on the ankles in this area.

Draught at the ankle region is normally defined 10 cm over the floor. Figure 4.31 show the velocity magnitude, or air speed, taken 10 cm over the floor as indicated in the sketch in the right bottom corner of the figure. This indicates that the near zone will be approximately 0.25 m from the wall since velocities over 0.18 m/s is defined as draught. In figure 4.28 we see that this air will have a temperature between 16°C and 17°C .

The zone of occupancy can typically be defined from 10 cm to 1.8 m over the floor. For active displacement ventilation, it could also be a solution to avoid staying in the area under the jet. Figure 4.32 shows the suggested zone of occupancy for the room. A distance 0.5 m from the wall is chosen for the region where draught from the jet is expected. This area could, for example, be used for a passage area. In the case where each inlet diffuser supply air to more than one person the near zone is expected to increase since less air is entrained per volume supplied air as already discussed in section 4.4.1.2. The occupancy zone would then decrease.

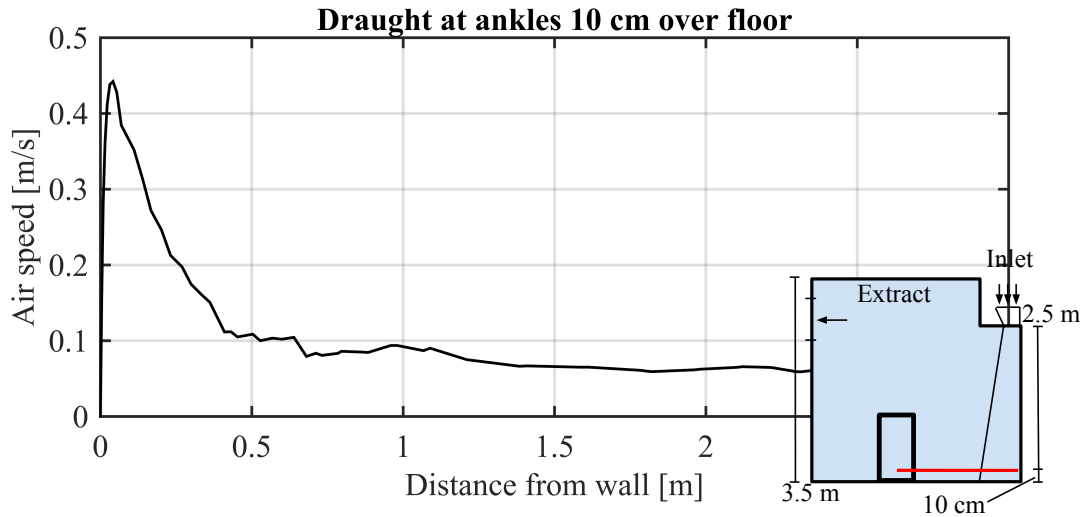


Figure 4.31: Draught at ankle height for active displacement ventilation

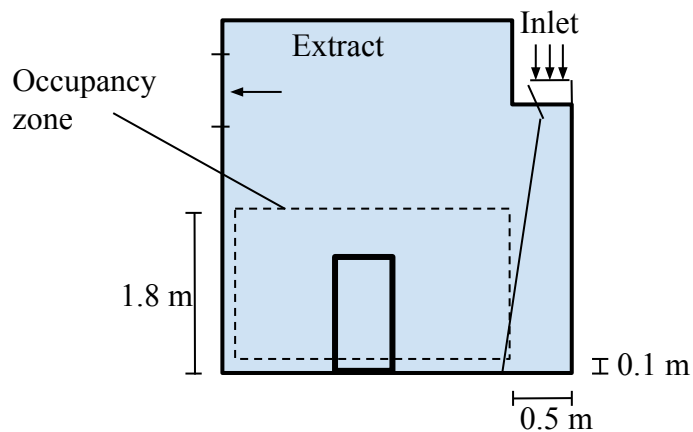


Figure 4.32: Sketch of suggested occupancy zone

4.5 Discussion of active displacement ventilation

The presentation and discussion of the results will be rounded off in this section. Humidity, comparison with other air supply methods, energy use, and the application of the results will be the focus areas.

4.5.1 Humidity

The humidity in the room is assumed to behave similarly as the CO_2 -particles. This means that the humidity that is transported from human exhalation will mix with the inlet air and be transported down to the lower zone causing a circulation of the vapor. At winter conditions

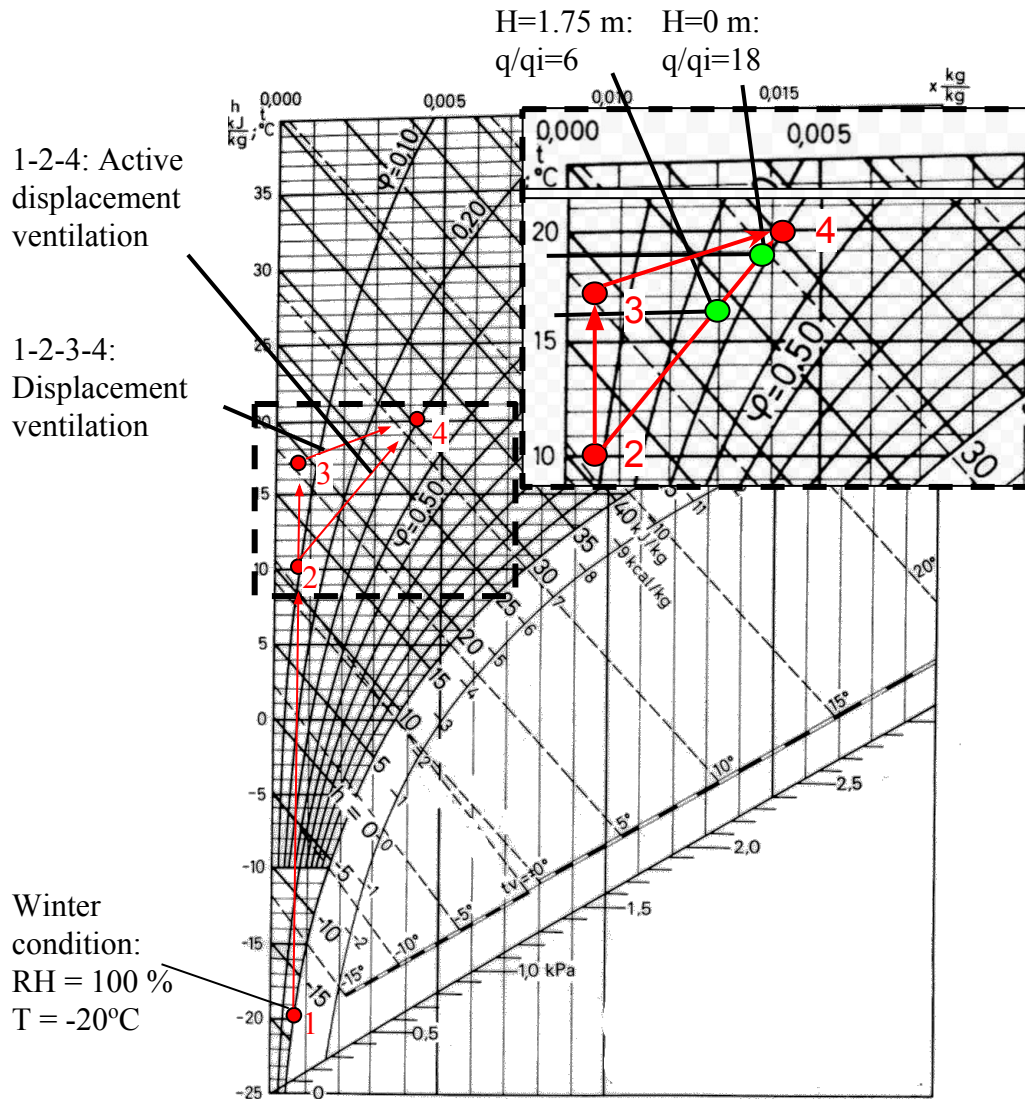


Figure 4.33: Mollier diagram with state changes for active and ordinary displacement ventilation

this can be an advantage since the air often is dry when it is heated from low temperatures without any humidification. For winter conditions the temperature can typically be $-20^{\circ}C$ for the coldest days in Norway. This is indicated as state 1 in figure 4.33 where the relative humidity (RH) is set to 100 %. Figure 4.33 illustrate the state changes for active and ordinary displacement ventilation. If air is heated to $17^{\circ}C$ without any humidification the inlet relative humidity will be approximately 8 %, which is below the lower requirement for relative humidity in buildings. The suggested indoor relative humidity is typically between 20 % and 40 %. If the humidity from the occupants and processes could be reused and not just transported to the upper zone, a more healthy environment could be obtained in the breathing zone. This is an advantage for active displacement ventilation compared to ordinary displacement ventilation since more air is entrained before the air reaches the breathing zone.

In figure 4.33 it is assumed that the average humidity in the room is 30 %. For active displacement ventilation, the inlet air is set to $10^{\circ}C$. For this temperature empirical relations

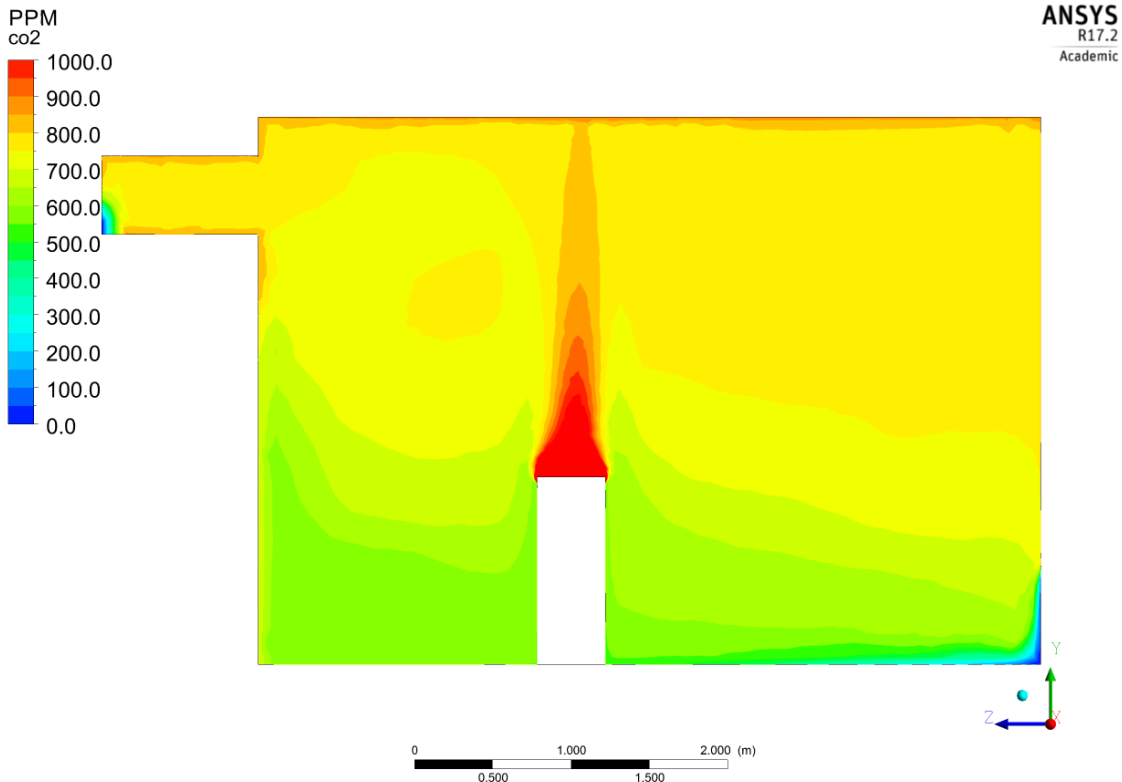


Figure 4.34: CO_2 for ordinary displacement ventilation ventilating. $Q_i = 6 \text{ l/s}$, $T_i = 17^\circ\text{C}$

and the Mollier diagram are used to calculate the humidity at the stratification height ($H=1.75 \text{ m}$), and at the floor ($H=0 \text{ m}$). The ratio between the entrained air and inlet air at these heights are approximately 6 and 18 respectively. This is indicated in the figure as green circles, and the relative humidity is approximately 25 % and 28 % for the two states which satisfies the requirement for relative humidity. State 3 is typically the state of the inlet air for ordinary displacement ventilation if the air is not humidified. As we see the relative humidity is less than 10 %, which is assumed as unhealthy low humidity. Of course, some humid air will be entrained as the inlet air approaches the breathing zone, but it is assumed that the humidity in the breathing zone will be noticeably lower for ordinary displacement compared to active displacement ventilation.

4.5.2 Comparison with ordinary displacement ventilation

A simple case of ordinary displacement ventilation is simulated in ANSYS Fluent. The same geometry and boundary condition is chosen as for active displacement ventilation except for the inlet conditions. Only one case will be presented in this thesis since this is sufficient for a simple comparison of the two methods. Several cases were simulated, and the case with the lowest airflow rate giving acceptable indoor air quality was when 6 l/s was supplied. The inlet temperature was set to 17°C , and lower temperatures are not recommended. This is to reduce the chance of cold draught in the occupancy zone.

Figure 4.34 and 4.35 show the contour plot of the CO_2 -concentration and air temperature

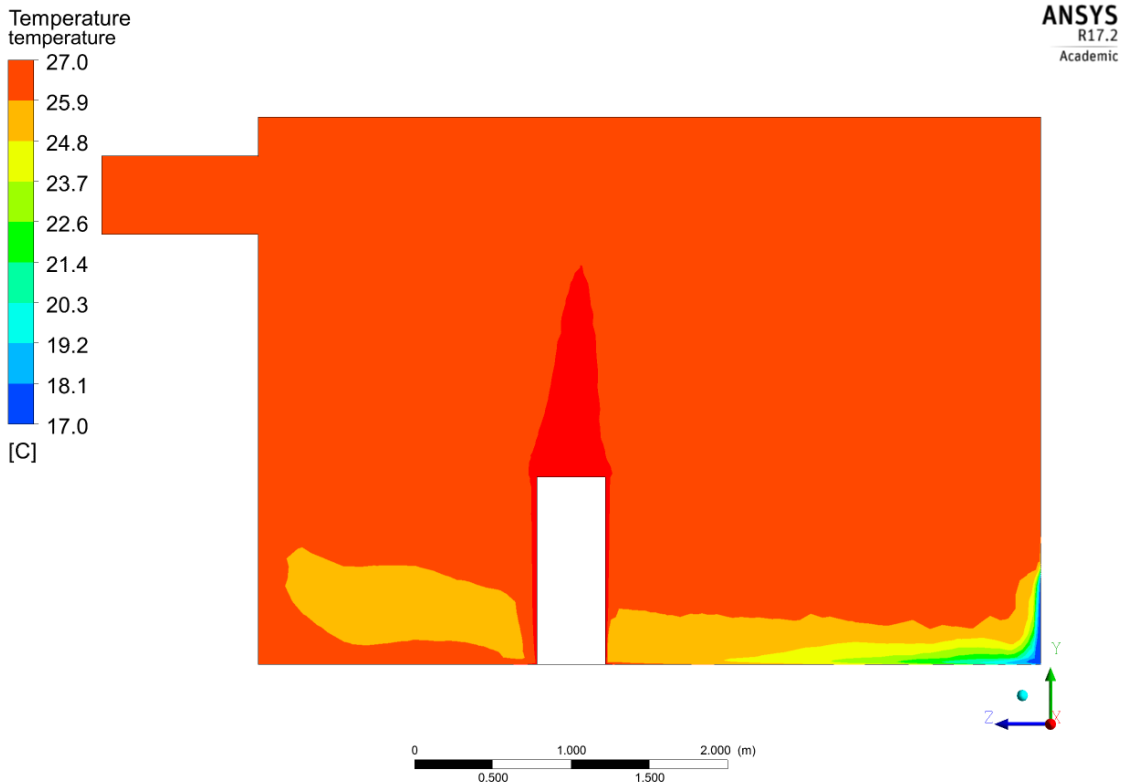


Figure 4.35: Temp. for ordinary displacement ventilation where $Q_i = 6 \text{ l/s}$, $T_i = 17^\circ\text{C}$

in the room. The CO_2 concentration in the breathing zone is approximately 600 ppm. This means that the airflow rate can be set to a lower value than for active displacement ventilation if the only requirement is the atmospheric environment. We see that the temperature in the zone of occupancy is higher than what is recommended since a temperature between 25.9°C and 27°C is expected. Therefore, the thermal environment is not satisfied for this case. Opening windows could be an alternative for summer conditions to let some of the heat out, but for winter conditions this is not necessarily an option due to the risk of cold draught. It will be a larger heat loss through walls and windows for winter conditions, so the temperatures are expected to be slightly lower for cold winter days than what is calculated from the simulation where all surfaces are adiabatic BC. Another option could be to increase the ceiling height to get a larger temperature gradient and lower temperature in the occupancy zone.

One way of cooling the room is increasing the airflow rate. By assuming that the exhaust temperature must be 26°C to obtain satisfactory temperatures in the occupancy zone, which is 24°C for winter condition, the inlet airflow rate must be set to 8 l/s . Equation 3.8 from section 3.6 is used for the calculation. Obviously, active displacement has an advantage when it comes to free cooling of the room since air with lower temperature can be supplied without the same risk of cold draught in the occupancy zone.

In the two zone model, the lower zone is assumed having the same concentration as the inlet. In this case, this means that the lower zone should have a concentration of 0 ppm. This is obviously not the case since air is entrained as it approaches the heated cylinder. This gives reasons to believe that the two-zone model for the design of ordinary displacement

ventilation using this kind of supply diffuser with this airflow rate is not ideal. However, in the case where we have larger supply devices and more supply air, less air will be entrained, and the concentration in the lower zone would possibly be lower. This is similar to what Xing et al. [10] said about how the design of the supply diffusers affect the air quality in the breathing zone. The zone height is typically lower for ordinary than active displacement ventilation, and the occupants are often dependent on fresh air being transported along with the body due to natural convection. This tendency is seen in figure 4.34 where the green area around the cylinder indicate that natural convection from the cylinder wall is transporting fresh air up to the breathing zone. This is equivalent to the experiments done by Sandberg [8] presented in section 2.2.1.2

Both ordinary and active displacement ventilation is well suited for natural and hybrid low-pressure ventilation systems due to the low supply air velocity. This is beneficial when one is interested in designing buildings based on thermal forces and low specific fan power (SFP). Heat exchange is beneficial both for active and ordinary displacement ventilation, but the need for pre-heating of the air is bigger for ordinary displacement ventilation.

4.5.3 Comparison with mixing ventilation

Assuming that there will be no cold draught in the zone of occupancy, table 4.6 can be generated for the design of mixing ventilation based on calculations presented in section 3.7. In the case where one take cold draught into account, one must investigate the ratio between air temperature and air velocity in the occupancy zone to evaluate the lowest air temperature for the given airflow rate that is accepted. The type of inlet diffuser will have a large influence on the inlet temperature. This means that thermal neutrality is obtained while thermal comfort is not necessarily obtained for the design. Both the room temperature and atmospheric environment will here be satisfactory, so no cooling or heating is necessary. The room temperature is limiting the inlet air temperature. The requirement is set to $22 \pm 2^\circ C$ which is required for winter conditions for classrooms.

One can often accept lower inlet air temperatures for mixing ventilation than for ordinary displacement ventilation. The reason is that warm air is entrained for mixing ventilation before it enters the occupancy zone which reduces the chance for cold draught. This is the same principle as in active displacement ventilation, and we see that the lowest inlet temperature is in the same range for mixing and active displacement ventilation. In fact, if the inlet diffuser is placed very high on the wall for active displacement ventilation the situation is almost identical to mixing ventilation since the air will approximately have the same concentration everywhere due to the high amount of entrained air in the supply air.

Table 4.6: Calculations for complete mixing ventilation

$Q_i=9 \text{ l/(s}\cdot\text{person)}$		
Inlet temperature [°C]	Room temperature [°C]	[CO ₂] over outdoor concentration [ppm]
10.8	20	617
14.8	24	617
$Q_i=10 \text{ l/(s}\cdot\text{person)}$		
Inlet temperature [°C]	Room temperature [°C]	[CO ₂] over outdoor concentration [ppm]
11.7	20	555
15.7	24	555
$Q_i=11 \text{ l/(s}\cdot\text{person)}$		
Inlet temperature [°C]	Room temperature [°C]	[CO ₂] over outdoor concentration [ppm]
12.5	20	505
16.5	24	505
$Q_i=12 \text{ l/(s}\cdot\text{person)}$		
Inlet temperature [°C]	Room temperature [°C]	[CO ₂] over outdoor concentration [ppm]
13.2	20	463
17.2	24	463

How air should be supplied for mixing ventilation is not studied in detail in this thesis, but the assumption is that the lower the temperature of the air is, the more difficult the design will be. Draught and early detachment from the wall are challenges for mixing ventilation with cold inlet air. Nielsen et al. [23] used a temperature difference $\Delta T_0 = 12.5^\circ\text{C}$ for the design of mixing ventilation in the design of the $q_0 - \Delta T_0$ - charts presented in section 2.5.2. This means that the inlet temperature is 12.5°C less than the room temperature. If this is used as a design criterion, all cases presented in table 4.6 will give thermal comfort.

The airflow rate is higher for mixing ventilation than active displacement ventilation in these calculations. The reason is that for complete mixing ventilation the upper zone must also meet the requirement for the thermal and atmospheric environment, and warm and polluted air can not be stored in the upper zone of the room.

When mixing ventilation is applied, heat exchangers are typically used to preheat the air to save energy. Mixing ventilation is not used for low-pressure ventilation systems since high inlet velocities are required.

4.5.4 Energy use and reduction of greenhouse gases

One of the main advantages of applying active displacement ventilation is the saved energy from reusing warm air in the upper zone of the room. Lower energy use in building reduces the emission of GHG. According to the results in this thesis, the difference in temperature between ordinary and active displacement ventilation can be as high as 7°C . It is then

assumed that the inlet air temperature for ordinary displacement ventilation should not be less than 17°C to avoid cold draught in the occupancy zone.

Building integrated ventilation and ventilation systems with low-pressure losses have been discussed in the theory section in the thesis. Active displacement ventilation is well suited for such systems. As we saw for the Swedish model, preheating air in a double wall and culvert system reduces the need for preheating. The fact that the air does not need to be heated to more than approximately 10°C means that a lot of energy can be saved for cold days where the air must be pre-heated. In Norway, where the temperature can approach -20°C in the winter, the culvert system and double wall are not assumed to be sufficient for pre-heating, and additional heating should be considered to reduce the chance of water-containing equipment from freezing.

4.5.5 Application of the results

Two main aspects will be discussed in this section. The first is an evaluation of the application of simple empirical relations used for the design of active displacement ventilation. This is also one of the main questions to be answered in the thesis. The second is an evaluation of the supply methods that are investigated in the thesis where they are compared against each other based on the thermal and atmospheric environment. Based on the results it is also possible to come up with recommendations on when each method should be used by visualizing them in charts.

4.5.5.1 Application of empirical relations

In this thesis we have seen how the design of active displacement ventilation using empirical relations and CFD simulations have given similar results when it comes to the CO_2 - and temperature distribution in a simple room. This means that using empirical relations in the design of active displacement ventilation together with heat- and mass balance is possible and recommended if the equations are applied correctly. There is still some uncertainty around the value of the pole distance for wall jets, which is a very important parameter in ventilation design. Values between $2.25d_0$ and $0.7d_0$ are so far recommended for free jets. Suggestions on the use of empirical relations will here be listed to clarify how the relations should be used in the design.

Calculation for wall jet Friction is neglected for wall jets. Calculation are done as presented in section 2.5.4

The validity of the relations The empirical relations are valid after ca. 5 diameters from the inlet. In the design of active displacement ventilation, the distance between the inlet and the stratification height should, therefore, be at least $5d_0$. For wall jets, it is the imaginary diameter that must be used to see whether the relation is valid or not.

No interaction of jets For precise flow calculations the jets should not interact with each other before they reach the stratification height. This means that there is a restriction on the

number of diffusers for each wall. The width is calculated from geometry when the pole distance and jet angle are known.

Diffuser variables The diffuser height, inlet area, and the number of diffusers are variables that will affect the thermal and atmospheric environment and are important in the optimization of active displacement ventilation. The variables affect the amount of entrained air. Placing many small diffusers high on the wall will increase the amount of entrainment, increase the CO₂-concentration in the lower zone, and increase the temperature in the lower zone. Large diffusers placed low on the wall will do the opposite. Draught is also a factor that must be taken into consideration.

4.5.5.2 Recommendations and comparison of supply methods

Active displacement-, ordinary displacement- and mixing ventilation has been investigated and analyzed for simple room situations. The goal for a ventilation designer will always be to minimize the energy use while the indoor climate is still satisfactory. Table 4.7 gives an overview of which cases that are considered to be the most energy efficient cases for each supply method. The methods are evaluated based on five different criteria. The criteria are the main factors of the thermal and atmospheric environment and are explained in the table. The results are based on the discussion in the previous sections.

In the design, the focus has been to fulfill the atmospheric environment (air pollution) first and then correct for the thermal environment (temperature in occupancy zone, draught and humidity). The thermal environment is usually the most important and is the factor an average person will first complain about. In this case, the only source of cooling is the ventilation, so if the temperature is not satisfactory one must either increase the flow rate or decrease the inlet temperature.

4.5. DISCUSSION OF ACTIVE DISPLACEMENT VENTILATION

Table 4.7: Overview of results for winter condition where the energy use is minimized while an acceptable thermal and atmospheric environment is still achieved

Complete mixing ventilation									
	Q_i	T_i	$[CO_2]_1$	T_1	Air temp. low zone	Draught	Humidity	Radiative asymmetry	Air pollution
	[l/s]	[°C]	[ppm]	[°C]					
1*	9	11	600	20	✓	-	✓	✓	✓
Displacement ventilation									
	Q_i	T_i	$[CO_2]_1$	T_1	Air temp. low zone	Draught	Humidity	Radiative asymmetry	Air pollution
	[l/s]	[°C]	[ppm]	[°C]					
2*	8	17	<600	≈24	✓	✓	-	✓	✓
Active displacement ventilation									
	Q_i	T_i	$[CO_2]_1$	T_1	Air temp. low zone	Draught	Humidity	Radiative asymmetry	Air pollution
	[l/s]	[°C]	[ppm]	[°C]					
3**	7	10	610	21	✓	✓	✓	✓	✓

How to fulfill requirements:

- ✓ Temperature: Temperature in the occupancy zone must be in the range 20 – 24°C [3]
- ✓ Draught: Air with velocity larger than 0.18 m/s is not expected in the occupancy zone and temperatures are in the range of the recommended room temperature [3]
- ✓ Humidity: The relative humidity is expected to be higher than 30 % for winter conditions in the occupancy zone without any humidifiers
- ✓ Radiative asymmetry: Based on an evaluation of the risk of being close to cold/warm surfaces
- ✓ Air pollution: CO_2 concentration is less than 600 ppm over outside concentration in the occupancy zone [95]

Explanation:

- ✓ Requirement fulfilled
- Requirement not fulfilled or assumed hard to fulfill
- * Heat- and mass balance used for calculation
- ** CFD used for calculation

Comment: The overview gives an indication of the indoor climate for rooms with one air supply device and one person. Results might vary with room design, diffuser design, the number of diffusers, heat load and pollution load. The index 1 indicate the lower room zone

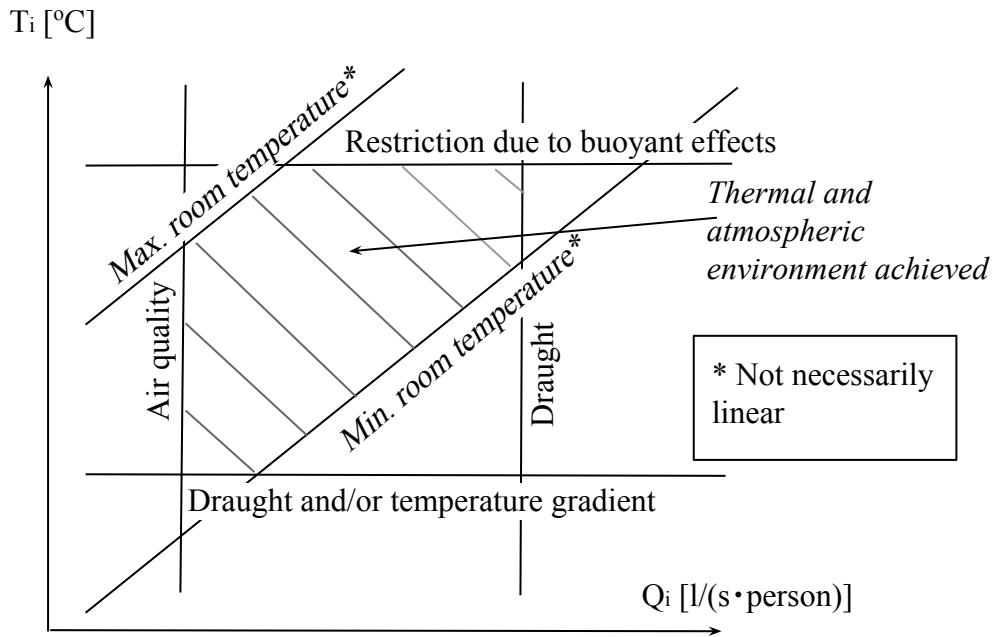


Figure 4.36: Explanation of design chart

4.5.5.3 Design chart for air supply methods

A chart inspired by the $q_0 - \Delta T_0$ - chart by Nielsen [22] will be presented in this section where mixing, displacement and active displacement ventilation will be compared. The main difference from the chart by Nielsen [22] is that the variable ΔT_0 is replaced by the inlet temperature T_i . Since a high ΔT_0 correspond to a low T_i the chart will be opposite in the y-direction. This means that the restriction "Draught and/or temperature gradient" will be at the bottom of the chart instead of in the upper part. This change is done to show which inlet temperatures that are suggested for the design.

Figure 4.36 show the restriction lines for the flow rate and inlet air temperature. Some lines are added in addition to the ones used by Nielsen. The sloped lines are restrictions on the supplied air temperature to fulfill the required room temperature. These are independent on draught and temperature gradients. The lines are sloped since the room temperature is both a function of the inlet temperature and the airflow rate. Another added restriction is the restriction due to buoyant effects. In ordinary and active displacement ventilation the supply temperature must hold a certain under-temperature compared to the ambient to ensure sufficient buoyant effects. This restriction line will vary from method to method and will be higher for ordinary displacement ventilation than active displacement ventilation.

Figure 4.37 indicate for which T_i and Q_i each supply method is recommended to be used. In addition to information about the inlet temperature and flow rate, it is possible to read the expected room temperature and expected CO_2 -concentration for each of the methods for different T_i and Q_i . The CO_2 -concentration is only dependent on the flow rate and is therefore not varying with the inlet temperature. The room temperature is depending both on flow rate and inlet temperature.

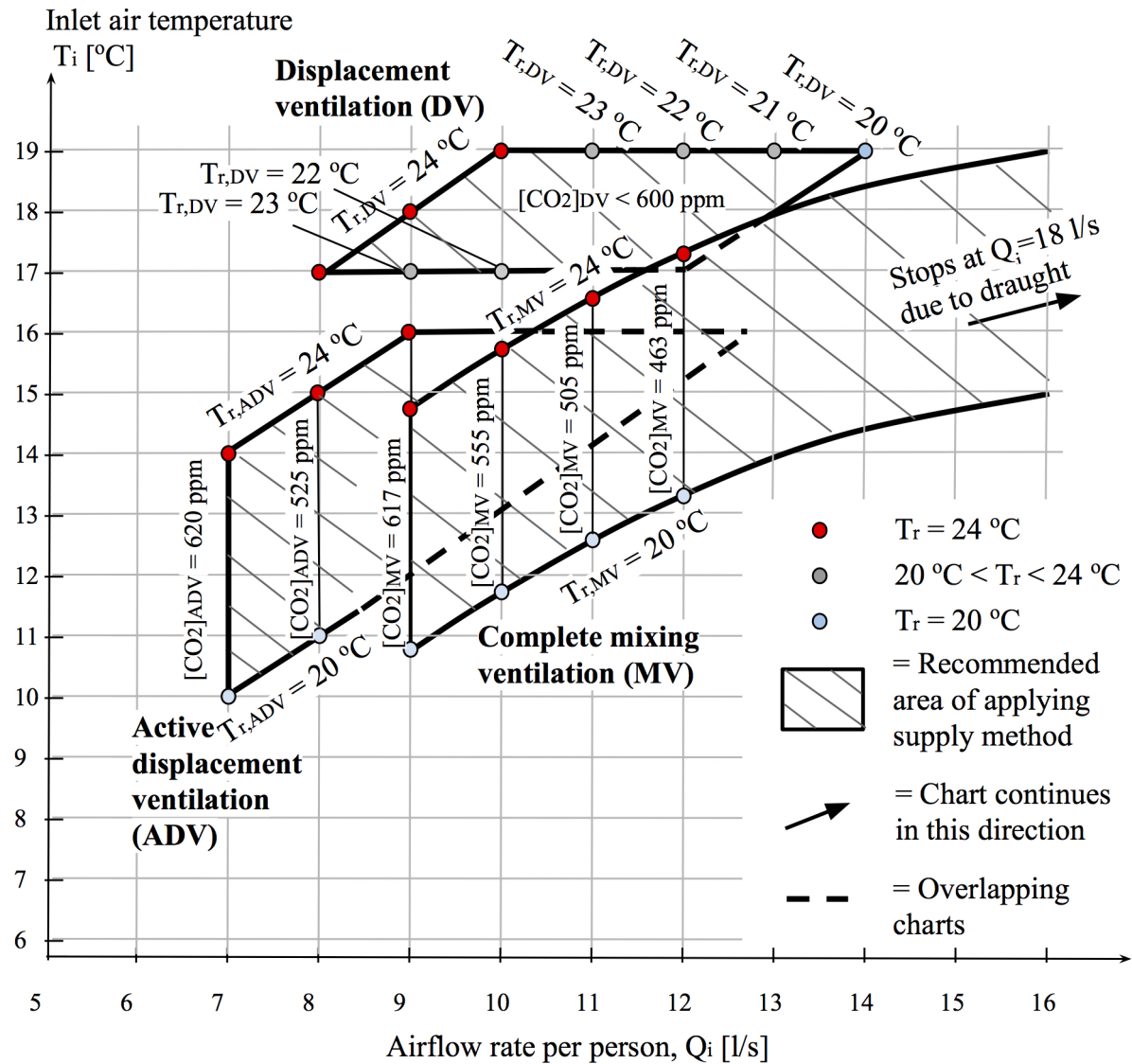


Figure 4.37: Graphical illustration of the use of supply methods

The further down to the left, the less energy is used since the airflow rate and the inlet air temperature are minimized. Therefore, according to these calculations, active displacement has the potential to be more energy-efficient than other methods.

Displacement ventilation is the method that is dependent on the highest temperature. This is due to the restriction of draught and/or temperature gradient. The restrictions for the different supply methods are visualized in figure 4.38. Because of this restriction, the airflow rate must be increased due to the restriction of maximum room temperature. In other words, it is not the air quality that is the limiting factor for displacement ventilation when it comes to the airflow rate per person, but the cold draught. As we saw in section 4.5.2 it was possible to obtain a satisfactory atmospheric environment for $Q_i = 6$ l/s. The upper restriction for displacement ventilation is the buoyant effects.

Mixing ventilation is limited to draught and/or temperature gradient after the suggested value of $\Delta T_0 = 12.5$ °C by Nielsen et al. [23]. However, the restriction for minimum room temperature is over this restriction and is thus the limiting factor for the lower inlet

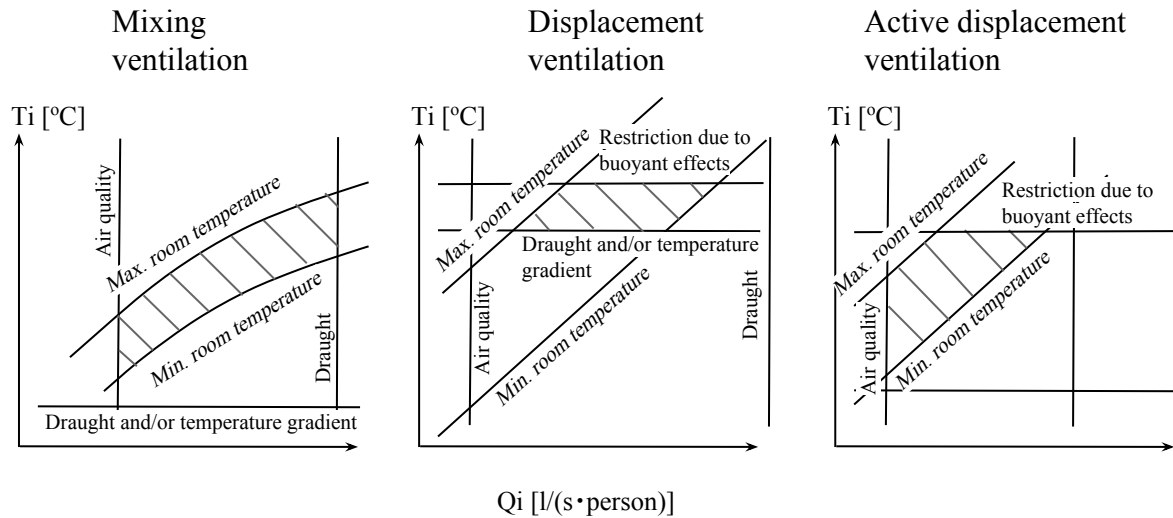


Figure 4.38: Illustration of the restrictions for each of the supply methods

temperature. Maximum airflow rate is set to 18 l/s due to draught.

Active displacement is also restricted to the buoyant effects, and the upper limit is set to 16°C. As for mixing ventilation the lowest airflow rate is limited by the indoor air quality in the occupancy zone.

4.5.6 Design of a classroom situation

A simple classroom situation will be designed to show an example of how one can use empirical relations in the design of active displacement ventilation. A room with 30 people, each radiating 100 W heat, are investigated where there is no heat loss except through the ventilation duct. The convective plumes from the occupants are assumed not to interact with each other. A sketch of the room is seen in figure 4.39 where room dimensions are specified. The area under the jets is used as a passage area to avoid people to stay in an area with risk of cold draught for a longer time.

The goal is to decide the following parameters:

- Airflow rate
- Inlet temperature
- Inlet area per diffuser
- Number of diffusers
- Height of diffusers

With this amount of variables, a large number of situations exist. The case where the supply flow rate is 7 l/(s·person) and the supply temperature is 10°C will be investigated. Since the inlet temperature is 10°C it is assumed that we have a typical winter situation where the ventilation air is preheated. It could also be a situation for other times of the year where the outdoor air temperature is close to 0°C and preheated in a culvert and a double wall. We are now left with deciding the inlet area, the number of diffusers and the height of the diffusers.

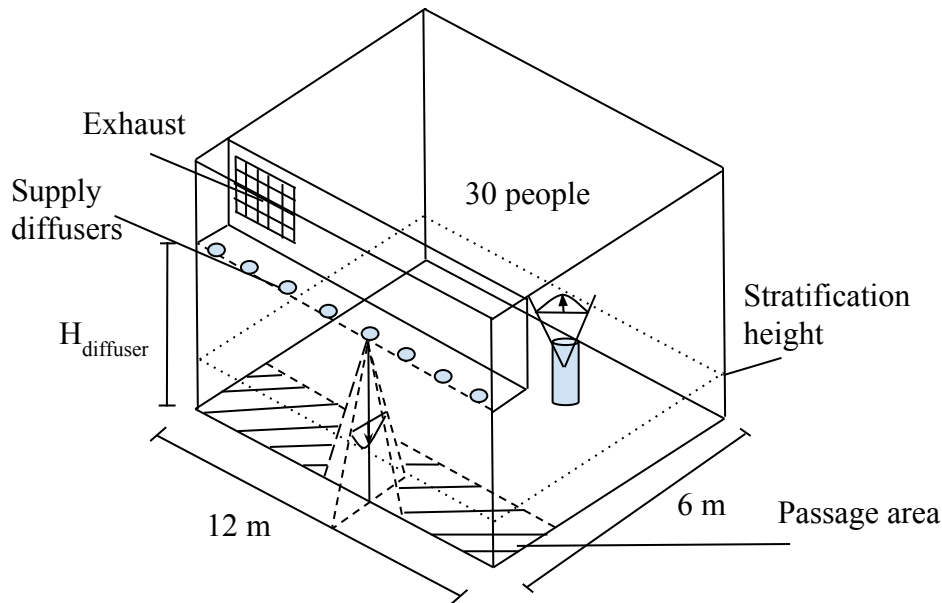


Figure 4.39: Illustration of the restrictions for each of the supply methods

The inlet area can not be too large since the jet must be developed before it reaches the stratification height. If not, the empirical relations are not suggested to be used since the relations will over predict the velocity in this region (see figure 4.8 for comparison of empirical relation and CFD simulation of buoyant jet). Since the jet is developed after ca. $5d_0$, and the zone height is between 1 m and 1.5 m, the value of d_0 should not be much more than 0.25 m. Larger diameters can, of course, be used for active displacement ventilation, but it will be hard to perform calculations using the relations presented in this thesis for large inlet areas. Table 4.8 show the distance it takes for different inlet areas to develop. We are looking on circular inlets placed close to a wall as illustrated in figure 4.39. It is here the imaginary diameter, d_{im} , that is used for the calculation of the distance. We see that if the inlet area is 0.25 m, it will take 1.75 m for the jet to develop. This means that the distance between the inlet and the stratification height must be equal or more than 1.75 m. It is not ideal to have a too small inlet area since the CO_2 concentration in the lower zone will be high due to the high amount of entrained air per volume inlet air. In addition, the inlet velocity and pressure losses will be higher when the total inlet area is decreased.

Table 4.8: Distance before jet is developed for different inlet areas

Inlet diameter	0.1 m	0.15 m	0.2 m	0.25 m
Imaginary diameter, d_{im}	0.14 m	0.21 m	0.28 m	0.35 m
Distance before developed ($6d_{im}$)	0.70 m	1.05 m	1.40 m	1.75 m

The inlet diameter, diffuser height and the number of diffusers will be varied to see for which cases the thermal and atmospheric environment are satisfactory. The inlet velocity is also calculated for each case. In some cases, the calculations are not valid since the jet is either not developed when it reaches the stratification height, or the jets interact with each other before they reach the stratification height. To distinguish between the reason for invalid empirical relations, square and round brackets are used as indicated in the bottom of the

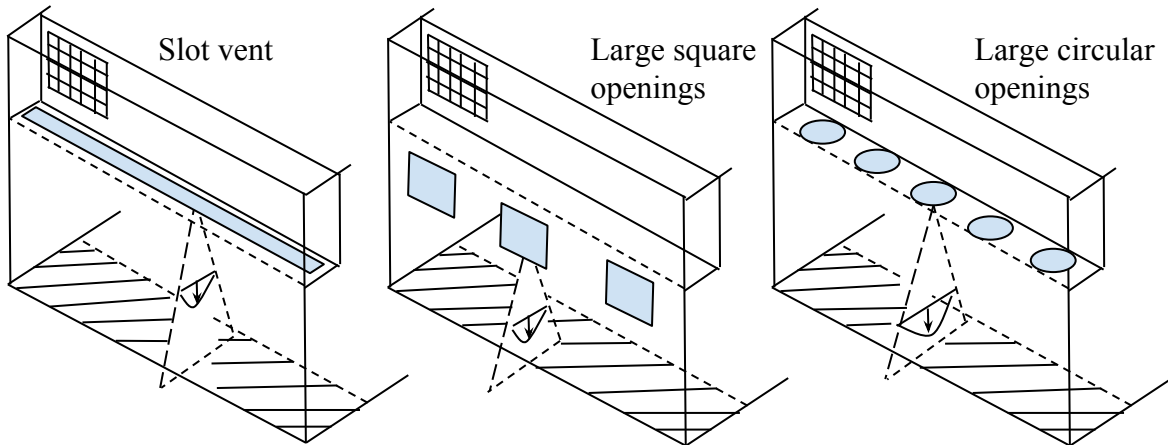


Figure 4.40: Suggestions on other inlet air devices that are assumed to decrease the pressure losses and velocity and improve the atmospheric environment

table 4.9 and 4.10. From the discussion of the velocity along the centerline for free buoyant jets in section 4.1.3, it is clear that there will be a large error if the empirical relations are used before approximately 5 diameters from the inlet. The error that arises when the jets are interacting before the stratification height are assumed to be smaller. In both cases where the empirical relations are invalid the flow will be overestimated.

Table 4.9 and 4.10 show calculations when the inlet diffuser diameter is 0.2 m and 0.25 m respectively. For each case the height and number of diffusers are varied, and the CO_2 -concentration and inlet velocity is calculated. The room temperature will be approximately equal for the different cases since the inlet temperature and total flow rate is the same.

Six different cases are calculated where each case has four different possibilities for the diffuser height. Case 1-3 is for the inlet diameter 0.2 m, and case 4-6 is for the inlet diameter 0.25 m. The cases are numbered in table 4.9 and 4.10. Ideally, the inlet velocity should be as low as possible to reduce pressure losses in the system and reduce the chance of cold draught in the occupancy zone. This means that one should look for cases where the inlet diameter is 0.25 m. Also, the inlet velocity is decreased when the total number of diffusers are high since the total inlet area is larger. Based on these criteria, case 6 would be the best case. As we see, none of the calculations for case 6 are valid. For the diffuser height 2.5 m and 3.0 m the jet will not be developed as it reaches the stratification line, while for the height 3.5 m and 4.0 m the jets interact with each other before they reach the stratification line.

Case 5 where the diffuser height is 3.5 m is assumed to represent the best design of the 6 cases since the inlet velocity is minimized, and the atmospheric environment is nearly satisfactory. The inlet velocity should ideally be lower. This could be done by increasing the diameter and/or installing more inlet devices to increase the total inlet area. It would then be hard to predict the indoor environment with the methods presented in this thesis. An option is to install diffusers on other walls as well. If the other 12 m wall was also used for supplying air, twice as many diffusers could be installed, and the inlet velocity could be reduced to 0.21 m/s which is assumed to be satisfactory for a low-pressure system.

4.5. DISCUSSION OF ACTIVE DISPLACEMENT VENTILATION

It is important to emphasize that better solutions for applying active displacement ventilation most likely exist. An inlet velocity of 0.42 m/s is assumed to be too high for a low-pressure system. Three suggestions on other inlet devices that would possibly decrease the inlet velocity due to the increased inlet area are illustrated in figure 4.40. The three suggestions are a slot vent, large square openings on the wall, and large circular openings.

Table 4.9: Design of classroom with active displacement. Inlet diameter 0.2 m

Supply flow rate per person, Q_i [l/(s·person)]	7			
Inlet air temperature, T_i [°C]	10			
Room temperature, T_1 [°C]	≈20			
Inlet diameter, d_0 [m]	0.20			
Diffuser height [m]	2.5	3.0	3.5	4.0
Case 1: Number of diffusers = 8				
Zone height [m]	[1.23]	1.38	1.54	(1.67)
Max. no. of diffusers on wall	[14]	12	10	(9)
[CO ₂] ₁ [ppm]	[534]	588	630	(653)
[CO ₂] ₂ [ppm]	[794]	794	794	(794)
Inlet velocity [m/s]	[0.83]	0.83	0.83	(0.83)
Case 2: Number of diffusers = 10				
Zone height [m]	[1.25]	1.43	1.57	(1.74)
Max. no. of diffusers on wall	[14]	12	10	(9)
[CO ₂] ₁ [ppm]	[544]	605	637	(665)
[CO ₂] ₂ [ppm]	[794]	794	794	(794)
Inlet velocity [m/s]	[0.67]	0.67	0.67	(0.67)
Case 3: Number of diffusers = 12				
Zone height [m]	[1.30]	1.46	(1.64)	(1.82)
Max. no. of diffusers on wall	[14]	12	(11)	(9)
[CO ₂] ₁ [ppm]	[563]	613	(650)	(676)
[CO ₂] ₂ [ppm]	[794]	794	(794)	(794)
Inlet velocity [m/s]	[0.55]	0.55	(0.55)	(0.55)
<p>[]: The jets are not developed and the empirical relations will overestimate the flow rate</p> <p>(): The jets will interact before they reach the stratification height and the flow is slightly overestimated.</p>				

Table 4.10: Design of classroom with active displacement. Inlet diameter 0.25 m

Supply flow rate per person, Q_i [l/(s·person)]	7			
Inlet air temperature, T_i [°C]	10			
Room temperature, T_1 [°C]	≈20			
Inlet diameter, d_0 [m]	0.25			
Diffuser height [m]	2.5	3.0	3.5	4.0
Case 4: Number of diffusers = 8				
Zone height [m]	[1.25]	[1.40]	1.54	1.70
Max. no. of diffusers on wall	[13]	[11]	9	8
[CO ₂] ₁ [ppm]	[544]	[596]	630	659
[CO ₂] ₂ [ppm]	[794]	[794]	794	794
Inlet velocity [m/s]	[0.53]	[0.53]	0.53	0.53
Case 5: Number of diffusers = 10				
Zone height [m]	[1.30]	[1.47]	1.61	(1.78)
Max. no. of diffusers on wall	[13]	(11)	10	(9)
[CO ₂] ₁ [ppm]	[563]	[613]	643	(671)
[CO ₂] ₂ [ppm]	[794]	[794]	794	(794)
Inlet velocity [m/s]	[0.42]	[0.42]	0.42	(0.42)
Case 6: Number of diffusers = 12				
Zone height [m]	[1.35]	[1.52]	(1.68)	(1.86)
Max. no. of diffusers on wall	[14]	[12]	(10)	(9)
[CO ₂] ₁ [ppm]	[580]	[626]	(655)	(681)
[CO ₂] ₂ [ppm]	[794]	[794]	(794)	(794)
Inlet velocity [m/s]	[0.34]	[0.34]	(0.34)	(0.34)

[]: The jets are not developed, and the empirical relation will overestimate the flow rate
 (): The jets will interact before they reach the stratification height and the flow is slightly overestimated.

Conclusion

The conclusion is divided into three parts. The first is about the investigation of the buoyant and isothermal jets, the second is related to active displacement ventilation and the use of empirical relations, while the third is for the comparison of different supply methods. The two first parts are directly connected to the tasks to be answered in the thesis, while the third is included to show the potential active displacement ventilation has to reduce the emission of GHG from buildings.

5.0.1 Application of CFD on buoyant and isothermal jets

Buoyant and isothermal jets were simulated with ANSYS Fluent where the goal was to compare them with the empirical relations developed by E. Skåret [1]. The geometrical model and boundary conditions were therefore created to imitate the ideal situation the equations are derived for. A nearly uniform ambient air temperature was obtained, and the walls, floor, ceiling, and extract were assumed to have a small impact on the free jets. The velocity and air temperature of the centerline corresponded well with the empirical relations. It is thus concluded that the empirical relations developed by E. Skåret yield for ideal conditions. The equations were valid after ca. $5-6d_0$ for the buoyant jet, while it was valid after ca. $4-5d_0$ for the isothermal jet. E. Skåret suggested that they were valid from $6-10d_0$ from the inlet. The similarity profile from the CFD simulations coincided with the theoretical similarity profile developed by Abramovich [27].

When the jet was placed next to a wall, the velocity increased while the temperature decreased compared to the free jet. This result is assumed to be wrong since the friction should slow down the jet. It is not clear for the author why these results are obtained, but it is assumed that one of the reasons is that the turbulence models used (Realizable $k-\epsilon$ and RNG $k-\epsilon$) perform poorly for wall jets. Similar observations are found in the literature review for versions of the $k-\epsilon$ equations.

The Realizable $k-\epsilon$ and RNG $k-\epsilon$ gave similar results except for the velocity distribution of buoyant free jets where the Realizable $k-\epsilon$ gave lower velocities than RNG $k-\epsilon$. RNG $k-\epsilon$ corresponded best with the empirical relations for buoyant free jets and was thus used for the simulation of active displacement ventilation.

The pole distance was close to zero for the buoyant free jet, while it was close to $5d_0$ for the isothermal free jet for the inlet device that was modeled. No suggestions on the pole distance

for wall jets are given since the results obtained are not reliable. The jet angle for the free jets, both buoyant and isothermal, corresponded well with the studied literature. The half angle was between 11.5° and 12.4° for the studied cases.

5.0.2 Evaluation of the application of simple empirical relations used for design of active displacement ventilation

A room with dimensions $w = 5$ m, $l = 5$ m and $h = 3.5$ m with a heat load of 100 W was investigated where the air was supplied 2.5 m over the floor. A heated cylinder was used to model the person, and the only heat loss was through the ventilation duct. A CO_2 - emission of 0.02 m³/(h·person) was used. The CO_2 concentration and air temperature calculated with empirical relations coincided with results obtained with CFD simulations. Only small deviations were observed. It is therefore concluded that the empirical relations developed by E. Skåret are recommended for the design of active displacement ventilation together with mass- and heat balance.

For active displacement ventilation, the CO_2 concentration became too high when the inlet airflow rate was 6 l/(s·person). When the flow rate was increased to 7 l/(s·person) the indoor air quality became nearly satisfactory. The CO_2 concentration is almost independent of the inlet air temperature since the relative temperature differences in the room are the same.

It is assumed that it is easier to reach satisfactory indoor air quality if one can use air inlet devices with larger inlet area since less air is entrained per volume inlet air. This will, on the other hand, increase the chance of cold draught in the occupancy zone.

The zone height/ stratification height was approximately 1.5 m for the CFD simulations while it was 1.75 m when empirical relations was used. The contaminant removal efficiency and temperature effectiveness were 1.23 and 1.05 respectively for the empirical relations, and 1.25 and 1.05 respectively for the CFD simulations.

When the inlet air temperature was decreased to under $10^\circ C$ the room had a need for heating when active displacement ventilation was used, while for inlet temperatures higher than approximately $14^\circ C$ the room had a need for cooling. This is valid when the inlet flow rate is 7 l/(s·person).

Humidity is assumed to behave similarly as contaminants for active displacement ventilation. This is beneficial for winter conditions since the dry inlet air is mixed with humid air before it enters the occupancy zone. Compared to ordinary displacement ventilation, where the air is transported directly to the occupancy zone, the humidity level can easier be kept at a satisfactory level.

Occupants should not stay in the zone bounded by a circle with a radius of 0.25 m from the centerline of the jet due to cold draught with air velocities over 0.18 m/s. This area could, for example, be used as a passage area. If the supply airflow rate and inlet area are larger, the radius is assumed to increase.

A classroom situation with 30 people was designed with empirical relations where the diffuser diameter, diffuser height and number of diffusers were varied. A case with 10 diffusers with diameter 0.25 m placed 3.5 m over the floor was assumed to be the best scenario when the inlet air flow rate was 7 l/(s·person) and inlet temperature was 10°C for this specific classroom. The criterion is then that the empirical relations are valid for the calculations.

The restrictions for such design is that the jets must be developed (have traveled $5d_0$) before it reaches the stratification line, and that the jets do not interact with each other before they reach the stratification height. These restrictions are a drawback in the design using empirical relations since relatively small inlet areas must be chosen in addition to an upper limit for the amount of diffusers per wall. It is assumed that it would be an advantage to have larger inlet areas and more diffusers to reduce the inlet velocity and pressure losses. The atmospheric environment would also be improved if the inlets were larger as already mentioned.

5.0.3 Comparison of supply methods

Air with lower supply temperature can be used for active- compared to ordinary displacement ventilation. This reduces the energy need and emission of GHG from buildings. The airflow rate for displacement ventilation is assumed to be somewhat lower than for active displacement ventilation for the diffusers investigated in this thesis when the atmospheric environment is the limiting factor. In the case where the room air temperature also must be satisfactory, the airflow rate for ordinary displacement ventilation must be increased to approximately 8 l/(s·person) to meet the requirement for room air temperature which is $22\pm 2^\circ\text{C}$ for winter conditions.

Complete mixing ventilation requires approximately 9 l/(s·person) which is a somewhat larger airflow rate than for active displacement ventilation. The supply temperature can be as low as 11°C for this case, but is still higher than for active displacement ventilation where the lowest supply temperature was 10°C.

A $q_0 - \Delta T_0$ - chart inspired by P.V. Nielsen (figure 4.37) was used to illustrate for which combination of flow rate and inlet air temperature each of the supply methods are suggested to be used. Active displacement ventilation has the potential of reducing the emission of GHG from buildings due to its low supply airflow rate and supply air temperatures along with satisfying conditions for thermal comfort, thermal stratification, draught risk, air quality and level of humidity.

Further Work

There are many opportunities for extending the scope of this thesis. Some suggestions are presented in this section.

The investigation of vertical jets, both buoyant and isothermal, along walls, was done in this thesis, but the CFD simulations were not as expected and are assumed to be unphysical. A further investigation of CFD for wall flow are therefore relevant for further work. It is suggested to consider using direct numerical solving or other turbulence models for further investigation of this problem. This would be helpful in the evaluation of empirical relations for jets supplied along walls.

In this thesis, only a circular opening in the ceiling was modeled with CFD for active displacement ventilation. The design of the inlet air devices has a large influence on the indoor environment. Other devices could also be modeled with the goal to optimize the amount of entrained room air, and reducing the inlet airflow rate. Larger circular inlets and slot vents are suggestions on inlet air devices that could be investigated. For slot vents, empirical relations for line sources could be used for comparison.

Simulations with heat loss through walls and windows will give more realistic room situations, and will better predict the performance of the ventilation methods for different seasons. This would reduce the heat load for winter conditions, and would possibly reduce the flow rate for ordinary displacement ventilation where the lower restriction for the inlet flow rate was the thermal environment and not the atmospheric environment as for the other supply methods.

The energy use and energy savings have been discussed in this section when different supply methods have been compared, but no actual calculations are performed. It would be interesting to perform energy calculations where factors such as preheating of air, driving pressure, pressure losses in ducts and HVAC-unit, and natural driving forces were investigated more in detail.

Appendix

A.1 Relevant guidelines and regulations

Table A.1: Overview over relevant guidelines, regulations and in addition to draught, occupancy and heat/activity related values. Values are valid for classrooms, and for low polluting buildings

Description	Value	Comment
Operating temperature requirements		
Winter condition, ($\approx 1\text{met}^*$ and 1.5clo^{**})	$22^\circ\text{C} \pm 2^\circ\text{C}$	
Summer condition, $\approx 1\text{met}$ and 0.5clo	$24.5^\circ\text{C} \pm 1.5^\circ\text{C}$	
Indoor air quality; 20% dissatisfaction		
Air flow per person, q_p	$7\text{ l}/(\text{s}\cdot\text{person})$	
Air flow due to material emission, q_B	$0.7\text{ l}/(\text{s}\cdot\text{m}^2)$	
CO₂-concentration		
CO ₂ concentration over outdoor conc.	$\approx 500\text{ ppm}$	
Max. CO ₂ concentration in classrooms	1000 ppm	Folkehelseinstituttet [95]
CO ₂ emission per person, low activity work	$0.02\text{ m}^3/\text{h}$	engineeringtoolbox.com
CO ₂ emission per person, normal work	$0.08\text{-}0.13\text{ m}^3/\text{h}$	engineeringtoolbox.com
Humidity		
Relative humidity	$20 - 40\%$	http://www.inneklima.com
Draught in occupied zone		
Summer conditions	$< 0.22\text{ m/s}$	
Winter conditions	$< 0.18\text{ m/s}$	

*1 met = $58\text{ W}/\text{m}^2$ and is used as a measure on a persons activity level

**1 clo = $0.155\text{ m}^2\text{K}/\text{W}$ and is the thermal resistance between the skin's surface and the outside surface of the clothing. Equivalent to the amount of insulation required to keep a person comfortable at 21°C

Table A.2: Overview over relevant guidelines, regulations and in addition to draught, occupancy and heat/activity related values. Values are valid for classrooms, and for low polluting buildings

Description	Value	Comment
Occupancy		
Standard occupancy density for classrooms	2 m ² /person	
Height of occupied zone when standing	1.8 m	Awbi et al. [6, p.266]
Height of occupied zone when seated	1.1 m	Awbi et al. [6, p.266]
Heat and activity		
Heat from seated person (office, school)	1 met	Novakovic et al. [4]
Heat from standing person on job	1.6 - 2.1 met	Novakovic et al. [4]
Convective heat from a person	≈ 50 % of E_{tot}	

A.2 Clothing, activity and human metabolism

Table A.3: Table for clothing, activity and human metabolism. Table obtained from www.engineeringtoolbox.com

Sitting still		
Clothing [Clo]	Comfort temperature [°C]	Convection [W]
1	23.3	36
1	24.5	45
1	25.0	50
1	25.6	55
1.5	20.7	36
1.5	21.8	45
1.5	22.3	50
1.5	22.8	55

A.3 Integration constants

Table A.4: Integration constants from [1] for round free jets

Int. const.	Round free jets
I_1	0.431
I_2	0.256
I_3	0.1785
I_4	0.134
I_5	0.108

Table A.5: Integration constants from [1] for plane free jets

Int. const.	Plane free jets
I_1	0.6
I_2	0.45
I_3	0.368
I_4	0.316
I_5	0.277

A.4 Matlab script for calculations of active displacement ventilation

```
% This LaTeX was auto-generated from MATLAB code.

% This is a simplified version of the a matlab script used
% for the design of active displacement ventilation.
% Many details are avoided in order to simplify the script,
% and the only purpos is to give the reader an example
% of how the calculation procedure can be done

% define global values
global Ti To ... % and so on

% =====
% VARIABLES
% =====

% Vary these values to achieve the disered design. The values
% are examples of input parameters.
Number_of_people = 1;
Qi_per_person = 6; % l/s
h_inlet = 2:0.5:4; % heights for inlet air device
Ti = 12 + 273;
no_diffusers = 1; % Number of diffusers
d_0 = 0.390; % diameter of inlet air device

% =====
% BEFORE CALCULATIONS
% =====
% Defining air properties
cp = 1.005;g = 9.81;betha = 1/300;%... and so on

% Other constant values
T_r = 20 + 273; alpha = 12.5; Cb = tan(alpha);...
U_value = 1.2; P_pers = 100;... % and so on
```

A.4. MATLAB SCRIPT FOR CALCULATIONS OF ACTIVE DISPLACEMENT VENTILATION

```
% Room and window design
h_room = 5; l_room = 5; w_room = 5; ... % and so on

% The next lines defines step size and create the vector for the
nj = 100;
jmax = nj + 1;
start_height = 0;
for i = 1:length(h_diffuse) % for loop start. calculate several diffuser heights
dh =( h_diffuser(i) - start) / nj;
h = 0:dh:h_inlet;
% =====
% CALCULATIONS
% =====

% Each of the functions are programmed to perform
% the calculations in the way they are presented in
% this thesis.

% Convective plume-vector calculated
[Q_plume] = calculate_plume();

% Exhaust temperature calculated. Estimate
[T2] = calculate_T2();

% Flow- , temperature and velocity-vectors and t of the
% round plaque diffuser
[Q_diffuser, Um_diffuser, T_diffuser] = calculate_diffuser();

% Sum all the flow elements (diffuser/fabricair + plume + draught)
[Q_totdiff, Q_totfabric] = calculate_flowsum(Q_diffuser, Q_fabric);

% Finding height and flow of the stratification height
[H_stratdiff, Q_stratdiff] = calculate_strat(Q_totdiff);
[H_stratfabric, Q_stratfabric] = calculate_strat(Q_totfabric);

% Finding the temperature of air entering the lower zone
[T1] = calculate_T1();

% Calculate CO2-concentration for lower and upper zone
[CO2_1, CO2_2] = calculate_co2();

% Calculate temperature effectiveness and
% contaminant removal effectiveness
[T_eff, CO2_eff] = calculate_effectiveness();

% =====
% PLOT FIGURE AND CREATE TABLES
% =====
```

A.4. MATLAB SCRIPT FOR CALCULATIONS OF ACTIVE DISPLACEMENT VENTILATION

```
% Plot figure of velocity distribution along the wall
Plot(h,Um);

% Plot figure of the flow elements
Plot(h,Qplume, h, Qdraught, h, Qdiffuser, h , Qtot);

% Create additional plots if wanted to visualize the design

% Create a table with all values calculated
Category = {'Temp upper zone','Temp lower zone'...
    , 'Concentration lower zone', 'Concentration upper zone',...
    'stratification height'}; %.... can add more values
Value = [T2, T1, CO2_1, CO2_2, H_strat]; %
Table = table(value, 'RowNames',Category);
```


Bibliography

- [1] Eimund Skåret. *Ventilasjonsteknisk Håndbok*. Norsk byggforskningsinstitutt, Forskningsveien 3 B, Postboks 123, Blindern, 2000.
- [2] Standard. *NS-EN ISO 7730:2005 . Ergonomics of the thermal environment - Analytical determination and interpretation of thermal comfort using calculation of the PMV and PPD indices and local thermal comfort criteria*. Standard Norge, 2005.
- [3] Standard. *NS-EN 15251:2007+NA:2014. Indoor environmental input parameters for designing and assessment of energy performance of buildings addressing indoor air quality, thermal environment, lightning and acoustics*. Standard Norge, 2007.
- [4] Vojislav Novakovic, Stein Olaf Hanssen, Jan Vincent Thue, Ivar Wangensteen, and Frode Olav Gjerstad. *Energy Management in Buildings*. Gyldendal Norsk, 3 edition, 2007.
- [5] Per Erik Nilsson, editor. *Achieving the desired indoor climate*. The Commtech Group, 2003.
- [6] Hazim B. Awbi, Yuguo Li, Bjarne Olesen, Bluysen Philo, Claude-Alan Roulet, James Axley, and Peter V. Nielsen. *Ventilation Systems*. Taylor and Francis, 2008.
- [7] Bjørn Jenssen Wachenfeldt, Mads Mysen, and Peter G. Schild. Air flow rates and energy saving potential in schools with demand-controlled displacement ventilation. *Science Direct*, 2007.
- [8] Mats Sandberg. Ventilation effectiveness and purging flow rate-a review. proceedings, international symposium on room air convection and ventilation effectiveness. July 1992.
- [9] M. Mattsson and M Sandberg. Displacement ventilation - influence of physical activity. *Proceedings Roomvent*, 1994.
- [10] H. Xing, A. Hatton, and H.B. Awbi. Astudy of the air quality in the breathing zone in a room with displacement ventilation. *Department of Engineering Science, University of Oxford, Oxford, UK*, 2001.
- [11] Per Heiselberg and Mats Sandberg. Convection from a slender cylinder in a ventilated room. *Proceedings Roomvent*, 1990.
- [12] Elisabeth Mundt. Displacement ventilation systems - convection flows and temperature gradients. *Building and Environment, Vol. 30, No. 1*, 1995.
- [13] Thor Helge Dokka, Mads Mysen, Peter G. Schild, and Per Olaf Tjelflaat. *Bygningsintegrert ventilasjon*. Mars 2003.

BIBLIOGRAPHY

- [14] Per Heiselberg. Building integrated ventilation systems - modelling and design challenges. 2004.
- [15] Torkel Andersson and Håkan Gillbro. Fredkulla- och risebergsskolan - två av många moderne självdragsskolor. 2011.
- [16] Christian Drivsholm, Hans Olsen, Per Tage Jespersen, Claus Martin Hvenegaard, and Søren Draborg. *Energioptimering af Procesventilation of Udvikling af Fleksible Procesudrug til Store Industrielle Emner*. Teknologisk Institut, Juni 2013.
- [17] Howard Goodfellow and Esko Tahti, editors. *Industrial Ventilation Design Guidebook*. Academic Press, 2001.
- [18] Henning Hørup Sørensen. *Håndbog i industri ventilation*. Teknisk Forlag A/S, 1998.
- [19] Alexander M. Zhivov. *Ventilation guide for automotive industry*. HPAC Engineering, Penton Media Bldg. 1300 E. 9th Street Cleveland, OH 44114-1503, 2000.
- [20] Peter Vilhelm Nielsen. *Air Distribution in Aircraft Cabins Using Free Convection Personalized Ventilation*. Aalborg Universitet, 2006.
- [21] David Etheridge and Mats Sandberg. *Building Ventilation*. John Wiley and Sons, 1996.
- [22] P. V. Nielsen. The "family tree" of air distribution systems. *Aalborg Universitet*, 2011.
- [23] P. V. Nielsen, T. S. Larsen, and C. Topp. Design methods for air distribution systems and comparison between mixing ventilation and displacement ventilation. *Aalborg Universitet*, 2003.
- [24] Peter V. Nielsen. Ventilation in commercial and residential buildings. *Ventilation System and Air Quality*, 1998.
- [25] Tor G. Malmstrøm, Allan T. Kirkpatrick, Brian Christensen, and Kevin D. Knappmiller. Centreline velocity decay measurements in low-velocity axisymmetric jets. *Cambridge University Press*, 1997.
- [26] Hazim B. Awbi. *Ventilation of buildings*. Spon Press, 2 edition, 2003.
- [27] G. N. Abramovich. *The theory of turbulent jets*. MIT Press, 1963.
- [28] Leif Steensaas. *Ventilasjonsteknikk*. Gyldendal Norsk Forlag, 2001.
- [29] Cao Guangyu. Modelling the attached plane jet in a room. *Dissertation for the degree of Doctor of Science in Technology*, 2009.
- [30] H. Skistad. Displacement ventilation. *Journal of the experimental and Technical Physics*, 1994.
- [31] Helsedirektoratet. "fysisk aktivitet blant voksne og eldre i norge". *Resultater fra en kartlegging i 2008 og 2009*, 2009.
- [32] P.O. Fanger. *Indeklima*, chapter 2 in "Varme og klimateknikk". 1992.
- [33] D.A. McIntyre. *Indoor Climate*. Applied Science Publishers LTT, 1980.

- [34] Thor Helge Dokka and Per Olaf Tjelflaat. A simplified model for human induced convective air flows - model predictions compared to experimental data. n.d.
- [35] P Kofoed. *Thermal plumes in ventilated rooms*. PhD thesis, University of Aalborg, 1991.
- [36] E Mundt. *The performance of displacement ventilation systems; Experimental and Theoretical studies*. PhD thesis, Royal Institute of Technology, Stockholm, 1996.
- [37] Per Olaf Tjelflaat and Mats Sandberg. Assessment of ventilation- and energy- efficiency in design for large enclosures. 1996.
- [38] John C. Tannehill, Dale A. Anderson, and Richard H. Pletcher. *Computational Fluid Mechanics and Heat Transfer*. Taylor and Francis, 1997.
- [39] Paul D. Bates, Stuart N. Lane, and Robert I. Ferguson, editors. *Computational Fluid Dynamics*. John Wiley and Sons, 2005.
- [40] J. Blazek. *Computational Fluid Dynamics: Principles and Applications*. ELSEVIER, 2005.
- [41] Stephen B. Pope. *Turbulent Flows*. Cambridge University Press, 2000.
- [42] Henk Tennekes and John L. Lumley. *A First Course in Turbulence*. MIT Press, 1972.
- [43] ANSYS. *ANSYS Fluent Theory Guide*. 275 Technology Drive, Canonsburg, PA 15317, 2013.
- [44] ANSYS. *ANSYS Fluent User's Guide*. 275 Technology Drive, Canonsburg, PA 15317, November 2013.
- [45] M. F. Modest. Radiative heat transfer. *Series in Mechanical ENgineeringMcGrawHill*, 1993.
- [46] Jihong Wang, Shugang Wang, Tengfei Zhang, and Francine Battaglia. Assessment of single-sided natural ventilation driven by buoyancy forces through variable window configurations. *Energy and buildings*, 2017.
- [47] Y. Ji, M. J. Cook, and V. Hanby. Cfd modelling of natural displacement ventilation in an enclosure connected to an atrium. *Building and Environment*, 2005.
- [48] M. P. Wan and C. Y. Chao. Numerical and experimental study of velocity and temperature characteristics in a ventilated enclosure with underfloor ventilationsystems. *Indoor Air*, 2005.
- [49] Sara Gilani, Hamid Montazeri, and Bert Blocken. Cfd simulation of stratified indoor environment in displacement ventilation: Validation and sensitivity analysis. *Building and Environment*, 2015.
- [50] William Craig Reynolds. *Computation of turbulent flows*. 1976.
- [51] Helge I. Andersson. Turbulence modelling. *Lecture Notes in subject 76572 Turbuent Flow*, 1988.
- [52] B. Moshfegh and Robert Nyiredy. Comparing rans models for flow and thermal analysis of pin fin heat sinks. *15th Australasian Fluid Mechanics Conference*, 2004.

- [53] M. Chmielewski and M. Gieras. Three-zonal wall function for k-e turbulence models. *Warsaw University of Technology, Institute of Heat Engineering*, 2013.
- [54] M. Alejandra Menchaca-Brandan, F. Alonso Dominguez Espinosa, and Leon R. Glicksman. The influence of radiation heat transfer on the prediction of air flows in rooms under natural ventilation. *Energy and buildings* 138, 2016.
- [55] M. J. Cook, Y. Ji, and G. R. Hunt. Cfd modelling of natural ventilation: combined wind and buoyancy forces. *International Journal of ventilation*, 2003.
- [56] Y. Huo, F. Haghghat, J. S. Zhang, and C. Y. Schaw. A systematic approach to describe the air terminal device in cfd simulation for room air distribution analysis. *Building and Environment*, 1999.
- [57] Francesco Russo and Nils T. Basse. Scaling of turbulence intensity for low-speed flow in smooth pipes. *Flow Measurement and Instrumentation* 52, 2016.
- [58] Peter Vilhelm Nielsen. Fifty years of cfd for room air distribution. *Building and Environment*, 2015.
- [59] Bernhard Muller. Lecture notes from tep4280 introduction to computational fluid dynamics, 2015.
- [60] Peter G. Schild. *Accurate prediction of indoor climate in glazed enclosures*. PhD thesis, NTNU, 1997.
- [61] Yihuan Yana, Xiangdong Li, Lin Yang, and Jiyuan Tu. Evaluation of manikin simplification methods for cfd simulations in occupied indoor environments. *Energy and buildings*, 2016.
- [62] Alain Makhoul, Kamel Ghali, and Nesreen Ghaddar. Low-mixing coaxial nozzle for effective personalized ventilation. *Indoor and Built Environment* 2015, 2013.
- [63] Claus Topp, Peter Vilhelm Nielsen, and Dan N. Sørensen. Application of computer simulated persons in indoor environment modeling. *ASHRAE Transactions*, 2002.
- [64] Syoginus Aloysius and Luiz C. Wrobel. *CFD comparison of buoyant and non-buoyant turbulent jets*. Brunel University West London, 2007.
- [65] M. Coussirat, A. Guardo, E. Jou, E. Egusquiza, and P. Alvedra. Performance and influence of numerical sub-models on the cfd simulation of free forced convection in double-glazed ventilated facades. 2008.
- [66] C. A Rundle, M. F Lightstone, P. Oosthuizen, P. Karava, and E. Mouriki. Validation of computational fluid dynamics simulations for atria geometries. *Building and Environment*, 2010.
- [67] Y. Ji and M. J. Cook. Numerical studies of displacement natural ventilation in multi-storey buildings connected to an atrium. *Institute of Energy and Sustainable Development, De Montfort University*, 2007.
- [68] Pei-Chun Liu, Hsien-Te Lin, and Jung-Hua Chou. Evaluation of buoyancy-driven ventilation in atrium buildings using computational fluid dynamics and reduced-scale air model. *Energy and Environment* 44, 2009.

- [69] Tomas Norton, Da-Wen Sun, Jim Grant, Richard Fallon, and Vincent Dodd. Applications of computational fluid dynamics (cfD) in the modelling and design of ventilation systems in the agricultural industry. *Science Direct*, 2007.
- [70] P. Rohdin and B. Moshfegh. Numerical predictions of indoor climate in large industrial premises. a comparison between different k-epsilon models supported by field measurements. *Linköping Institute of Technology, Sweden*, 2005.
- [71] Nobukazu Kobayashi and Qingyan Chen. Floor-supply displacement ventilation in a small office. *Indoor and Built Environment*, 2003.
- [72] Christine Walker, Gang Tan, and Leon Glicksman. Reduced-scale building model and numerical investigations to buoyancy-driven natural ventilation. *Energy and buildings* 43, 2011.
- [73] Zhiqiang John Zhai, Zhao Zhang, Wei Zhang, and Qingyan Yan Chen. Evaluation of various turbulence models in predicting airflow and turbulence in enclosed environments by cfd: Part 1 - summary of prevalent turbulence models. *HVAC and R Research*, 2011.
- [74] Qiongxiang Kong and Bingfeng Yu. Numerical study on temperature stratification in a room with underfloor air distribution system. *Energy and buildings* 40, 2006.
- [75] Zhao Zhang, Wei Zhang, Zhiqiang John Zhai, and Qingyan Yan Chen. Evaluation of various turbulence models in predicting airflow and turbulence in enclosed environments by cfd: Part 2-comparison with experimental data from literature. *HVAC and R Research*, 2011.
- [76] M. J. Cook and K.L Lomas. Buoyance-driven displacement ventilation flows: evaluation of two eddy viscosity models for prediction. *Building Services Engineering Research and Technology*, 1998.
- [77] V. Yakhot, S.A Orszag, S. Thangham, and T. B Gatski. Development of turbulence models for shear flows by double expansion technique. *Physics of Fluids. A.Fluid Dynamics*, 1992.
- [78] Q. Chen. Comparison of different k- epsilon models for indoor air flow computations. *Numerical Heat Transfer*, 1995.
- [79] Hanne Liland Bottolfsen. Undersøkelse av aktiv fortregningsventilasjon for bruk i klasserom. Master's thesis, NTNU: Norwegian University of Science and Technology, June 2014.
- [80] Y. Bartosiewicz, Z. Aidoun, P. Desevaux, and Y. Mercadier. Cfd experiments integration in the evaluation of six turbulence models for supersonic ejectors modelling. *Proceedings of intergrating CFD and experiments conference*, 2003.
- [81] A. Stamou and I. Katsiris. Verification of a cfd model for indoor airflow and heat transfer. *Building and Environment* 41, 2005.
- [82] Tengfei Zhang, Kisup Lee, and Qingyan (Yan) Chen. A simplified approach to describe complex diffusers in displacement ventilation for cfd simulations. *Indoor Air* 19, 2009.

- [83] Shafqat Hussain and Patrick H. Oosthuizen. Validation of numerical modeling of conditions in an atrium space with a hybrid ventilation system. *Building and Environment* 52, 2011.
- [84] Shafqat Hussain, Patrick H. Oosthuizen, and Abdulrahim Kalendar. Evaluation of various turbulence models for the prediction of the airflow and temperature distributions in atria. *Energy and buildings* 48, 2012.
- [85] V. Yakhot and S.A Orszag. Renormalization group analysis of turbulence: I. basic theory. *Journal of Scientific Computing*, 1, 1-51, 1986.
- [86] F. Boysan. Advanced turbulence modeling. Short Course Notes at the University of Leeds, Fluent Europe Ltd, pp. 1279-1298, 1995.
- [87] Hazim B. Awbi and A. A. Setrak. Numerical solution of ventilation air jet. *5th CIB Int. Symp. on the use of computers for environmental engineering related to buildings*, 1986.
- [88] Hazim B. Awbi and A. A. Setrak. Air jet interference due to ceiling-mounted obstacles. *Air distribution in ventilated spaces symp. Roomvent* 87, 1987.
- [89] Guilherme Anrain Lindner, Roberto Mathias Susin, Viviana Cocco Mariani, and Katia Cordeiro Mendonca. Comparison of different turbulence models for indoor airflow computations. *Mechanical Engineering Department - Pontifical Catholic University of Parana - PUCPR*, 2007.
- [90] Andrius Jurelionis and Edmundas Isevicius. Cfd predictions of indoor air movement induced by cold window surfaces. *Journal of Civil Engineering and Management*, 2010.
- [91] A. Schlin and P. V. Nielsen. Impact of turbulence anisotropy near walls in room airflow. *Indoor Air 2004: 14*, 2003.
- [92] Peter Vilhelm Nielsen. Computational fluid dynamics in ventilation design. *Aalborg Universitet*, 2008.
- [93] A. D. Lemaire. Room air and contaminant flow, evaluation of computational methods. *Summary Report of IEA Programme for Energy Concervation in Buildings and Community systems*, 1993.
- [94] M. Deevy, Y. Sinai, P. Everitt, L. Voigt, and N. Gobeau. Modelling the effect of an occupant on displacement ventilation with computational fluid dynamics. *Science Direct Energy and Buildings* 40, 2007.
- [95] Folkehelseinstituttet. *Anbefalte faglige normer for innneklima*, 2015.